ION SPECIFICITY AND CONONSOLVENCY EFFECTS ON NEUTRAL MACROMOLECULES

A THESIS SUBMITTED TO

THE GRADUATE SCHOOL OF ENGINEERING AND SCIENCE

OF

BILKENT UNIVERSITY

IN PARTIAL FULFILLMENT OF THE REQUIREMENTS FOR

THE DEGREE OF

MASTER OF SCIENCE

IN

CHEMISTRY

BY

YAREN SEVVAL OZDOGAN

SEPTEMBER 2025

ION SPECIFICITY AND CONONSOLVENCY EFFECTS ON NEUTRAL MACROMOLECULES

BY YAREN SEVVAL OZDOGAN

SEPTEMBER 2025

We certify that we have read this thesis and that in our opinion it is fully adequate, in scope and in quality, as a thesis for the degree of Master of Science.

_____

Halil Ibrahim Okur (Advisor)

_____

Özgül Persil Çetinkol

_____

Ömer Dağ

Approved for the Graduate School of Engineering and Science:

_____

Orhan Arıkan

Director of the Graduate School

ABSTRACT

ION SPECIFICITY AND CONONSOLVENCY EFFECTS ON NEUTRAL MACROMOLECULES

YAREN SEVVAL OZDOGAN

M.S. in Chemistry

Advisor: HALIL IBRAHIM OKUR

SEPTEMBER 2025

Ions, osmolytes, and other small molecules can interact with macromolecules and affect their properties, such as solubility and hydration. The ion specificity has been an important research topic since Franz Hofmeister published the "*Hofmeister Series*", which ranks the anions and cations based on their ability to increase or decrease the solubility of macromolecules. It is known that the weakly-hydrated anions can interact with macromolecules, while the strongly hydrated ones are excluded from the macromolecular surface due to having strongly interacting hydration shells. In this thesis, the ion-specific effects are extended to sugar-based macromolecules from commonly studied amide-based ones. Methylcellulose (MC), hydroxypropyl cellulose (HPC), and dextran were utilized as model polymers for investigating whether the Hofmeister anions can interact or not. Lower Critical Solution Temperature (LCST) measurements showed that MC and HPC are affected by the Hofmeister anions with the same way as the amide-based macromolecules. Namely, SCN^- act as a surface-active ion, and salts-in whereas SO_4^{2-} ion salts-out macromolecules via ion exclusion mechanism. The proton nuclear magnetic resonance (^{1}H-NMR) spectroscopy

measurements showed that the methyl groups of MC are responsible for the interaction between the Hofmeister anions and the polymer.

In the second part, “cononsolvency” which is an important phenomenon that occurs when two good solvents decrease the solubility of the macromolecule when they are mixed. For understanding the mechanism of this phenomenon, poly(*N*-isopropylacrylamide) (PNIPAM) and poly (*N, N* - diethylacrylamide) (PDEA) were used as model macromolecules. PNIPAM showed cononsolvency behavior via the addition of methanol, ethanol, and isopropanol, while PDEA did not exhibit the same anomaly, rather showed cosolvency. Attenuated Total Reflection – Fourier Transform Infrared (ATR-FTIR) spectroscopy combined with Multivariate Curve Resolution (MCR) analysis showed that both the changes in the bulk properties of solvent-cosolvent mixtures and the hydration shell of the macromolecules in the collapsed state cause the cononsolvency behavior for PNIPAM. Our results show that the interface and preferential alcohol adsorption dictate the cononsolvency phenomenon.

Keywords: Hofmeister series, Specific ion effects, Thermoresponsive polymers, PNIPAM, PDEA, MC, HPC, Dextran, Cononsolvency

ÖZET

NÖTR MAKROMOLEKÜLLER ÜZERİNDE SPESİFİK İYON VE EŞ ÇÖZÜNMEZLİK ETKİLERİ

YAREN SEVVAL OZDOGAN

Kimya | Yüksek Lisans

Danışman: HALİL İBRAHIM OKUR

EYLÜL 2025

İyonların, ozmolitlerin ve diğer küçük organik moleküllerin makromoleküllerle etkileşimleri, makromoleküllerin çözünürlük ve hidratlanma gibi fiziksel özelliklerini etkiler. Bu bağlamda iyona özel etkiler, "*Hofmeister serileri*" Franz Hofmeister tarafından yayınlandığından bu yana önemli bir araştırma konusu olmuştur. Hofmeister serileri, iyonların makromoleküllerin çözünürlüğünü arttırması veya azaltması özelliğine göre sıralayan bir seridir. Bu seride "zayıf hidratlanmış" olarak adlandırılan anyonların makromoleküllerle hidrojen bağları ya da diğer elektrostatik kuvvetlerle doğrudan etkileşime girerek onların su içerisindeki çözünürlüklerini arttırdığı bilinmektedir. Öte yandan, "güçlü hidratlanmış" anyonlar etraflarındaki katı hidrasyon kabuğu sebebiyle makromoleküllerle doğrudan etkileşim kuramazlar ve varlıkları makromolekülerin su içindeki çözünürlüğünü azaltır. Bu çalışmada, Hofmeister anyonların makromoleküller üzerindeki etkilerini daha iyi anlamak amacıyla amid bazlı makromoleküller yerine şeker bazlı makromoleküller kullanılmıştır. Hofmeister anyonlarının şeker bazlı makromoleküller üzerinde nasıl etkileri olduğunu anlamak amacıyla metilselüloz, hidroksipropil selüloz ve dekstran model polimerler olarak seçilmiştir. Metilselüloz (MC) ve hidroksipropil selülozun

(HCP) faz değiştirme sıcaklıklarının (LCST) Hofmeister anyonlarının varlığında amid bazlı polimerlerle aynı trendleri sergilediği Faz Değiştirme Sıcaklığı ölçümleri ile gösterilmiştir. SCN^- gibi zayıf hidratlanmış Hofmeister anyonları yüzey aktif iyon olarak davranırken, SO_4^{2-} gibi güçlü hidratlanmış Hofmeister anyonların tam tersi etkiye sebep oldukları gösterilmiştir. Ek olarak nükleer manyetik rezonans spektroskopisi (^{1}H-NMR) ölçümleri, metilselülozun fonksiyonel grubu olan metil gruplarının zayıf hidratlanmış anyonlar ile olan etkileşimlerinden sorumlu olduğunu göstermiştir.

İyona özel etkilere ek olarak "eş çözünmezlik" etkisi de makromoleküllerin çözünürlük mekanizmalarını anlamak açısından önemli bir fenomendir. Bu etki iki iyi çözücünün belirli oranlarda karıştırıldığında kötü bir çözücüye dönüşmesi ve makromolekülün çözünürlüğünü düşürmesini ifade eder. Bu etkinin mekanizmalarını anlamak amacıyla poli(*N*-izopropilakrilamid) (PNIPAM) and poli(*N, N*-diethylakrilamid) (PDEA) model polimerler olarak kullanıldı. Eş solvent olarak kullanılan metanol, etanol ve izopropanolün eklenmesi PNIPAM'in su içerisindeki çözünürlüğünü azaltırken çok benzer bir moleküler yapıysa sahip olmasına rağmen PDEA'de aynı etki gözlenmedi. Zayıflatılmış Toplam Yansıma - Fourier Dönüşümlü Kızılötesi spektroskopisi (ATR-FTIR) ve Çok Değişkenli Eğri Çözünürlüğü (MCR) algoritması analizi, hem çözücü-eş-çözücü karışımlarının kütle özelliklerindeki değişikliklerin hem de çökmüş durumdaki makromoleküllerin hidrasyon kabuğundaki değişimlerin PNIPAM için eş çözünmezlik davranışına neden olduğunu göstermiştir.

Anahtar kelimeler: Hofmeister serileri, Spesifik iyon etkileri, Termoresponsif polimerler, PNIPAM, PDEA, MC, HPC, Dekstran, Eş çözünmezlik

ACKNOWLEDGEMENT

I would like to thank my advisor, Dr. Halil I. Okur, for his unlimited support, guidance, and patience. His academic depth, experience, and broad scientific knowledge made my first research experiences invaluable. His optimistic and indulgent attitude, combined with his deep kindness, has grown me both personally and academically. When I look back on what I have learned and achieved in the last few years, I could not have done it without him as my advisor. I extend my greatest gratitude to Dr. Halil I. Okur. Thank you sincerely, hocam. I feel fortunate to have had the opportunity to work with you, and I hope our correspondence will continue.

I would also like to thank all the former and present Okur Research Group Members. Especially, Dr. Ezgi Yılmaz Topuzlu, Sobia Farooq, Umay Eren Ertekin, and Cansın Ayvaz. Besides the academic help and guidance, I thank you all for making our research group feel like a home to me. I wish you all the best.

I would like to thank Prof. Ömer Dağ and Prof. Özgül Persil Çetinkol for their kind acceptance of serving on my thesis committee, their feedback, and our valuable discussion.

The friends that Ankara gave to me, I am grateful to all of them. To Pelin, Ezgi, Umut Mert, and Gözde for the years in the Bilkent University, Chemistry Department were invaluable and unforgettable. Additionally, I thank Özgür, Özge, and İpek for their ongoing support throughout this journey.

I thank Mehmet Ali for being my best friend for thirteen years and always supporting me, even though he has been far away from me for the last five years; he always made me feel at home.

I thank Ertan for being by my side and making all the roads we walk together enjoyable and for being my strongest support system.

Lastly, I thank my parents, Erhan and Figen. I could not be where I am right now without their support and the sacrifices that they made. I love them so much, and I am dedicating this thesis to my sister Nisa Ceren, who will be a greater researcher than I am in the future.

Table of Contents

List of Figures

List of Tables

List of Abbreviations

ATP	Adenosine triphosphate
ATR-FTIR	Attenuated Total Reflectance Fourier Transform Infrared Spectroscopy
CD	Circular Dichroism
ELP	Elastin-like Polypeptide
HPC	Hydroxypropyl Cellulose
ITC	Isothermal Titration Calorimetry
K_A	Acid Dissociation Constant
LCST	Lower Critical Solution Temperature
MC	Methylcellulose
MCR	Multivariate Curve Resolution
MD	Molecular Dynamics
NAD	Nicotinamide Adenine Dinucleotide
NMR	Nuclear Magnetic Resonance
PcyPOx	Poly(2-cyclopropyl-2-oxazoline)
PDEA	Poly (*N*, *N*-diethylacrylamide)
PEG	Polyethylene glycol
PEI	Polyethyleneimine
PiPOx	Poly(2-isopropyl-2-oxazoline)

PNIPAM	Poly (*N*-isopropylacrylamide)
PVCL	Poly(N-vinylcaprolactam)
SIE	Specific Ion Effects
TMAO	Trimethylamine *N*-oxide
UV-Vis	Ultraviolet-Visible
VPGVG	Valine-Proline-Glycine-Valine-Glycine

Chapter 1 – Introduction

Biological macromolecules are crucial for living organisms, and understanding their interactions with the environment is vital for understanding the fundamentals of life. This class of macromolecules primarily consists of proteins and carbohydrates, which exhibit unique behaviors in their solutions. Their properties, such as solubility, conformational changes, aggregation, hydration, enzymatic activity, and denaturation, can be altered by their intrinsic structural properties -sequence, composition, and surface chemistry- and environmental factors. These factors can be exemplified as temperature, pH, ionic strength, and the presence of additives. [2–6] Especially, the Hofmeister series and the addition of some small organic molecules to the solution of macromolecules are known to affect their behavior crucially. In this chapter, the well-known examples related to the behaviors of biological macromolecules and how they are affected by the presence of different additives in their aqueous solutions from the literature are presented.

1.1 Interactions and Behaviors of Macromolecules: From Ions to Osmolytes

1.1.1 Aqueous Phase Behaviors of Biomacromolecules and Hofmeister Series

Among the factors that affect the behavior of macromolecules, the significance of dissolved ions in the solution is particularly notable. This effect can be described as the concept of the *specific ion effect* (SIE), a term used to explain how different salts

impact various physicochemical and biological phenomena. In this manner, Franz Hofmeister and his coworkers published their work in the late 19th century, which revealed the effect of different salts on protein solubility, which would be called the *"Hofmeister Series"* later.[7–11] This series contains both anions and cations and is ranked based on the hydration properties of the ions. The "weakly hydrated" anions cause "salting-in" (i.e., SCN^-, ClO_4^-, I^-, and NO_3^-) while the "strongly hydrated" anions cause "salting-out" (i.e., CO_3^{2-}, SO_4^{2-}, $H_2PO_4^-$, F^-) effects.[12,13]

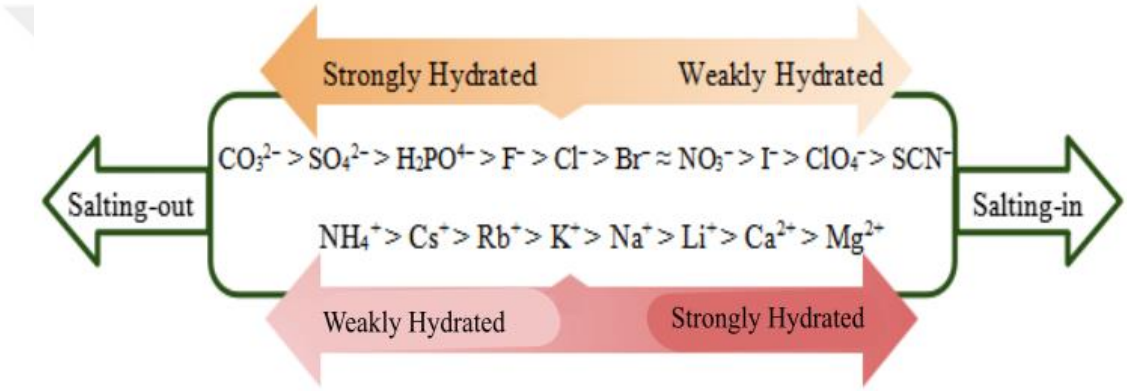

Figure 1: A rank order for Hofmeister anions and cations that one may come across in the literature, ordered from most salting-out (left) to most salting-in (right). The anion series is shown above, and the cation series below. Note that the ordering of the two series based on strongly to weakly-hydrated is inverted. The ordering is generic, but it was inspired by references Zhang *et al.*[11] and Bruce *et al.*[12]

The context of the Hofmeister series expanded from only protein solubility to protein folding and misfolding, aggregation and self-assembly, enzymatic activity modulation, nucleic acid duplex stability, micelle and vesicle formation, colloid stability, and interfacial behaviors like surface tension and bubble coalescence. [14–26] However, in contrast to its diverse application areas and long history, the underlying mechanism remains elusive due to the complex nature of the concept. Unlike the electrostatic interactions, SIE is context-dependent on specific molecular-level

interactions, such as ion hydration, preferential exclusion/accumulation of ions on macromolecular surfaces, and ion effects on water structure and dynamics. [27–31] For this reason, these variations between different systems are adopted, and related research is mostly focused on explaining the diverse molecular-level mechanisms. This interest has led to utilization and improvement in experimental and spectroscopic techniques, as well as molecular dynamics simulations and theoretical modeling, which enable to understand the effect of ions on the macromolecules in aqueous media.

One widely utilized model macromolecule example is poly(N-isopropylacrylamide) (PNIPAM), an amide-based thermoresponsive macromolecule used to understand protein solubility behaviors. The effect of Hofmeister ions on the phase transition temperature (LCST) of PNIPAM has been investigated, and it was concluded that the weakly hydrated anions can act through the hydration shell of PNIPAM and can directly bind to the macromolecule. In contrast, the strongly hydrated ones cannot do it and cause salting-out behavior.[4] These findings are important in terms of understanding how hydration properties change with the addition of Hofmeister ions, rather than just the bulk properties. With the development of spectroscopic and thermodynamic techniques, this paradigm started to be shifted, and it appeared that the influence of the Hofmeister ions on the water network alone was shown to not a sufficient explanation. [32–34]

1.1.2 Molecular-Level Mechanisms on Specific Ion Effects

The experimental background of the Specific Ion Series goes back to the pioneering work of Franz Hofmeister performed in the late 19th century. [7–11] These studies were performed using egg-white proteins and enabled Hofmeister and his

coworkers to rank the ions based on their ability to "salt-in" or "salt-out" from the aqueous solution. One strong explanation of this phenomenon is mainly centered on the effect of ions to alter the bulk water structure and gives rise to the use of the terms "structure maker" and "structure breaker" or "kosmotrope" and "chaotrope." [35,36] In this paradigm, kosmotropic ions are strongly hydrated, small, and of high charge density are referred to as "structurer", while chaotropic ions are larger, weakly hydrated, and thought to be "disorderer" in terms of the bulk properties of water. However, this model was too generalized and has never been proven with empirical techniques.

Some influential studies were performed using femtosecond pump-probe spectroscopy by Bakker and coworkers, who were able to observe the orientational correlations of water molecules in different contents of salt solutions. [37–41] The findings concluded that the presence of ions increases the correlation times of water molecules found only in the first hydration shells and does not affect the dynamics of the water molecules present in bulk water, even at elevated concentrations.

Another groundbreaking technique used to investigate the effect of Hofmeister ions on water structure is vibrational sum frequency spectroscopy (VSFS). Cremer and coworkers were able to observe the Hofmeister effects on the phase transition behavior of a surfactant (octadecylamine) monolayer spread on the air/water interface of D_2O and H_2O.[42,43] In these studies, the vibrational signals corresponding to the interfacial structure are isolated by VSFS, and it is shown that, in the presence of salt effects, the surface potential decreases compared to its absence, due to the positive charge on the

surfactant molecules. This indicates that anions penetrate the monolayer. For sodium salts of Hofmeister anions, it was found that alkyl chain disorder and the degree of anion penetration show a parallel trend with the Hofmeister series. Still, the effect on the water structure deviated from this order.

Using smaller model systems was one of the most significant advancements in understanding the more complex biological macromolecular systems. Since the proteins contain a variety of different amino acids with variable charges and have a diverse and complex nature, oligopeptides were one of the most proper models, since they contain peptide bonds, which are common among all proteins. These findings concluded that there are preferential interactions between the peptide bond and weakly-hydrated anions (e.g., I^- and SCN^-) and strongly-hydrated cations (e.g., Li^+).[44–46] It was also shown that the carbonyl groups of the oligopeptide are responsible for the interactions between the strongly-hydrated cations via hydrogen bonding, and the specific ion interactions between the oligopeptide and Hofmeister ions are directly proportional to the number of peptide units.[44]

Even the oligopeptides are good models for understanding the specific ion effect on proteins, factors like molecular size and charged capping of termini groups of oligopeptides, caused complications.[47–49] To overcome these complications, synthetic model macromolecules became preferable due to their ability to mimic proteins and being thermoresponsive. These materials are water-soluble with a random coil conformation under the "lower critical solution temperature (LCST)" and undergo a phase transition above this point, which is indicated by a macroscopically observable

cloud-point. [50,51] These polymers are tailorable for different sizes, charges, hydrophobicity, and other characteristics, resulting in a wide range of different polymers used in literature. [52–56] Among these models, the most widely used model macromolecule is poly(*N*-isopropylacrylamide) (PNIPAM), which is an amide-based macromolecule that undergoes a sharp transition around 35 ^{o}C.[32] PNIPAM has hydrophobic backbone groups and the isopropyl group on the side-chain, and also a hydrophilic amide group on the side-chain, which enables it to mimic the natural proteins, and a suitable model for observing the specific ion effect on a protein mimic. Alongside the PNIPAM, with a very similar molecular structure, Poly (*N*, *N* – Diethyl acrylamide) (PDEA), which shows a phase transition temperature around 32 °C, is another widely-used model macromolecule (Figure 2).[57] Also, elastin-like polypeptides (ELP), more specifically V_5-120 or a more hydrophobic example, $V_5A_2G_3$-120 have great significance for the investigation of the specific ion effects since they are good mimics of the proteins and can be utilized in applications such as therapeutic purposes. [58]

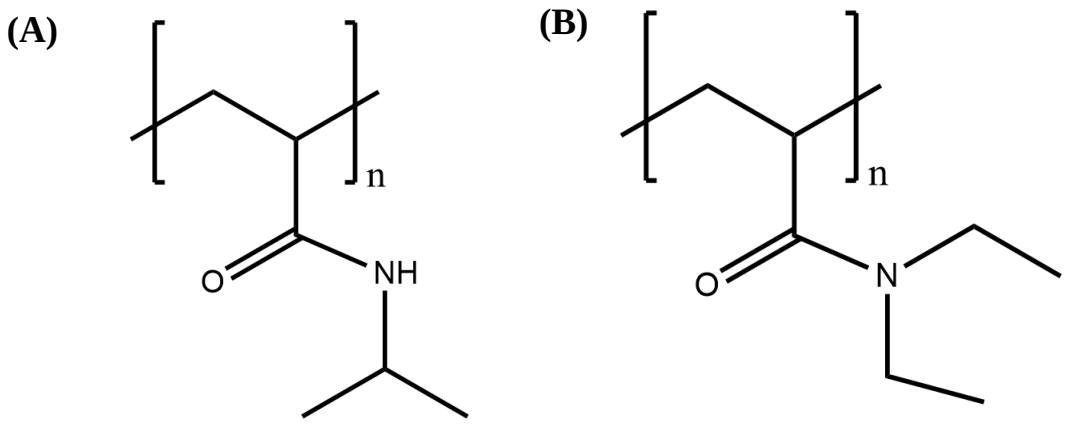

Figure 2: The molecular structure of (A) PNIPAM and (B) PDEA

Zhang *et al*. showed the interactions between the 11 sodium salts of Hofmeister anions and PNIPAM and how the LCST of PNIPAM changes in the presence of these salts by utilizing the microfluidic/dark field microscopy set-up developed by the group.[59] The findings showed that PNIPAM follows the direct anionic Hofmeister series: strongly-hydrated anions cause salting-out behavior, which is indicated by a linear decrease of the LCST of PNIPAM with increasing salt concentration. The weakly-hydrated anions cause salting-in behavior, which causes a nonlinearity in the lower salt concentrations. The authors provided an empirical formula to fit their data, which consists of a constant, a linear term, and a Langmuir isotherm:

$$T = T_0 + c[M] + \frac{B_{max}.\mathrm{K}_A[M]}{1 + \mathrm{K}_A[M]} \qquad (1)$$

In this formula, T_0 is the LCST in the absence of any salts, and T is the observed LCST of PNIPAM dependent on the salt concentration ([M]). The coefficient c has the units ^{o}C/M or K/M, and the nonlinear terms are a Langmuir-type binding isotherm. K_A is the apparent association equilibrium constant for PNIPAM and ion interaction, where the B_{max} is the maximum change in LCST of PNIPAM, which can be correlated with saturation concentration. Their data confirmed that the behavior caused by all the salts obeys this fitting formula, and they came up with three different mechanisms for salting-in and salting-out behaviors: the strongly-hydrated anions cause the salting-out effect by preventing the hydrophobic hydration of the polymer by elevating the interfacial surface tension. The weakly-hydrated anions are found to bind directly to the side-chain amide moieties, which led to polymer salt-in and stabilized the coil conformation of the macromolecule. This behavior is shown via the Langmuir-type isotherm shown with the nonlinear term of Equation 1, which models a saturable

binding. The ranking of the B_{max} values of binding anions matches the order of the Hofmeister series.

To understand if the proposed mechanisms published by Zhang *et.al.* are plausible for other systems, closer to the natural proteins, the same experiments were performed using ELP instead of PNIPAM by Cho et.al. with 11 sodium salts of Hofmeister anions.[60] In this study, both the V_5-120 and $V_5A_2G_3$-120 were used to understand how these ELPs interact with Hofmeister anions. V_5-120 has an LCST at around 28 °C, and $V_5A_2G_3$-120 has it at around 42 °C. The trends for the changes in the LCST of both ELPs were very similar to the trends observed for the PNIPAM case, as shown by Zhang et al.: strongly-hydrated anions cause a linear decrease in LCST while the weakly-hydrated anions cause a nonlinear behavior, indicating the ion-specific binding. This data was also fitted by the same empirical formula, shown as Equation 1.

For understanding the site-specific binding of the anions to ELPs, Rembert *et al.* performed externally-referenced ^{1}H-NMR spectroscopy to observe how the protons of ELPs behave in the presence of anions.[61] The same 11 Hofmeister anions as the sodium salts were utilized for these measurements, and reference standard sodium 2,2-dimethyl-2-silapentane-5-sulfonate (DSS) was used as external referencing for preventing chemical contact with the sample. All the measurements performed below the LCST, and the position of each proton peak, were plotted as a function of the concentration of the salts. The protons at the α-position on the backbone were shown to be changed nonlinearly in terms of the chemical shift in the presence of the salts of

weakly-hydrated anions, while the other proton peaks displayed only a linear decrease in their chemical shifts. The resulting curves showed a similar behavior to the LCST curves and were fitted to a similar empirical fit:

$$\Delta\delta = -c[M] + \frac{\Delta\delta_{max}[M]}{K_D + [M]} \qquad (2)$$

In this formula, the change in chemical shift is related to a saturable interaction with the weakly-hydrated anions. The dissociation constant (K_D) for such interactions was found to be around 50 mM for the binding of SCN^- to α-position protons.

More recently, a relation between the monomer number of polymers and their shape has been shown to have a role in their interactions with Hofmeister ions.[62] In this study, it was observed that the weakly hydrated anions, such as SCN^-, are repelled from the hydration shell of monomers of model macromolecule polyethylene glycol (PEG), while they are attracted to the oligomers and larger polymers. Additional information lies under the hydration behavior of the different sites of the macromolecules. The authors showed that the different parts of the macromolecules show different binding behavior since they have differing hydration properties. Termini groups have a more ordered water network around them, which is hard to break by the ions and causes ions to get repelled from their hydration shell. On the other hand, the water structure around central groups is less ordered, and it is easier to break the hydration and bind to the central groups for ions.

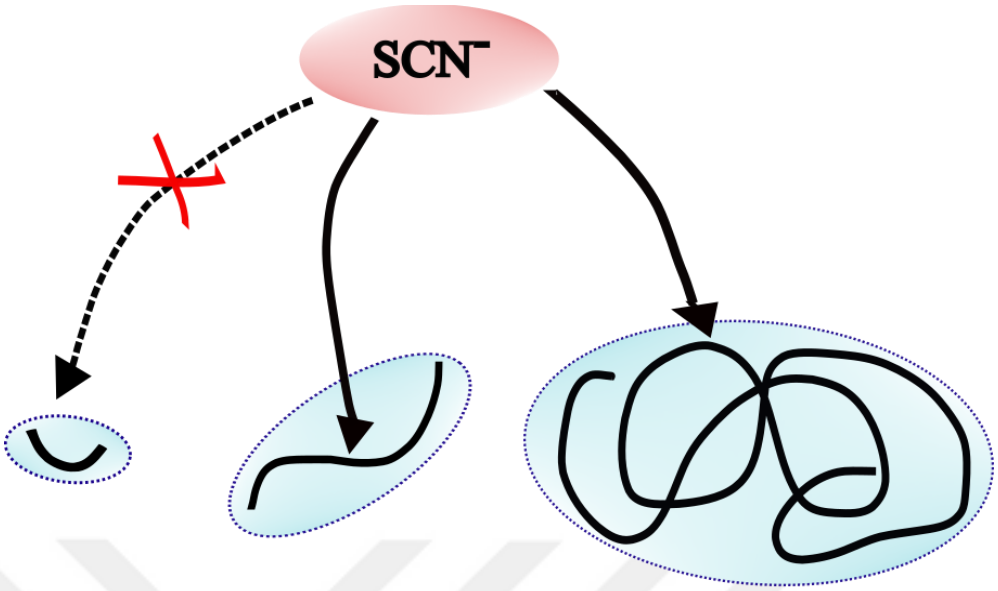

Figure 3: The proposed mechanism for the binding of weakly hydrated Hofmeister anion, SCN^- to a monomer, an oligomer and a macromolecule. Adapted from reference 60.

1.1.3 Effect of Osmolytes on Biomacromolecules

Osmolytes are small organic compounds found in living organisms, either synthesized or accumulated due to external factors such as osmotic and thermal changes. From a more biological perspective, osmolytes are small organic molecules found in biological systems besides many complex functionalities, and they give rise to osmotic pressure. This class of molecules is generally utilized as cellular protectants to maintain protein homeostasis and cellular integrity in hyperosmotic or denaturing environments. Under some stress conditions, osmolytes function as protein, membrane, and amino acid protectants without preventing the normal biological functions from being processed. Polyols, amino acids, methylamines, and urea are the most commonly referred osmolyte categories in literature. [63–68] These osmolytes can

be classified under two main categories in aqueous conditions: “stabilizers" and “denaturants.”

Stabilizer osmolytes such as trimethylamine N-oxide (TMAO), proline, betaine, and glycine are preferentially excluded from the surface of the proteins instead of directly binding to them. This behavior increases the solvent accessible surface area of the macromolecule and promotes a folding conformation.[69,70] This mechanism resembles the “salting-out” behavior, which is associated with the behavior of the strongly hydrated Hofmeister anions in aqueous macromolecules, which promotes their stability. On the other hand, “denaturant” osmolytes like urea and guanidium chloride (GnCl), interact directly with the protein backbone and side-chain and, by lowering the energy barrier for denaturation, favor the unfolded states of the proteins.[71–74] For instance, urea can form several hydrogen bonds with polar groups of the peptide backbone and prevent the intramolecular interactions, resulting in the loss of the secondary and tertiary structure of the protein.[75,76] This behavior matches the “salting-in” behavior, which occurs in the presence of weakly hydrated Hofmeister anions in aqueous media of macromolecules. The structures of the most common osmolytes can be found in Figure 4.

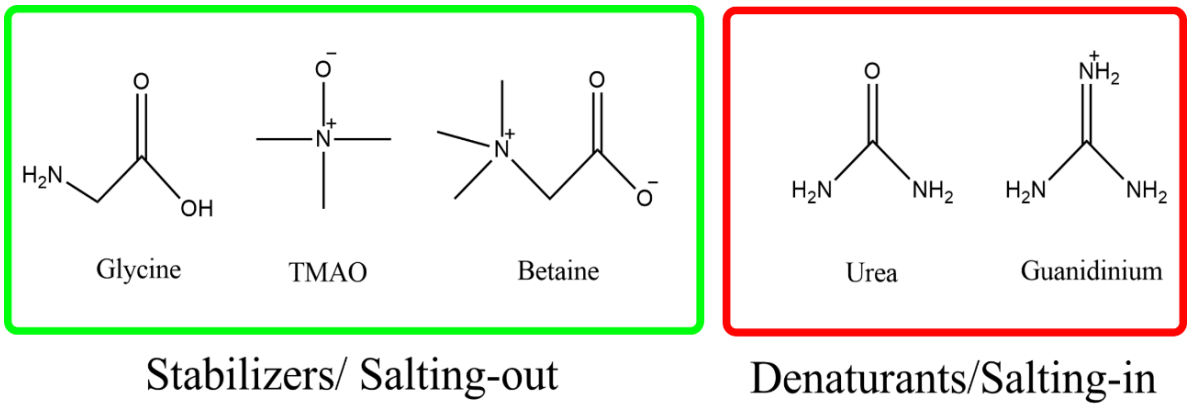

Figure 4: The molecular structures of glycine, TMAO, betaine, urea and guanidinium as examples of the most common osmolytes

Deciphering the underlying mechanism of the influence of the osmolytes on the proteins led to a wide range of research. Spectroscopic and thermodynamic techniques like NMR spectroscopy, Circular Dichroism (CD), and LCST measurements were the techniques that are commonly used for achieving this aim, as well as the molecular dynamics (MD) simulation techniques. For example, by using CD, differential calorimetry, NMR, and MD simulations, Heyda et.al. showed that GndCl and urea promote the denaturation of Tr-cage miniprotein.[77]

CD results in this study concluded that the ability of guanidium to change the alpha helical structure of Tr-cage is two times more effective compared to urea, and NMR results showed that the denaturation strategies of these two osmolytes are different from each other: urea binds to the backbone of the protein while guanidium targets the aromatic and charged groups instead.

Okur and his coworkers expanded this study to ELP VPGVG-120, which is a synthetic polymer that mimics protein folding/unfolding, utilizing FTIR spectroscopy, LCST measurements, and MD simulations.[78] Their results showed that the change of the counter anion of the guanidinium significantly affects its influence on the protein-like polymer. When the guanidium is paired with a strongly hydrated anion, such as sulphate, both ions are depleted from the hydration shell of the ELPs and cause the favorable collapsed/folded state, and act as a stabilizer osmolyte. On the contrary, pairing guanidium with a weakly hydrated/salting-in anion like thiocyanate results in two different types of behavior at two different concentration regimes. In the lower concentration of the guanidinium thiocyanate salt, polymer-polymer cross-linking is promoted, which favors the collapsed state. In the elevated concentrations, both ions

participated in the hydration shell and favored the unfolded/extended state of the ELPs. GndCl fell between these two cases with a constant promotion of the unfolded state. This study concluded that the identity of the osmolyte does not solely depend on its ionic properties, but also additive with the environmental content.

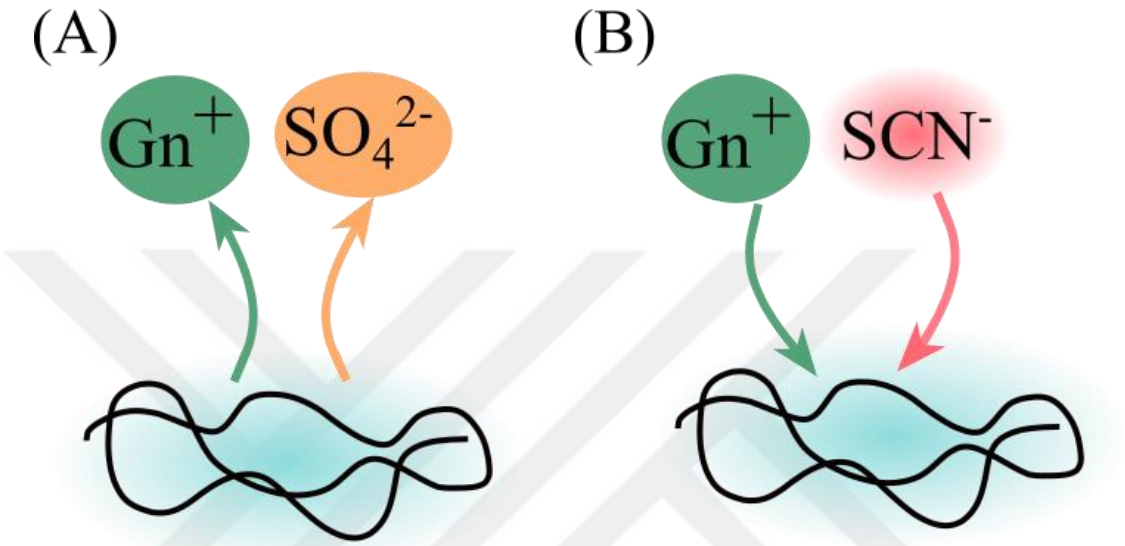

Figure 5: The representation of the interactions of guanidinium depending on its counter anion. (A) When the guanidinium is added with a strongly hydrated anion, sulphate, both ions are depleted from the hydration shell. (B) On the other hand, when guanidinium is added with a weakly hydrated anion, thiocyanate, both the anion and cation are attracted by the polymer and included in its hydration shell.

Osmolytes are important in real biological systems as well as model systems. Their most common duty in nature is to prevent cells from being damaged by extreme environmental conditions, such as salinity, extreme heat or cold, and dehydration. For example, marine species like sharks use destabilizing agents like urea and counterbalancing stabilizers such as TMAO to maintain protein functionality in differing ocean temperatures.[79] Likewise, proline accumulation is observed in plants to decrease osmotic stress caused by salinity or lack of water.[80] In addition to these

physiological roles of osmolytes, they also have growing importance in the medical and therapeutic areas of research. Numerous neurodegenerative diseases, such as Alzheimer's, Parkinson's, Huntington's, and ALS, are caused by protein misfolding and aggregation, and some stabilizer osmolytes play crucial roles in promoting the native structure of the proteins. [81] They can alter the hydration shell of the proteins and reorganize the solution dynamics. Thanks to this property, osmolytes have control over protein behavior both inside and outside of the cell [82–84] and are seen as a potential new direction for therapeutic developments and linking molecular biology and clinical applications. [85–88]

1.2 Beyond Hofmeister and Osmolytes: A Cononsolvency Study

Alongside the specific ion effects and the osmolytes, the interactions between the small molecules and osmolytes hold a crucial role for the biological systems and for basic fundamental understanding of aqueous systems. Small organic molecules with relatively low molecular weight and a size of around 1 nm are considered "small molecules". These types of molecules are widely encountered in biological systems as inhibitors or activators and are responsible for the regulation of various biological processes. For instance, some of the small molecules act as inhibitors that compete for the binding sites with enzymes [89,90] or can increase enzymatic activity by acting as an activator. [91,92] Additionally, small-molecule metabolites such as NADH or ATP can interact with biomacromolecules and influence their behavior throughout the biological processes. Thanks to this ability, small molecules can be involved in regulating gene expression, affecting processes such as transcription and translation,

as well as the stability of RNA and proteins.[93–99] Because of these diverse applications of small molecules, investigating the mechanisms of small molecules with biological macromolecules is crucial.

Klotz *et al.* showed that synthetic water-soluble polymers favorably bind to organic ions via different mechanisms.[100] They performed a study to observe how methyl orange interacts with protein-mimicking polymers such as polyethyleneimine (PEI) and its derivatives: lauryl-PEI, hexanoyl-PEI, and poly (acrylic acid) modified with carbobenzoxytryptophan (PA-Z-Trp). Utilizing techniques like Ultraviolet-Visible (UV-Vis) Spectroscopy, titration assays, and Scatchard analysis, the authors showed that methyl orange can form complexes with PEI derivative polymers via hydrophobic interactions and π-π stacking. Especially lauryl-PEI shows a high binding affinity with a high K_A value up to 10^6 M^{-1} even at the low degrees of lauryl substitution. After this study, Klotz expanded his work to real biological proteins rather than the model macromolecules and investigated how a wide range of small molecules, including caffeine, nicotinic acid, imidazole, and ATP, interact with proteins such as hemoglobin and albumin.[101] He put forth a broad review of how the proteins interact with different small molecules with different mechanisms utilizing spectrophotometry, fluorescence spectroscopy, Isothermal Titration Calorimetry (ITC), and Circular Dichroism (CD). He showed that the protein ligand bindings include Langmuir-type single-site binding, multiple independent binding sites, positive and negative cooperative binding, and allosteric regulation.

1.2.1 Cosolutes, Cosolvency, and Cononsolvency Phenomenon

In some contexts, the small molecules and osmolytes mentioned in previous subsections are referred to as “cosolutes”, which indicates their ability to dissolve along with the main solute (biomacromolecules in this case) and to alter the properties of the solutions.[102] One of the primary studies showed the interactions between the cosolutes, including alcohols, salts, and surfactants, and how they affect the properties of the aqueous solutions of neutral polymers such as ethyl(hydroxyethyl)cellulose (EHEC), methylcellulose (MC), poly(ethylene oxide) (PEO), etc. [103] The author refers to the phase transition temperature as “cloudy point (CP)” and they determined the CP visually via optical spectroscopy. The findings showed that low-molecular-weight alcohols, methanol and ethanol, caused an increase in CP, while the longer chain alcohols, like heptanol, caused a dramatic decrease in the CP of the polymers. The effect of the inorganic salts obeys the Hofmeister series; Na_2SO_4 caused a sharp decrease in CP, and NaI and NaSCN caused salting-in behavior.

Another important concept for the ternary systems is “cosolvency,” since the addition of a second solvent can alter the properties of the polymer solutions. In the late 20th century, Wolf and Blaum demonstrated that the addition of cosolvents to polymer solutions alters the phase transition behaviors of the polymers through complex mechanisms.[104] The authors used poly (methyl methacrylate) (PMMA) as the model macromolecule, 1-chlorobutane as the solvent, and 4-heptanone and 2-butanol as “cosolvents”. They visually probe the phase transition of the polymer in solvent mixtures using optical setups. 4-Heptanone is a good solvent for PMMA, while 2-butanol and 1-chlorobutane are poor solvents. The solubility of PMMA in the mixtures

of 4-heptanone and 1-chlorobutane gradually increases with increasing 4-heptanone content and decreases with increasing 1-chlorobutane content and shows a "monotonic behavior." On the other hand, the behavior of PMMA is not monotonic in the presence of 1-chlorobutane and 2-butanol. Even though the polymer is not soluble in either solvent, in the mixtures of these two solvents, the solvent power is enhanced, and PMMA becomes soluble in certain solvent-cosolvent mixtures. The authors called this nonideal and nonmonotonic behavior "cosolvency". This phenomenon plays an important role in the determination of the stimuli-responsive soft materials, tailoring the structures of polypeptides, and regulating the water-soluble drug formulations.[105–108]

"Cononsolvency", on the other hand, is a well-known but more rarely observed that some solvent-cosolvent mixtures cause a reverse effect. "Cononsolvency." is a phenomenon where two good and miscible solvents become a bad solvent for the same macromolecule when they are mixed at certain ratios. The first example of this phenomenon was published in 1923 by Mardles and investigated the solubility of cellulose acetate, which is soluble in aniline and in glacial acetic acid but not in a mixture of these two.[109]

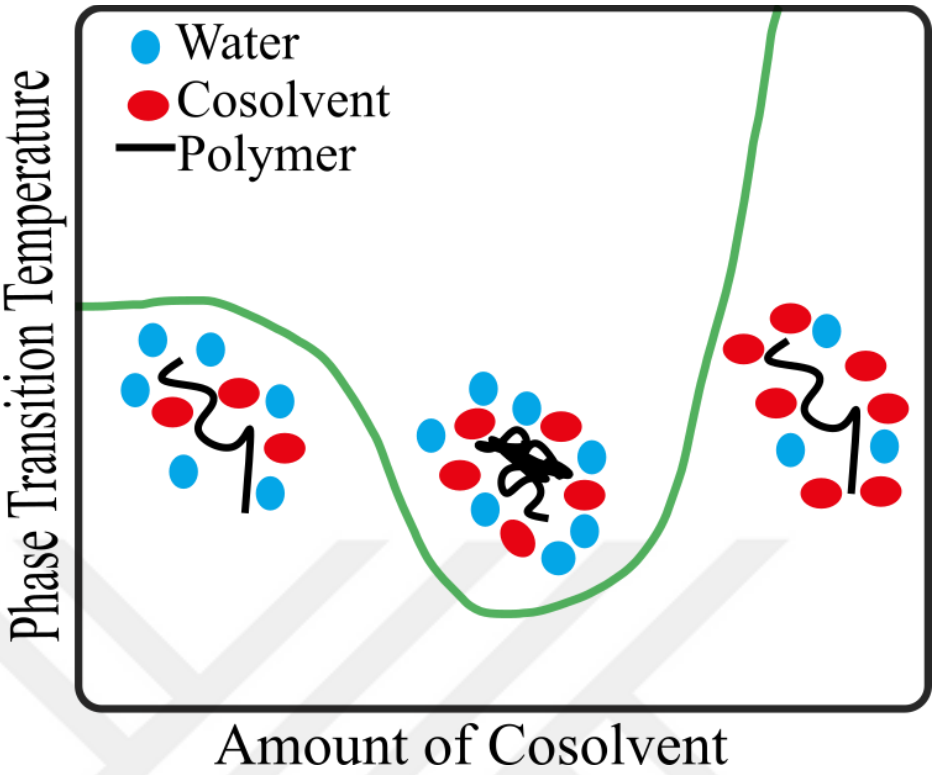

Figure 6: The schematic representation of the cononsolvency phenomenon. The solubility of the polymer in lower concentrations of cosolvent is high, and the polymer is in an extended form. As the amount of cosolvent increases, the solubility and phase transition of the polymer decrease, and the polymer is in an aggregated form. Finally, as the concentration of the cosolvent further increases, the polymer becomes extended, and its solubility starts to increase again.

After the first findings emerged in the literature regarding the "cononsolvency" phenomenon, PNIPAM also became a suitable model for this research area and a tool for investigating this unexpected behavior. In one of the first studies where PNIPAM was used, it was shown how the LCST of PNIPAM changes in methanol-water mixtures with different ratios.[110] The authors observed the LCST, cloud point, via turbidity changes of the samples and measured using a diode array spectrometer by heating the solutions at a constant rate of 0.2 °C/min. They used 1g/L PNIPAM for the aqueous solution preparation and performed the cloud point measurements in differing

mole fractions of methanol in water. Below the 0.05 mole fraction of methanol, the LCST of PNIPAM remains around 31 ^{o}C; however, as the mole fraction of methanol increases up to 0.35, the temperature constantly decreases and reaches a minimum of -7.5 ^{o}C at 0.35 mole fraction of methanol. As the methanol content further increases, the LCST increases again up to 14.5 ^{o}C at 0.45, and beyond this mole fraction, there is no cloud point detected up to 100 ^{o}C, PNIPAM remains soluble. As the underlying reason for this behavior, the study suggests that, at low concentrations of methanol in water, methanol forms "hydrogen-bonded cages" which prevent it from interacting with the polymer and cause little impact on the solubility. In moderate concentrations, methanol molecules compete for interaction and distort the hydration shell structure, which leads to a decrease in the solubility of the polymer. And, after 0.45 mole fraction of methanol, the methanol-water interactions become more attractive, water cages are broken, and enhance the methanol-polymer interactions, promoting the hydrated state of the polymer, which increases the polymer solubility. They concluded that this type of behavior is mostly driven by the enthalpic interactions among water, methanol, and polymer. These conclusions are dependent on the thermodynamic inferences and hypotheses, and up to this day, there is no experimental and spectroscopic evidence for elucidating the universal mechanism underlying cononsolvency phenomenon.

1.2.2 Proposed Mechanisms for Cononsolvency

The cononsolvency phenomenon is functional in a wide range of areas of applications like sensor design[111], catalysis[112], selective precipitation processes[113,114], self-assembly formations[115] and the development of different topological surfaces[116,117] since it enables the adjustable thermoresponsive abilities of the

materials. The cosolvents utilized in this research area are generally alcohols (most commonly: methanol and ethanol), and other organic solvents such as acetone, dimethyl sulfoxide (DMSO), and dimethylformamide (DMF). Notably, PNIPAM is most widely used as the model macromolecule, as well as the other poly(acrylamides), poly(n-propyl-2-oxazoline), poly(N-vinylcaprolactam), and elastin-like polypeptides (ELPs), a class of biomimetic macromolecules that exhibit thermoresponsive behavior.

For observing the underlying mechanism, lots of different characteristics of macromolecules are investigated, such as cloud point changes, thermodynamic aspects of the transition, the dynamics of the side groups or the chain or the solvent, and the chain length by utilizing a variety of techniques such as differential scanning calorimetry (DSC), nuclear magnetic resonance spectroscopy (NMR), quasi-elastic neutron scattering (QENS), and fluorescence correlation spectroscopy (FCS) and theoretical studies.[118–123] Even the more complex systems, such as polypeptides, gels, block copolymers, thin films, and grafted polymer brushes, are under consideration in this research area[124–128], the most studied system is PNIPAM, water, and methanol mixtures. The key takeaways from all these works mainly depend on the idea that the addition of methanol causes the alteration of the hydration shells of PNIPAM and changes the chain-chain interaction, which leads to the collapse of the polymer.

For the PNIPAM-containing systems, the interactions of polymers with solvent/cosolvent systems were observed. The work by Mukherji et.al. showed that methanol preferentially adsorbs on the side-chain of PNIPAM and encapsulates the side-chain as globules, resulting in a decrease in mobility of the side-chain.[120] The

authors combined ^{1}H-NMR measurements with MD simulations. The NMR measurements were conducted with a special sealed design of NMR tubes to prevent the evaporation of alcohol, containing 15% aqueous methanol, and 1.188 g PNIPAM over sixteen days, to observe the solvent intake by the polymer. The results showed that, in the first 3-4 days, the proton peak corresponding to methanol decreased linearly and then exhibited a plateau behavior. This decrease showed that the methanol content in the bulk solution decreased to 3% from 15%, which indicates that the methanol is adsorbed by the polymer. The hydrogen bonds per PNIPAM monomer are calculated by all-atom simulation and show that PNIPAM preferentially binds methanol, especially at methanol mole fractions $0.10 \leq X_m \leq 0.25$. The resulting mechanism can be concluded as: the OH group of methanol bonds to the amide group of PNIPAM, and its CH_3 goes toward the isopropyl group of another PNIPAM unit, causing a bridge-type interaction between the polymer segments, resulting in the collapse of the polymer. The other possible scenario is the bridging of two different PNIPAM monomers by two different methanol molecules.

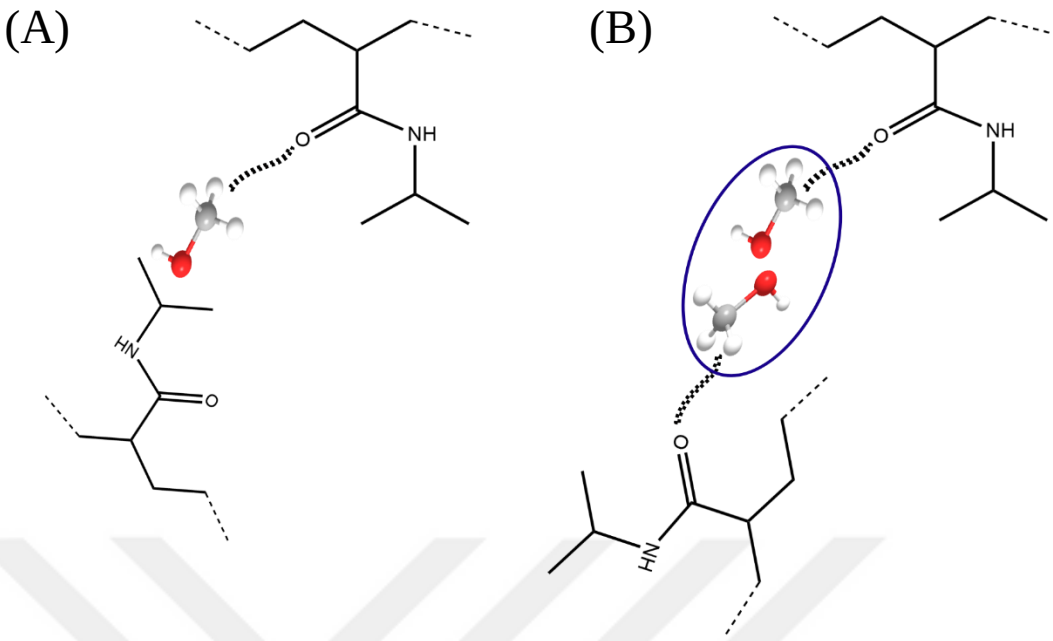

Figure 7: The two proposed mechanisms by Mukherji et.al. (A) displayed the OH group of methanol bonding to the amide group of PNIPAM, and its CH_3 goes toward to isopropyl group of another PNIPAM, and (B) shows both OH groups of two different methanol molecules coordinate two different PNIPAM monomers from isopropyl groups. Both scenarios suggest an increase in the molecular interactions between PNIPAM monomers, and caused the collapse of the polymer. Adapted from reference 116.

Besides the investigation of the effects of methanol, the effects of other alcohols have also been investigated. In the study by Wang et.al., Fluorescence Correlation Spectroscopy (FCS) is used for investigating how ethanol affects the chain conformation of PNIPAM in the dilute aqueous solutions.[129] The authors labeled PNIPAM in the presence of different concentrations of ethanol with dye and fluorescence correlation spectroscopy (FCS) to determine the hydrodynamic radii and the Flory exponent *n*. The Flory component in pure ethanol and water is around 0.57, indicating that PNIPAM is fully dissolved in both solvents. The addition of ethanol to aqueous solutions decreases to 1/3 of the pure solvent case, and the change from 0.09

to 0.25 occurs with the changing concentrations of ethanol as an indication of polymer collapse.

In another work that studied PNIPAM in D_2O and deuterated ethanol (d-ethanol, C_2D_6O), small-angle neutron scattering (SANS) was utilized by Hore and Hammouda.[130] It was observed that PNIPAM showed LCST behavior at low d-ethanol fractions, a miscibility gap at intermediate compositions, and UCST behavior at high d-ethanol fractions. The Flory-Huggins interaction parameters were calculated, and it was concluded that, for D_2O fractions up to a volume fraction of 40%, interactions between polymer and d-ethanol were favored over those between PNIPAM and D_2O or between D_2O and d-ethanol. This nonlinear dependence of interaction parameters on the concentration of ethanol suggests that there should be a competition between D_2O/d-ethanol complex formation and PNIPAM solvation, and this contributes to polymer collapse and results in cononsolvency behavior.

The other polymers, which are different than PNIPAM in molecular structure, also show cononsolvency. For example, Poly(N-vinylcaprolactam) (PVCL) was reported by Kirsh *et al*. to demonstrate bizarre behavior in different alcohol-water mixtures.[131,132] They showed that the LCST of PVCL slightly increases with the addition of methanol up to a volume fraction of methanol of 40% and the addition of ethanol, iso- or n-propanol, or tert-propanol lowers the cloud point up to 10–20 mol% of the alcohols, while it increases with the further addition of these alcohols. The cloud point for this polymer increases up to 80 ^{o}C at higher mole fractions of ethanol, iso- or n-propanol, or tert-propanol. In another study, the cononsolvency behavior was investigated on various poly(2-oxazoline) polymers by Pooch *et al.*[133]

The authors found that the cloud point of poly(n-propyl-2-oxazoline) (PnPOx) is depressed as the methanol content reaches to 35 vol%. However, this behavior is not observed for poly(2-isopropyl-2-oxazoline) (PiPOx) or poly(2-cyclopropyl-2-oxazoline) (PcyPOx). The Cloud point determination is made by calorimetric measurements, and thermograms were recorded for all three polymers. As a result of the comparison of these thermograms, it was concluded that the rotational freedom of the side groups is important for determining the occurrence of cononsolvency by changing the entropy/enthalpy compensation.

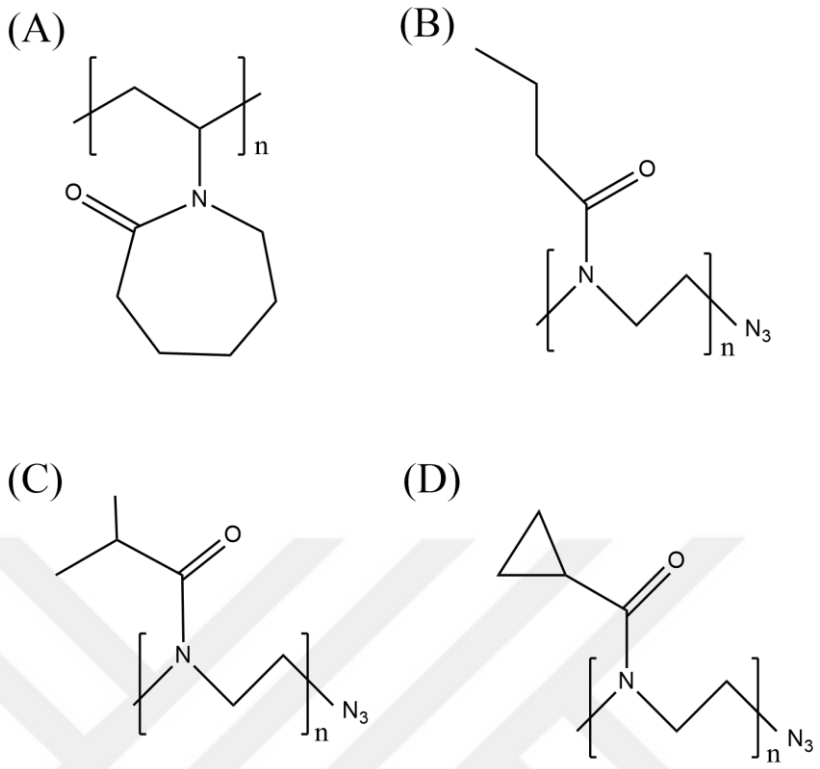

Figure 8: The structure of different polymers that were used for the investigation of cononsolvency behavior. (A) The structure of poly(N-vinylcaprolactam) (PVCL), which exhibits cononsolvency behavior in the presence of methanol, ethanol, iso- or n-propanol, or tert-propanol. Adapted from references 128, 129. (B) The molecular structure of poly(n-propyl-2-oxazoline) (PnPOx), which exhibits cononsolvency behavior in methanol-water mixtures. Adapted from reference 130. (C) and (D) The structures of poly(2-isopropyl-2-oxazoline) (PiPOx) or poly(2-cyclopropyl-2-oxazoline) (PcyPOx), which do not exhibit the cononsolvency behavior even though the structures are very similar to the structure of (B). Adapted from reference 130.

The molecular structures of the polymers are independent of the cause of this phenomenon since the structurally similar polymers do not exhibit the same behavior. Even though there are lots of different studies that contain different types of polymers and different solvent-cosolvent systems, the experimental studies are too short to elucidate the underlying mechanism of cononsolvency behavior. For this reason,

theoretical calculations and simulation studies are also utilized for understanding this mechanism.

1.2.3 Theoretical and Simulation Findings on Cononsolvency

Besides the experimental findings mentioned above, the theoretical findings and simulation studies hold great importance in understanding the reason why the cononsolvency phenomenon occurs. In one of the earliest theoretical studies, it is concluded that the reason for this phenomenon is probably caused by the strong solvent-cosolvent interactions.[134–136] At low cosolvent concentrations, the extent of the polymer's reach to cosolvent is lower because of these strong interactions. As the cosolvent content further increases, the excess amount of cosolvent weakens the solvent-cosolvent interactions, resulting in the resolvation of the polymer by these cosolvent molecules, instead of interacting with the main solvent.

In addition to this solution-theory-based opinion, another study suggests that the cononsolvency behavior is governed by the water-cosolvent mixing thermodynamic properties.[137] Bischofberger *et al.* suggest that the addition of small amounts of amphiphiles, alcohols in this case, lowers the energy of bulk water, making hydrophobic hydration less favorable. For amphiphilic polymers like PNIPAM, hydrophobic hydration ceases to be the key factor, and the coil-to-globule transition is more likely to occur. Since this scenario arises due to the thermodynamics between the water and the cosolvent, this mechanism is independent of polymer-specific factors, such as chain length or concentration.

These types of theory-dependent findings are both valuable and insufficient for considering the importance of interactions between solutes and solvent/cosolvent systems. To further understand the effect of polymer conformation on their interactions with the cosolvent, Heyda *et al*. performed coarse-grained MD simulation of a system containing a homopolymer chain including solvent effects in the polymer-polymer pair interaction potential, and also including explicit cosolvent effects.[138] The authors observed that there are three main interaction regimes corresponding to weak, intermediate, and strong interactions. Weak polymer-cosolvent interactions cause the cosolvent molecules to deplete from the hydration shell of the macromolecule and cause the polymer to collapse. This depletion is also the consequence of the strong cosolvent interaction. On the other hand, in the intermediate polymer-cosolvent interaction regime, the attraction drives the polymer swelling and the adsorption of the cosolvent. These two behaviors agree with the classical mechanism that suggests that the cosolvent depletion causes the polymer collapse and the cosolvent adsorption causes the polymer swelling. However, in the strong polymer-cosolvent interaction regime, cosolvent is preferentially adsorbed on the polymer and leads to the polymer collapsing. In this regime, the collapse is driven by the bridging type of interactions between the monomer-cosolvent molecules, binding the distant monomer units together.

Another MD study by Dalgicdir *et al.,* computational calorimetric measurement shows that the cononsolvency of PNIPAM in water-methanol mixtures is mainly governed by the hydration of the polymer.[139] Methanol is included in the hydration shell of the polymer and disrupts the formation of H-bonds between the NH moiety of PNIPAM and water. The cosolvent molecules pay the hydration energy

penalty for the polymer and lower the hydration shell of the macromolecule and cause the polymer to collapse.

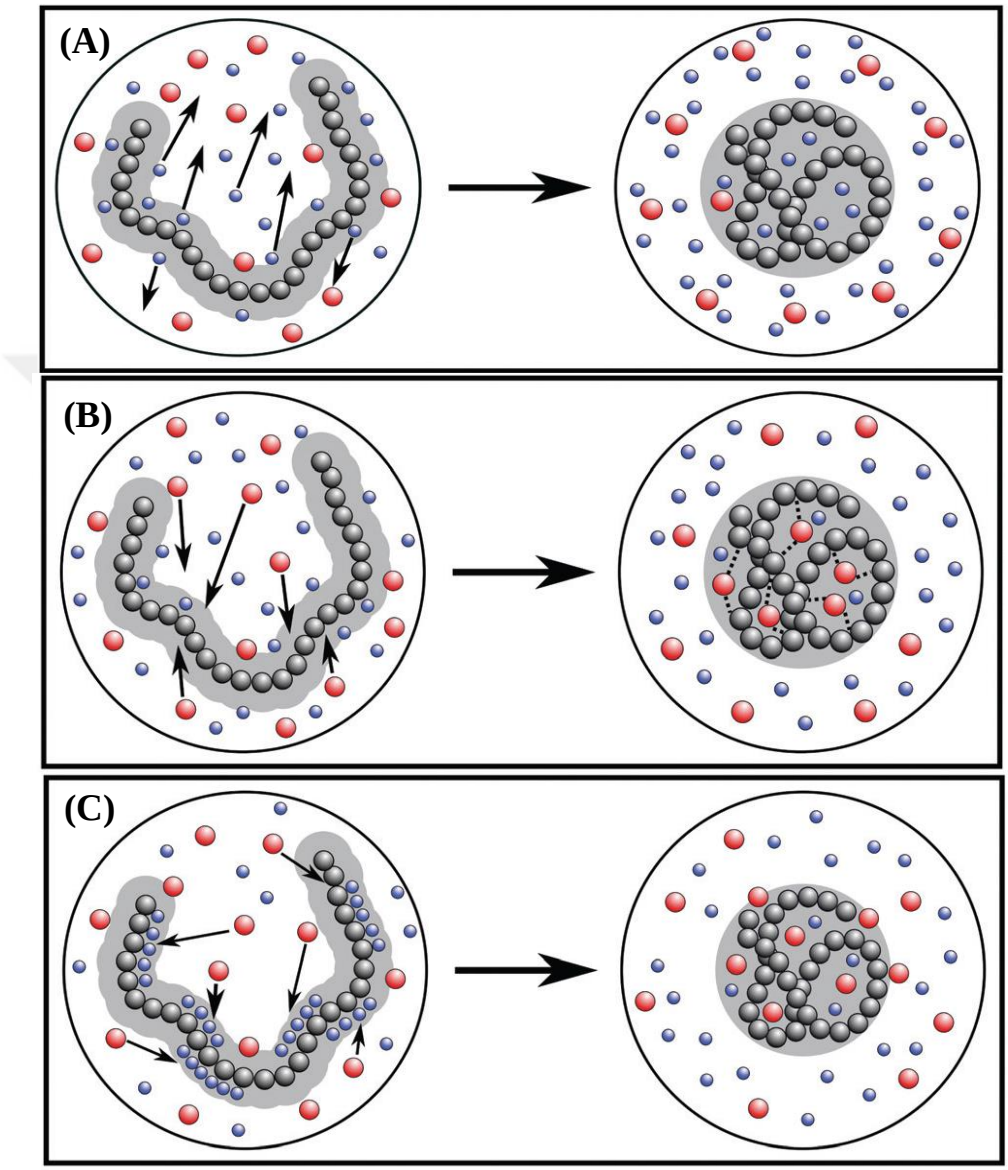

Figure 9: The proposed mechanisms as the results of theoretical and simulation studies explained above. (A) The strong solvent-cosolvent interaction causes the polymer to collapse, as explained in reference 131. (B) Enthalpic bridging mechanism, as explained in reference 134. (C) Geometric frustration caused by the preferential adsorption of the cosolvent, as explained in reference 135. The overall figure is adapted from reference 133.

In addition to these generalized proposed mechanisms mostly related to PNIPAM, there is also a bizarre behavior that is not universal for all the macromolecules, even though they are similar in molecular structure. For example, the addition of urea, which is an important osmolyte commonly found in living organisms, causes a solubility increase in poly (*N*-isopropylacrylamide) (PNIPAM), while it causes a decrease in the solubility of poly (*N*, *N*-diethylacrylamide) (PDEA) even though they have similar molecular structures.[140] Van der Vegt and his coworkers performed molecular dynamics simulations of 40-mer PNIPAM and PDEA chains in water and in aqueous urea solutions, and these simulations showed that urea collapses PNIPAM's secondary amide side chains but unfolds PDEA's tertiary amide side chains. These effects are dependent on the urea's preferential inclusion in the hydration shell of the polymer; however, the mechanism differs from polymer to polymer. For PNIPAM's collapse, the mechanism is entropically driven for the urea content lower than 4M; and for the higher concentrations, the collapsed state is stabilized by bivalent hydrogen bonding with urea. On the other hand, the unfolding of PDEA is governed by favorable water entropy gain since urea screens the large nonpolar interfaces and reduces the hydrophobic effects. These findings showed that the cononsolvency type of behavior is not only governed by the bulk properties such as solvent-cosolvent interactions, but it might be polymer-specific in some cases. These differences come from the difference in side-chain chemistry and the change in the "solvent-accessible surface area (SASA)". Since the PDEA has a larger SASA, it can interact with either solvent or cosolvent, and this leads to unfolding.

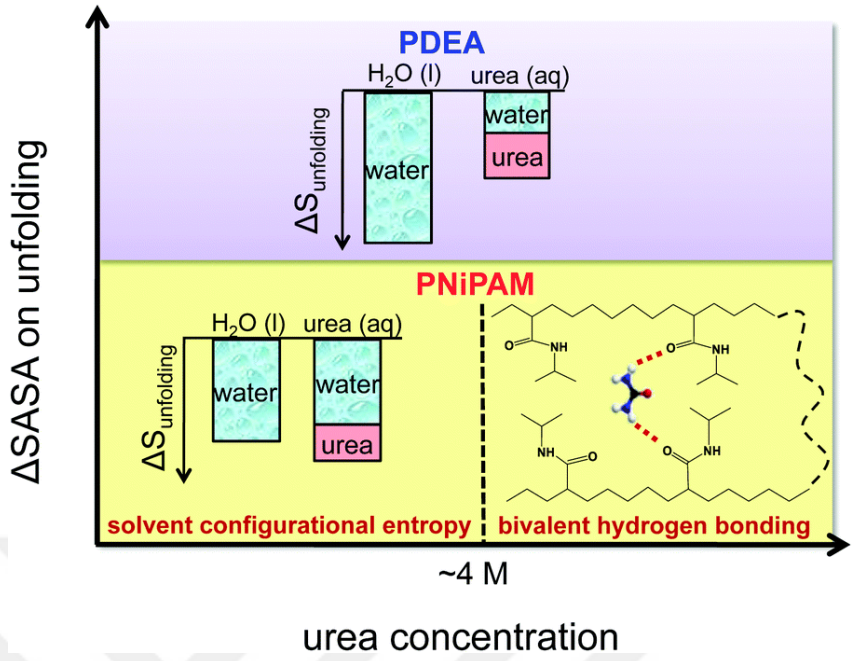

Figure 10: The proposed mechanisms for PNIPAM and PDEA in aqueous urea solutions. Image is from reference 136.

1.3 Beyond Amide-Based Macromolecules: Polysaccharides

Biological macromolecules are important for both living organisms and for other applications, such as tissue engineering.[2–6] Since the amide-based macromolecules are good mimic systems for proteins and most of them are thermoresponsive, for this type of application, the most used model systems are amide-based macromolecules, which are widely mentioned in previous sections. The most well-known ones are poly (*N*-isopropylacrylamide) (PNIPAM) and poly (*N*, *N*-diethylacrylamide) (PDEA) (see Figure 2 for the molecular structures). However, proteins are not the only important biological macromolecules for living organisms; sugar-based macromolecules are also important for living systems. The sugar-based macromolecules are mainly referred to as "glycans" and "polysaccharides," and they are found in different forms, such as glycoproteins or glycolipids.[141] These molecules

consist of O-glycosidic linkages of monosaccharides and have various roles in living cells. For example, cellulose and starch are the most widely found polysaccharides in the membrane of a plant cell wall.[142] In animals, glycogen is used as a primary storage polysaccharide in the liver and muscles.[143] Glycosaminoglycans such as hyaluronic acid, chondroitin sulfate, and heparin are used in connective tissue, cartilage, extracellular matrix, and blood vessels, and glycoproteins and glycolipids are located on cell membranes, used for signaling and recognition.[144–148]

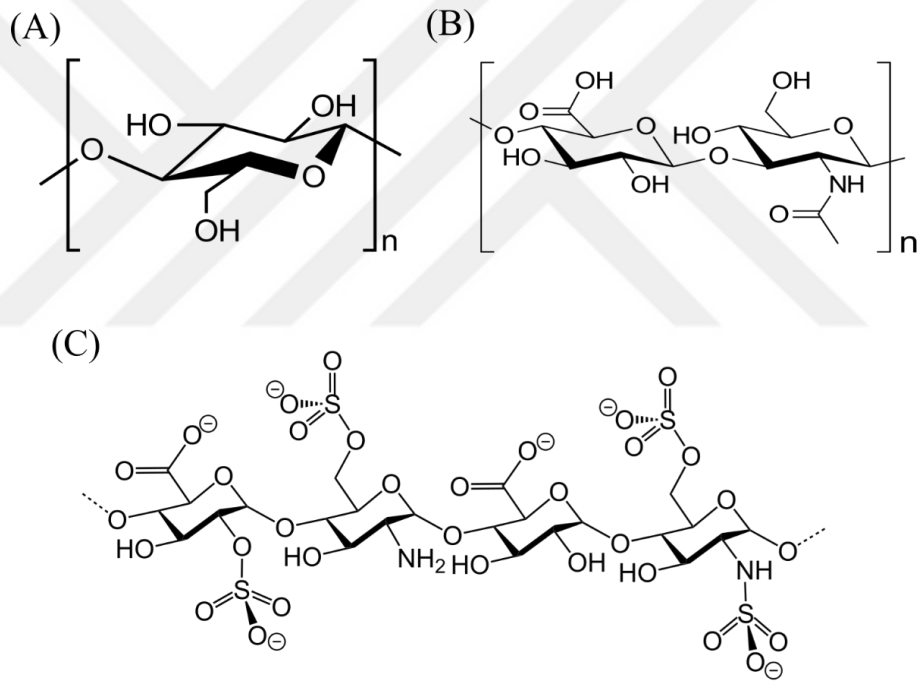

Figure 11: The molecular structures of the most commonly found polysaccharides in living organisms. (A) The structure of cellulose, (B) The structure of hyaluronic acid, and (C) The structure of heparin

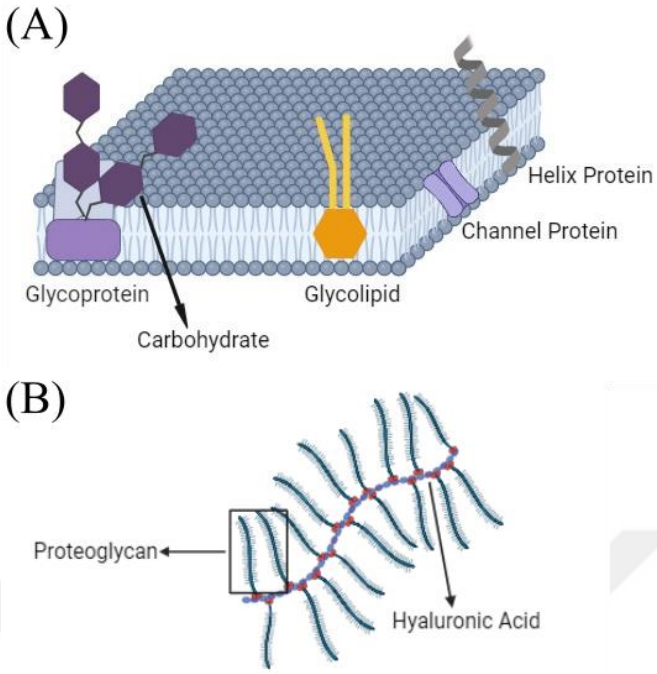

Figure 12: The representation of (A) the cell membrane and the polysaccharides located on it. (B) The structure of the proteoglycan complexed with hyaluronic acid, which is a component of the cartilage extracellular matrix and important for tissue functioning, is adapted from reference 145.

Besides these structural functions and important roles in living organisms, the polysaccharides are also used for other applications in science and technology, such as drug delivery, tissue engineering, gene delivery, and therapeutic purposes.[149–155] For example, Zhao *et al.* developed a biocompatible self-healing polysaccharide hydrogel for an injectable drug carrier for the delivery targeting for neural stem cells.[152] N-carboxyethyl chitosan (CEC) and oxidized sodium alginate are used as the backbone of the hydrogel. Herein, we developed a biocompatible self-healing polysaccharide-based hydrogel system as a novel injectable carrier for the delivery of neural stem cells. N-carboxyethyl chitosan (CEC) and oxidized sodium alginate (OSA) are the main backbones of the hydrogel networks, denoted as CEC-l-OSA hydrogel ("l"

means “linked-by”). This hydrogel has the same stiffness as the natural brain tissue and promotes the proliferation of neural stem cells. These hydrogels are useful because of their reproducibility, being cost-effective, scalable, and environmentally friendly.

Azzam *et al.* showed that the dextran conjugates can be used for gene delivery purposes.[156] The authors used different chain lengths of dextrans (5-380 kDa) that were oxidized with potassium periodate to form polyaldehydes, and then reacted with spermine via reductive amination. The resulting polycations are found to be water-soluble and form nanoparticles with plasmid DNA. Among almost 50 different types of spermine-dextran conjugates, only conjugates of ~6–8 kDa, with ~2 μmol/mg spermine and 25–30% branching, achieved a high transfection efficiency of 50% for HEK293 cells. Larger conjugates and lower spermine-content variants were found to be inefficient. This work emphasizes the importance of polymer size, branching, and functional group chemistry in designing effective, low-toxicity nonviral vectors.

In addition to the biological functions of sugar-based macromolecules, the energy materials are also a wide application area, such as for developing solid and gel electrolytes, electrodes, and active surfaces for energy harvesting devices.[157] Utilization of native polysaccharides, such as starch, agar, alginate, carrageenan, ulvan, chitin, chitosan, and bacterial cellulose derived from natural sources, such as potatoes, algae, and bacteria in areas such as the food industry or energy systems has been shown. These polysaccharide-based materials are biodegradable, biocompatible, and have low toxicity; they are good alternatives to other conventional materials. The important key parameters in polysaccharides, such as ionic conductivity, capacitance,

stability, and efficiency, have been investigated for compatibility in energy applications.

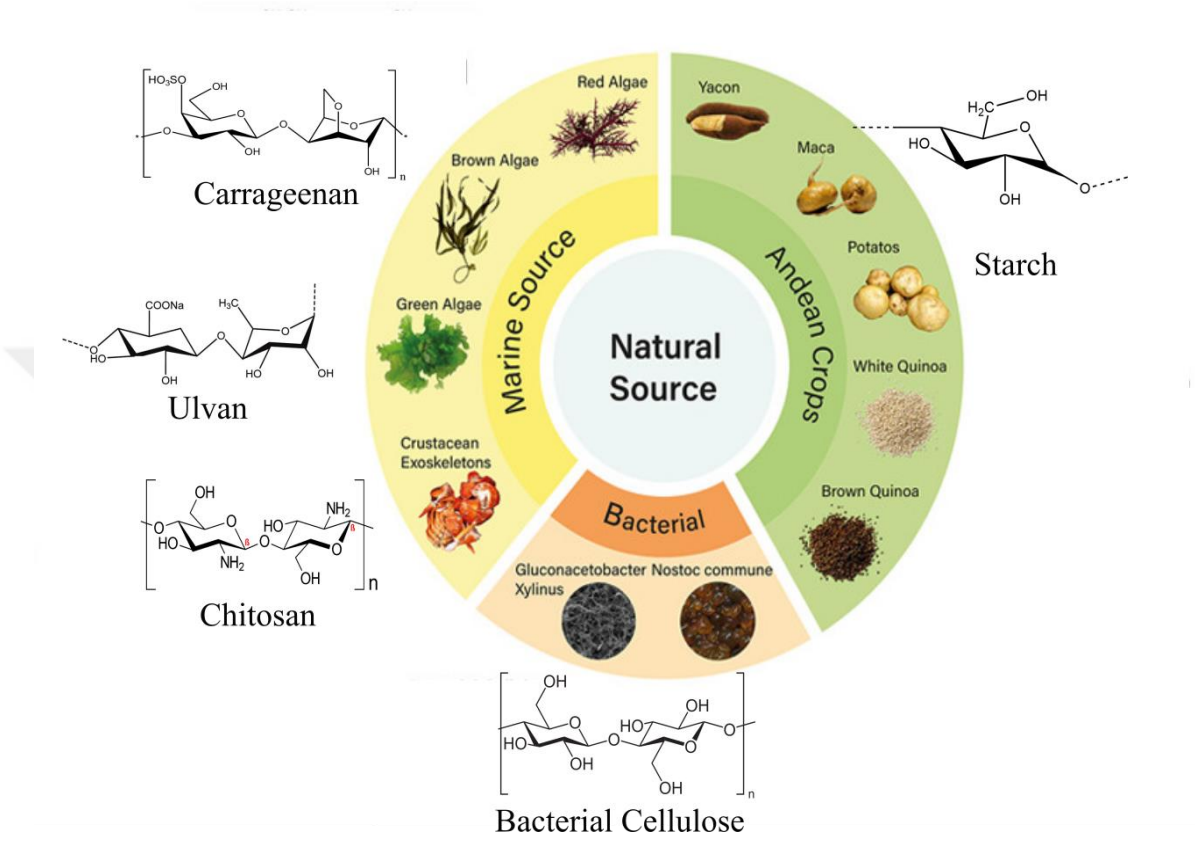

Figure 13: The molecular structures and the sources of native polysaccharides that are used for energy applications, adapted from reference 154.

The role of polysaccharides in both natural biological applications and technological developments make sugar-based macromolecules important and good alternatives to other polymers, such as amide-based ones.

1.4 Motivation and Aim of the Study

Understanding the interactions between the macromolecules and small molecules, such as ions or osmolytes, holds great importance for a variety of fields from fundamental science to industrial applications. While different studies present varying findings and approaches to understanding the interaction mechanisms, generalized mechanisms that apply to all systems remain elusive, and the model systems lack diversity. This work aims to expand our understanding of the interactions between Hofmeister ions and macromolecules and to systematically investigate the underlying mechanism for the cononsolvency phenomenon by utilizing a combination of both thermodynamic and spectroscopic techniques. Sugar-based macromolecules are used as model systems, since their molecular interactions with Hofmeister anions have not been covered in depth. In this regard, methylcellulose (MC), hydroxypropyl cellulose (HPC), and dextran are used for understanding how different sugar-based macromolecules interact with Hofmeister anions and what mechanisms underlie these interactions. Lower critical solution temperature (LCST) measurements and nuclear magnetic resonance (^{1}H-NMR) measurements were performed on these model macromolecules in the presence of Hofmeister anions. In the second part, the cononsolvency phenomenon on both amide-based and sugar-based macromolecules is investigated. Poly(*N*-isopropylacrylamide) (PNIPAM) and Poly(*N*, *N*-diethylacrylamide) (PDEA) were used as the main model systems, since they have similar molecular structures, and they are suitable for comparison. Lower critical solution temperature (LCST), the Attenuated Total Reflectance Fourier transform infrared spectrometer (ATR-FTIR), and Raman Spectroscopy measurements were

performed on the macromolecule-solvent-cosolvent ternary systems and solvent-cosolvent systems as well to show both the bulk properties and the surface properties of macromolecules.

Chapter 2 – Materials and Methods

2.1 Materials

2.1.1 Salts

All salts are purchased from Sigma Aldrich. Sodium thiocyanate (NaSCN) has 99.99+% purity. Sodium perchlorate hydrate ($NaClO_4$), sodium iodide (NaI), sodium nitrate ($NaNO_3$), and sodium chloride (NaCl) have 99.99% purity. Sodium phosphate monobasic ($NaHPO_4$) has 98% purity. Sodium sulphate (Na_2SO_4) has 99.00% purity. Sodium carbonate ($NaCO_3$) has 99.5% purity. The 2,2-dimethyl-2-silapentane-5-sulfonate sodium salt (DSS) (97%).

No further purification was performed before using the salt.

2.1.2 Polymers

Poly(*N*-isopropylacrylamide) (PNIPAM) was purchased from Polymer Source Inc. The average molecular mass of this polymer was reported as 118,500 Da and a polydispersity index (PDI) of 2.16, which was determined with Gel Permeation Chromatography (GPC). Poly(*N, N*-diethylacrylamide) (PDEA) was purchased from Polymer Source Inc. The average molecular mass was reported as 85,500 Da, and the PDI was 1.45. Methylcellulose (MC) was purchased from Sigma Aldrich, whose average molecular mass was later determined by Size Exclusion Chromatography (SEC) as a mixture of around 145 kDa average molecular mass with PDI of 1.2. (See Appendix A) Hydroxypropyl cellulose (HPC) was purchased from Sigma Aldrich with an average molecular mass of 10,000 Da. Two different dextran polymers were utilized: 70,000 Da and 6,000 Da. Both dextrans were purchased from Sigma Aldrich

with average molecular masses reported by the brand. Poly (Propylene Glycol) was purchased from Thermo Fisher with a reported weight average molecular weight of 4,000 Da. Polyethylene glycol is purchased from Sigma with a reported average molecular mass of 6,000 Da.

All polymer samples except the Methylcellulose samples used in Nuclear Magnetic Resonance measurements were lyophilized before usage according to the procedure explained in section 2.2.1.

2.2 Methods

2.2.1 Lyophilization and Preparation of Polymer Samples

To prepare the polymer samples, the solid polymers were weighed to the required mass in a volumetric flask filled with deionized water, then brought up to the target solution volume and homogenized using a vortex mixer. Stock solutions were kept for a day in the refrigerator before further application to ensure complete solubility. After a day of waiting, according to the required polymer mass after lyophilization, small portions of the stock solutions were put into 2 mL Eppendorf tubes by utilizing micropipettes. Tubes were enclosed by punctured caps to enable evaporation.

The tubes were frozen in liquid nitrogen and placed in a desiccator, which is connected to a vacuum pump, and samples were exposed to a vacuum condition overnight for complete dryness (see Figure 14 for the setup). The desiccator is sealed with vacuum grease, put on the lid, and the chamber. For further preparations, the dried

samples were dissolved again in the relevant solution in Eppendorf tubes and homogenized again with the help of a vortex mixer.

Figure 14: The setup for lyophilization. The desiccator (left) and vacuum pump (right) are seen in the figure, and there are linkages between them.

2.2.2 LCST Measurements

Lower Critical Solution Temperature (LCST) measurements were performed using the OptiMelt MPA100 instrument. This device simultaneously heats the sample and records the light scattering intensity using camera images (see Figure 15 for the setup). Samples in solution form, which were prepared as explained in the section above, were put into three different capillary tubes and could be measured three times at once. Recorded data is shown on the software of the device, MeltView 2.0.7 (Figure

16 for the screenshots from the software). The heating rate was 5 °C per minute for MC and HPC containing samples, and 1°C per minute for PNIPAM, PDEA, and PPG containing samples, since the phase transition temperature was not exhibited for MC and HPC in the slower heating rate.

Figure 15: OptiMelt instrument placed in the refrigerator.

Lower critical solution temperature, also referred to as “phase transition temperature”, is the temperature at which polymers aggregate suddenly and resulted in the formation of a cloudy solution with increasing temperature. At the exact point where the polymer solution becomes turbid, the light scattering intensity increases significantly, causing a sharp increase in the light scattering intensity vs. temperature graph. The onset point of this graph gives the LCST for that sample (see Figure 16 and 17 for the example and data processing). After exporting the data from MeltView software, further analysis was performed using OriginLab 2024.

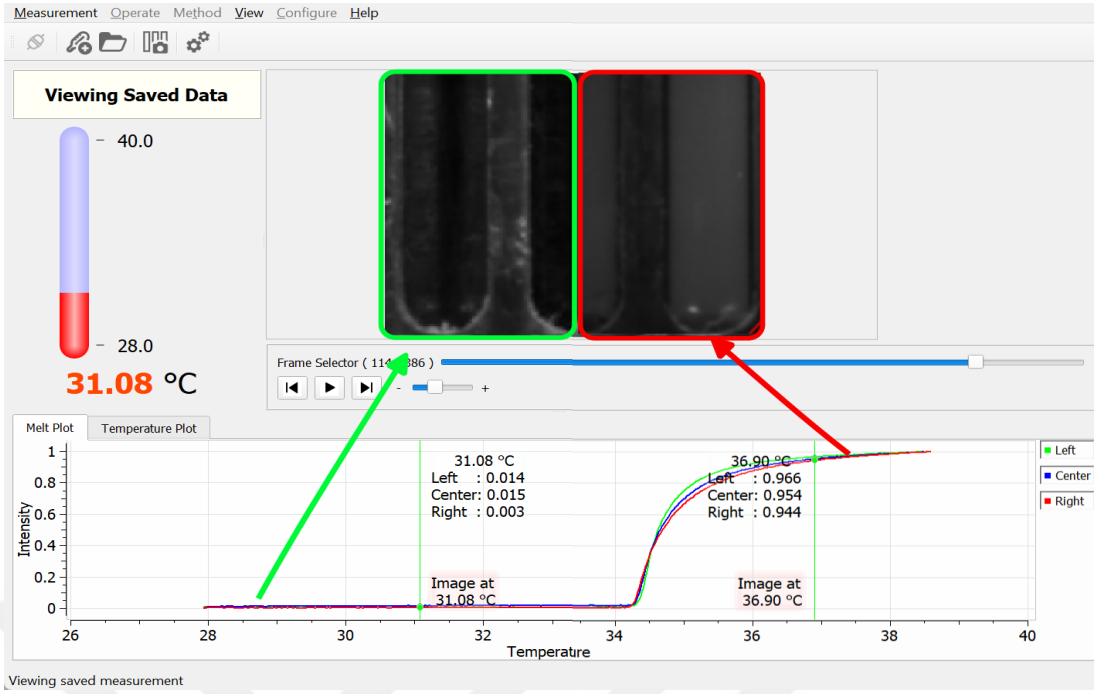

Figure 16: Screenshot from MeltView software containing a record for light scattering intensity vs. temperature graph for the below (inside the green box) and above LCST (inside the red box).

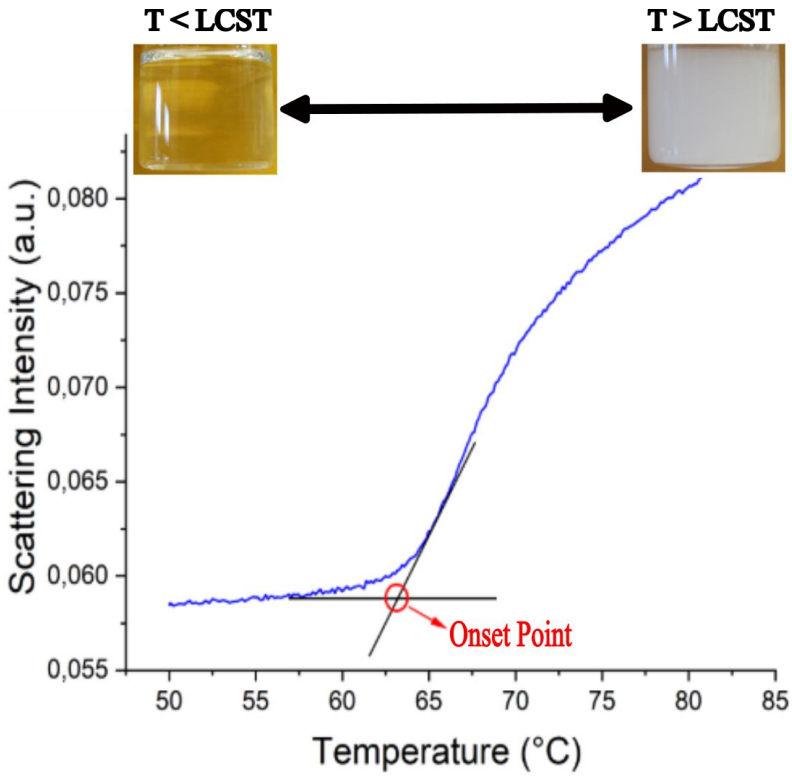

Figure 17: Representative graph of light scattering intensity vs temperature with the image of the sample polymer below (T < LCST) and above (T > LCST) phase transition temperature. As the temperature increases, inter- and intra-molecular interactions of the polymer increase, causing it to aggregate and result in a cloudy, turbid solution. This increasing trend generally shows a sharper increasing point for the amide-based macromolecule samples, such as PNIPAM. However, it shows a less sharp increase at the onset point, probably because of the high viscosity of the MC, but it is still sharp enough to assign the point where the light scattering intensity increases the most.

2.2.3 ATR-FTIR Spectroscopy Measurements

The Attenuated Total Reflectance Fourier transform infrared spectrometer (ATR-FTIR) used for conducting the ATR-FTIR measurements is a Bruker ALPHA FTIR spectrometer, equipped with a Platinum ATR module. The crystal of this device is a monoclinic diamond, and the source is blackbody radiation. For the measurements

that are not performed at room temperature, a water circulator, which can either decrease or increase the temperature of the sample, was utilized (see Figure 18 a). The tubing of the calculator was connected to a custom-made metal headpiece, which is located on the ATR plate, enabling tuning of the required temperature. This headpiece is fixed on the ATR plate during the measurement with the help of a rotatable arm, and a cap is put on the sample for minimal air exposure to the sample (see Figure 18 b for the setup). This setup makes it possible to conduct measurements both below and above the phase transition temperatures.

ATR spectra were obtained from a 50 µL sample with 4 cm^{-1} resolution in the range of 400 - 4000 cm^{-1} and 512 scans. Before all measurements, background spectrum measurements were obtained, and all spectra were ATR corrected by the instrumental software OPUS 7.2, but all further analysis and processing of spectra were performed in OriginLab 2024. Hydration spectra analysis was performed with the MCR algorithm macro embedded in Igor Pro(WaveMetrics), as explained in more detail in Chapter 3.2.

The ATR-FTIR measurements not used for hydration shell analysis yielded spectra from a 50 µL sample, with a 2 cm^{-1} resolution in the 400-4000 cm^{-1} range, and 32 scans.

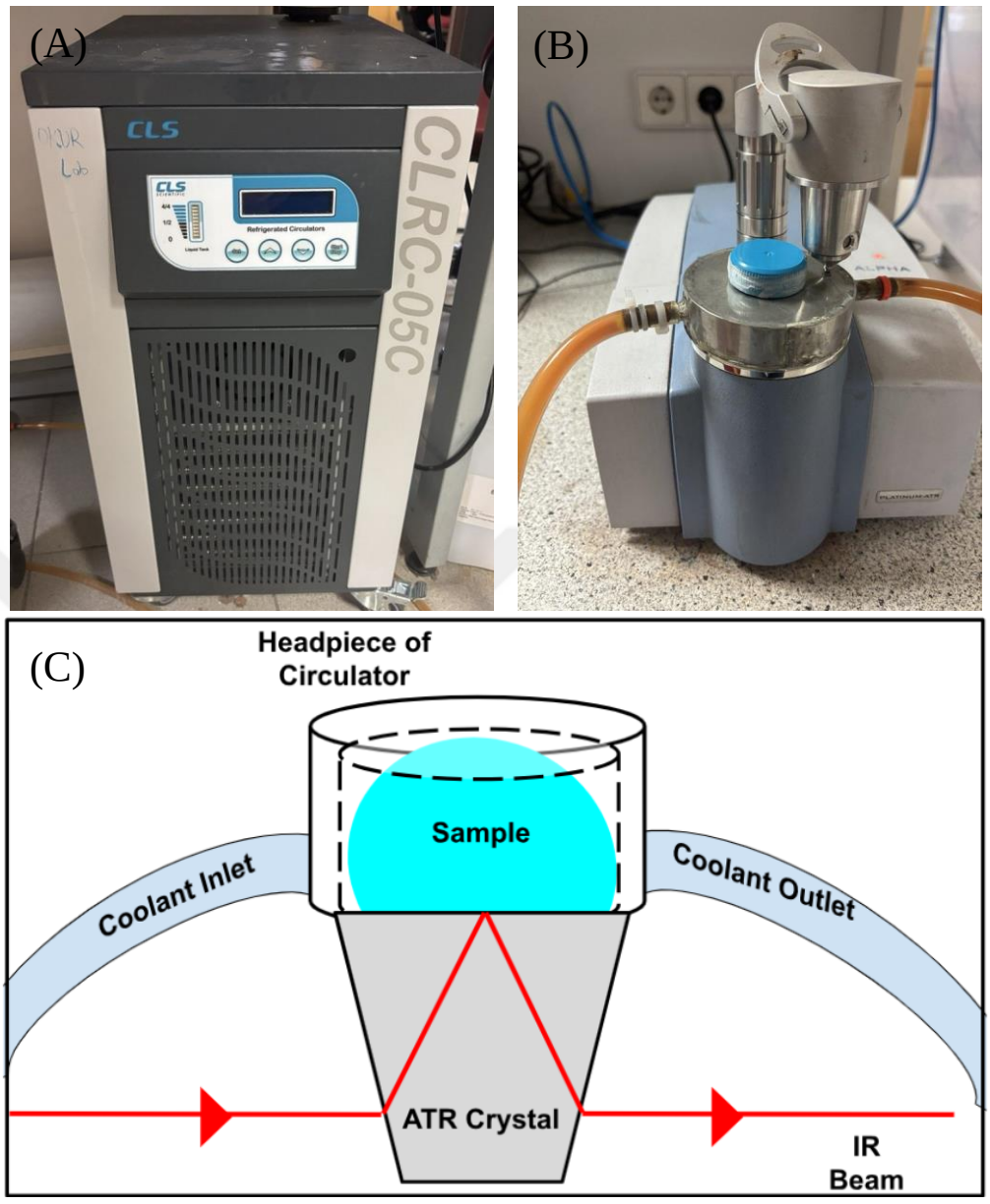

Figure 18: (A) Water circulation bath used for heating or cooling the samples during the measurements, (B) ATR-FTIR Spectrometer and the measurement setup containing water circulation headpiece fixed on the ATR plate with a cap closed over it, (C) Illustration of temperature-controlled ATR-FTIR measurement setup. The inlet and outlet enable the circulated water to flow through the metal headpiece.

2.2.4 ^{1}H-NMR Spectroscopy Measurements

Proton Nuclear Magnetic Resonance Spectroscopy measurements were performed using an Agilent Premium Compact 600 MHz spectrometer at room temperature. The external magnetic field of the instrument is 14.1 T. The free induction decay (FID) is 1.703 milliseconds, and the light application time is 3.9 microseconds. All the samples were lyophilized in the way explained in section 2.1.1 and then prepared using D_2O as the solvent.

SP Wilmad-LabGlass 5 mm thin-walled precision 7″ NMR tubes were used for holding the sample. An additional external chemical shift referencing, which contains 2,2-dimethyl-2-silapentane-5-sulfonate sodium salt (DSS) in D_2O solvent. This reference tube is always placed in the main sample tube during the measurements (shown in Figure 19). This method enables both the samples and the reference solution to be measured simultaneously without being in contact.

NMR spectra were obtained using 32 scans, and standard procedures, such as solvent locking and shimming, were performed automatically with the instrument's software, OpenVnmrJ. Data processing was carried out with OpenVnmrJ software from Agilent and MestreNova. After obtaining the spectra from the instrument's software, they are first converted to text files by MestreNova, and further analysis is carried out by using Origin 2025b software. The text files are imported to Origin 2025b, and their reference peaks, which are supposed to be placed at 0 ppm, are corrected by simple addition or subtraction to the X-axis values of the spectra. After this correction, the peak positions are determined. For this determination, a straight

line is placed horizontally on the full-width half-maximum position of the peaks, and the average value of the two intersection points is determined, and this value is used as the “peak position”.

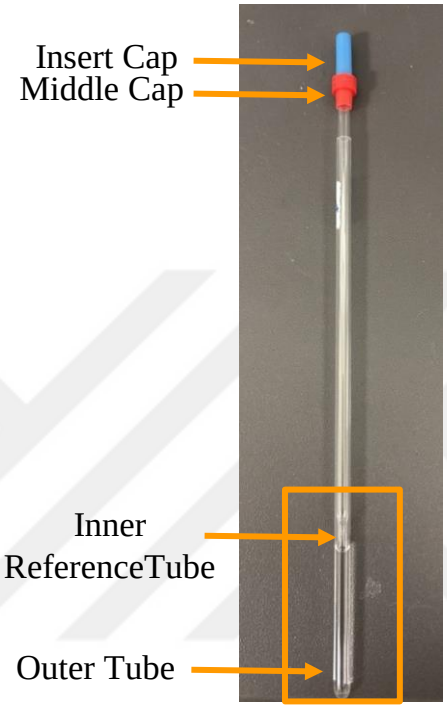

Figure 19: Outer NMR tube containing sample to be measured and the coaxial reference tube inside it. The volume of the sample is around 500 µL, and the volume of the inner reference is 60 µL.

2.2.5 Raman Spectroscopy Measurements

Raman spectra were obtained with a Jobin Yvon Horiba Raman System with an Andor charge-coupled device (CCD) camera (see Figure 20A). Using a Low-Noise Continuous Wave (CW) Diode-Pumped Solid-State (DPSS) Laser (Ventus 532) at 532 nm at 50 mW with 10 % attenuation as the excitation laser source, is employed by the Raman spectrometer (see Figure 20 B). The camera runs by a < 0.01

electron/pixel/second dark current response by thermo-electrically cooling the detector, which is set to -69 ºC. 12.5 x 12.5 x 45 mm Quartz spectrometer cuvettes were used for samples, and they were placed under the laser. The laser light was directed to the sample and collected with a 10x focus (see Figure 20 C). The collected light was directed to a 600 g/mm grating and finally measured by a 1024 x 256-pixel CCD camera. Unless specified otherwise, spectra were obtained using 150 scans with 2 seconds, resulting in a 5-minute integration time. All the measurements were performed at ambient temperatures.

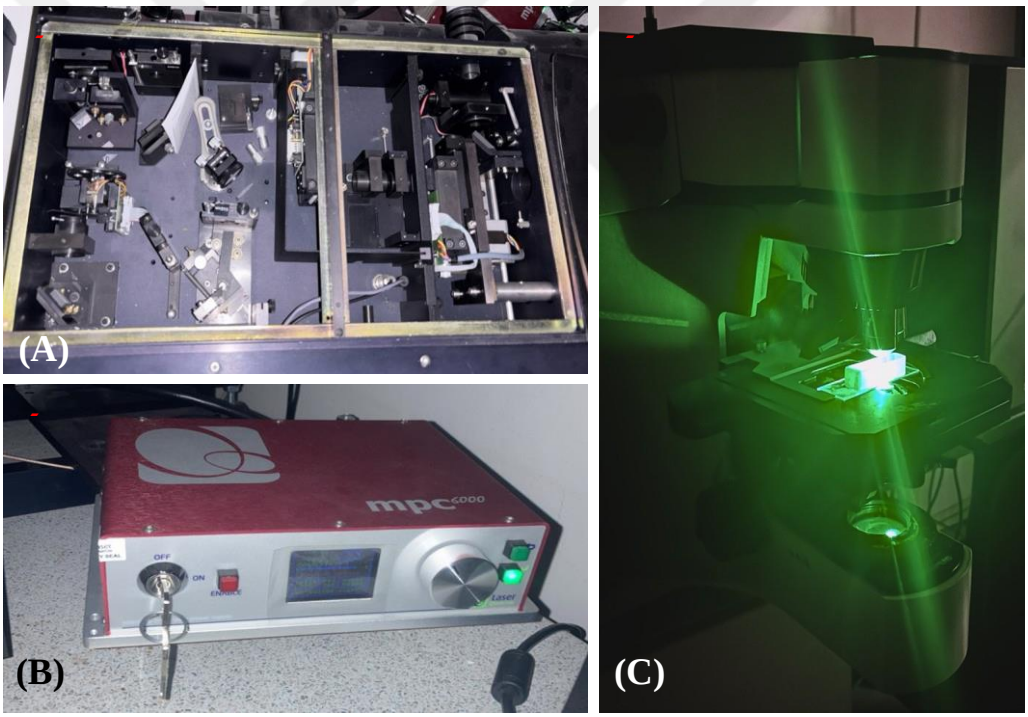

Figure 20: Setup for the Raman Spectroscopy measurements, (A) Compartments of the spectrometer, (B) The Diode-Pumped Solid-State (DPSS) Laser utilized by the spectrometer, (C) The focused green light on the sample, which is in the quartz cuvette

Data processing was performed using LabSpec software, and for further analysis, OriginLab 2024 and Igor Pro software (WaveMetrics) were used. Hydration

spectra analysis was performed with the Multivariate Curve Resolution (MCR) algorithm macro embedded in Igor Pro (WaveMetrics), as explained in more detail in Section 3.2.

Chapter 3 – Results

3.1 Interactions of Hofmeister Anions with Sugar-Based Macromolecules

The interaction of macromolecules with ions, osmolytes, and other small molecules holds great importance in many different aspects. This kind of interaction can alter the hydration behavior of the macromolecules, which can result in the display of changes in the role of these macromolecules in the systems. One of the most widely investigated interactions is the interaction between Hofmeister ions and amine-based macromolecules, which is a system that resembles proteins in biological systems. Understanding these interactions enables researchers to understand the interactions of proteins and pave the way to develop different applications, such as drug synthesis and drug delivery. Besides the importance of amide-based macromolecules, another class of macromolecules is also widely present in living systems: sugar-based macromolecules. By addressing this in the first part of this chapter, thermodynamic and spectroscopic evidence about how the Hofmeister ions interact with sugar-based macromolecules will be presented.

3.1.1 LCST and ^{1}H-NMR Measurements: Showing the Effects of Salting-in and Salting-out Anions on Methylcellulose and Site-Specific Evidence

As discussed previously in Chapter 1, the thermodynamic evidence of the interactions between Hofmeister ions and the macromolecules holds great importance and is also the motivation of the present chapter. Thermodynamic measurements are the preliminary data that reveal the effect of Hofmeister ions on macromolecules. The

presence of the Hofmeister ions affects the phase transition temperature of the thermoresponsive macromolecules. The increase in the lower critical solution temperature (LCST) with increasing ion concentration means a “salting-in” behavior, while the decrease means “salting-out” behavior.[12,13]

In this study, the molecular system consists of methylcellulose, which is a thermoresponsive and water-soluble derivative of cellulose as the model macromolecule, and the effect of the sodium salts of different Hofmeister anions. Just like cellulose, methylcellulose is composed of glucose units with β-1,4 glycosidic linkages and additional side-groups, methyl.

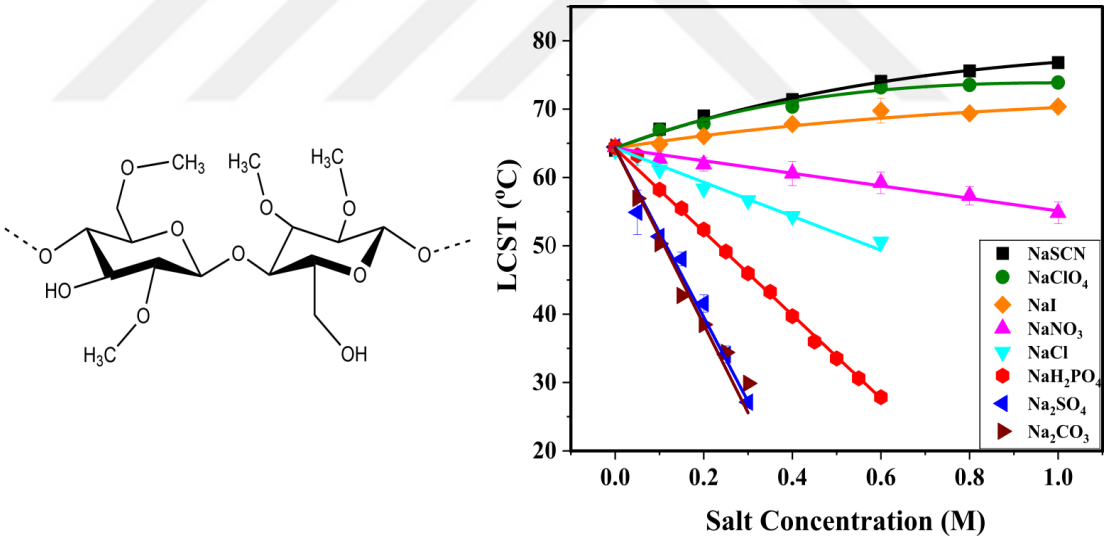

Figure 21: (Left) The molecular structure of Methylcellulose (MC) and (Right) the fitted curves for the lower critical solution temperature of MC as a function of sodium salts of eight different Hofmeister anions. Error bars indicate the standard deviation of the data for at least 3 replicates for each measurement.

Figure 21 shows the LCST measurements of a 5mg/mL MC sample, prepared as explained in Section 2.1.1, and dissolved in salt solutions of the salts indicated in

the graph. The LCST of MC in the absence of any salt is measured as 63.3 ± 0.4 °C. For all the samples in the presence of different salt concentrations, the LCST value was measured and recorded to show the trend with the increasing concentration. The data were fitted according to an empirical formula, which is widely used in the literature, as explained in Chapter 1. This formula contains both a linear and a nonlinear term. Both terms are used to fit the nonlinear salting-in type of graph, which involves a saturable anion binding at a particular concentration of weakly hydrated anions.

$$T = T_0 + c[M] + \frac{B_{max}.[M]}{[M] + K_D} \qquad (1)$$

In this formula, [M] is the molar salt concentration. c is the linear coefficient with units °C/M. The B_{max} and K_D refer to the maximum change in the phase transition temperature and the dissociation constant of the ion.

The LCST of MC nonlinearly increases as the salt concentration of salting-in ions, namely NaSCN, $NaClO_4$, NaI, and $NaNO_3$, increases (see the curves indicated with black squares, green circles, orange squares, and magenta triangles). This nonlinear trend is correlated to a saturable type of binding behavior, which indicates that there is a direct interaction between the macromolecule and the ion. In contrast, the LCST is decreasing as the salting-out ions, namely, NaCl, NaH_2PO_4, Na_2SO_4 and Na_2CO_3, increase. This linear decrease is evidence that there is no direct specific interaction between the macromolecule and the ion. As a result of this graph, the given Hofmeister anions act on the MC as expected and cause similar trends in the LCST values to the amide-based macromolecules scenario.[4]

Salt	Concentration Range	c (K.M^{-1})	K_D (M)	B_{max} (K)
NaSCN	0 - 1.0 M	-4.30	0.40	8.74
$NaClO_4$	0 - 1.0 M	-1.00	0.49	65.04
NaI	0 - 1.0 M	-2.50	0.58	5.90
$NaNO_3$	0 - 1.0 M	13.65	0.80	7.16
NaCl	0 - 0.6 M	-24.90	-	-
NaH_2PO_4	0 - 0.6 M	-61.00	-	-
Na_2SO_4	0 - 0.3 M	-123.50	-	-
Na_2CO_3	0 - 0.3 M	-129.00	-	-

Table 1: Fit values for the parameters c, K_D, and B_{max} according to the empirical fit (Equation 1) for the LCST values of MC solutions with salt content given in the second column. Note that the K_D values are not experimental; they are apparent values resulting from the fit equation. For the last four salts, the fit is linear, and there is no nonlinear term to report.

After showing that the Hofmeister anions cause a similar effect on methylcellulose, which is the model sugar-macromolecule for this research, as they do on amide-based macromolecules, the next step was to determine which part of the macromolecule is responsible for the interaction with the weakly hydrated Hofmeister anions. For site-specific evidence, ^{1}H-NMR measurements were performed. The ^{1}H-NMR technique that was employed in this study has been proven to be used for investigating the interactions between small molecules or ions and macromolecules. [60] In Figure 22, the ^{1}H-NMR spectrum of 5mg/mL MC in neat D_2O is shown with the assigned peak positions, including externally referenced DSS salt in D_2O. The structure of DSS is given in the figure as well.

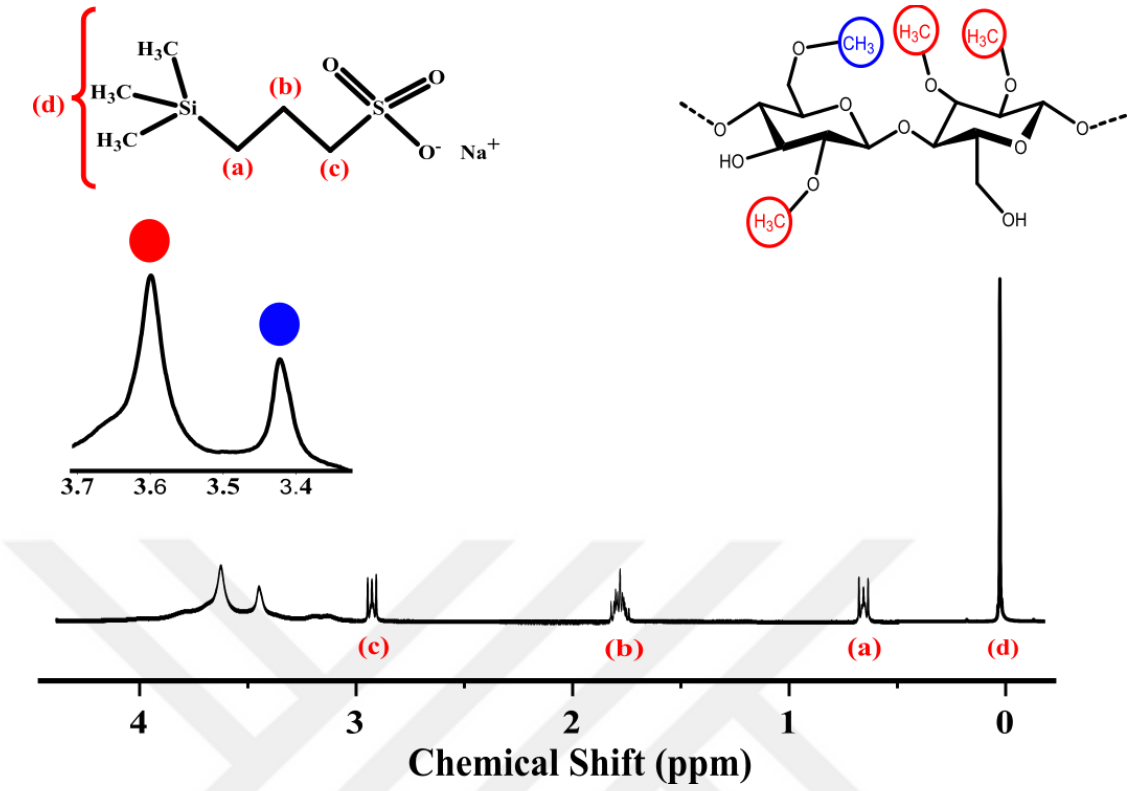

Figure 22: The example spectrum of MC in D_2O. The red and blue circles on the spectrum correspond to two methyl peaks of the side-chains of the MC located in different chemical shifts (ppm). The structure of MC is on the upper right side, and the different methyl groups are indicated in red and blue. The structure of DSS is located on the upper left side of MC, and its peaks are indicated using the letters (a), (b), (c), and (d).

Besides four different peaks coming from DSS hydrogens, there are two distinct and sharp singlet peaks around 3.4 and 3.6 ppm, which correspond to protons of two different methyl peaks of the side-chain of MC. Also, there are some other little peaks located between 3 - 3.4 ppm, which belong to the backbone hydrogens of MC, but they are broadened and have lower intensity because of high intermolecular interactions and the polymer network. The change in the position of these two methyl peaks was analyzed to understand the interactions between the MC and weakly hydrated anions. The change in the position of these peaks was plotted as a function

of concentration, and the trends show that the change in the peak position is a nonlinear behavior in the presence of a weakly hydrated anion, namely SCN^-, and for the strongly hydrated anions such as Cl^- or SO_4^{2-}, the behavior is a monotonic linear decrease.

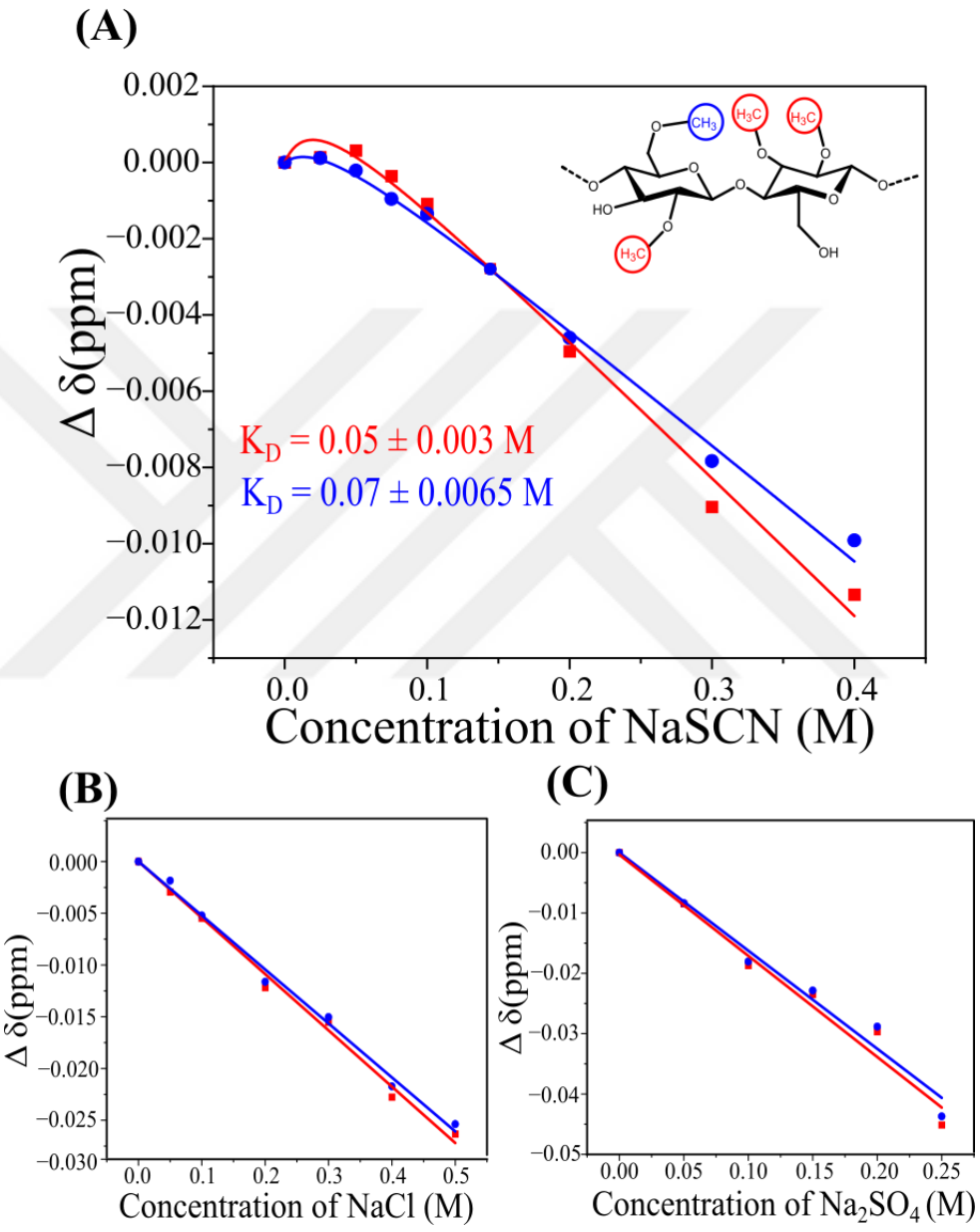

Figure 23: The changes in the ppm values of methyl peaks in the presence of different concentrations of (A) NaSCN, (B) NaCl, and (C) Na_2SO_4. Red and blue curves color color-coded for the two different methyl peaks shown with red and blue in the inset of the figure. The measurements were performed at least 3 times for each data set. The resulting trends are reported to be reproducible.

The data shown in Figure 23 is fitted using an empirical formula from the literature, which resembles equation (1). Again, it contains both a linear and a nonlinear term for modeling two different types of behavior.

$$\Delta\delta_H = c[M] + \frac{\Delta\delta_{max}[M]}{K_D + [M]} \qquad (2)$$

In this formula, again, c is the linear coefficient with units ppm/M, $\Delta\delta_{max}$ is the maximum change in chemical shift, i.e., at saturation, and K_D is the ion-polymer binding dissociation equilibrium constant. For fitting the data that contains NaSCN, both the linear and the nonlinear term of the formula were used, and K_D values were calculated as: 0.05 ± 0.003 M for the more deshielded methyl peak (occurs around 3.6 ppm) and 0.07 ± 0.0065 M for the less deshielded methyl peak (occurs around 3.4 ppm). The reported apparent binding constants are comparable with the ones belong the amide-based cases from the litearature. Since in NMR measurements, the binding of only one site is investigated, and the LCST measurements are more macroscopic and the K_D values for that measurements corresponds to whole macromolecule, the reported K_D values for LCST measurements and NMR measurements are quite different. These NMR measurements resulted in the binding of weakly hydrated anions such as SCN^- to the methyl groups of MC, i.e., the side chain of the macromolecule. The spectroscopic evidence also raises the question: Is the side chain of sugar-based macromolecules the only site for a specific interaction between the weakly hydrated anion and the macromolecule? The results are explained in the next section.

3.1.2 The Lack of Side-Chain Changes the Interactions of Sugar-Based Macromolecules with Hofmeister Anions

After showing that the side methyl group of MC is responsible for the interactions between the MC and weakly hydrated Hofmeister anions, the question arose as to whether another similar polymer without a side group would cause the same interactions. For this purpose, the same ^{1}H-NMR measurements were performed using dextran in the presence of the sodium salts of the Hofmeister anions, NaCl, NaSCN, and Na_2SO_4. Dextran is a branched sugar-based macromolecule composed of glucose units joined together with an α-1,6 glucoside linkage and has additional branches from α-1,3 linkages. It is water-soluble; however, it does not show an LCST behavior and is not thermoresponsive. For this reason, dextran is investigated only via ^{1}H-NMR measurements. The main dextran chemical shifts can be seen in the range of 3.4 -4.1 ppm. The NMR spectrum and assigned chemical shifts can be seen in Figure 24.

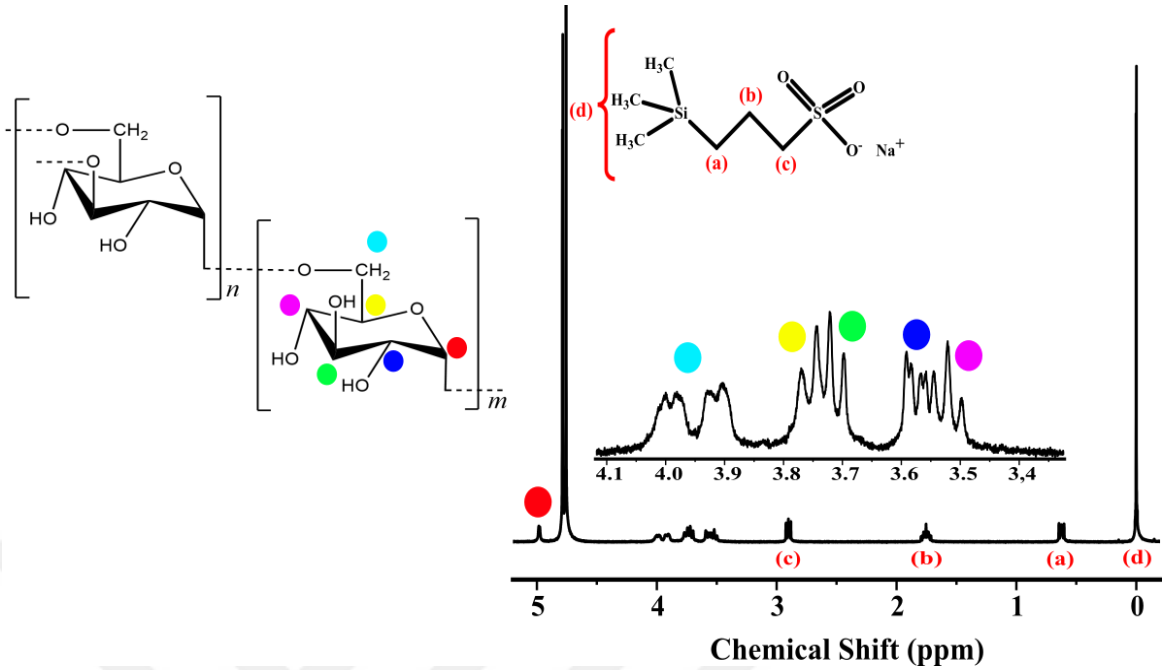

Figure 24: (Left) The structure of dextran, and (Right) the ^{1}H-NMR measurement of dextran in D_2O using DSS as the reference. The colorful dots are used to assign the peaks from different hydrogens of dextran.

The change of the position of all the hydrogen peaks is observed with increasing NaSCN concentration to see if there is a binding of the SCN^- anion to dextran, even though it does not contain a side-chain, see Figure 25.

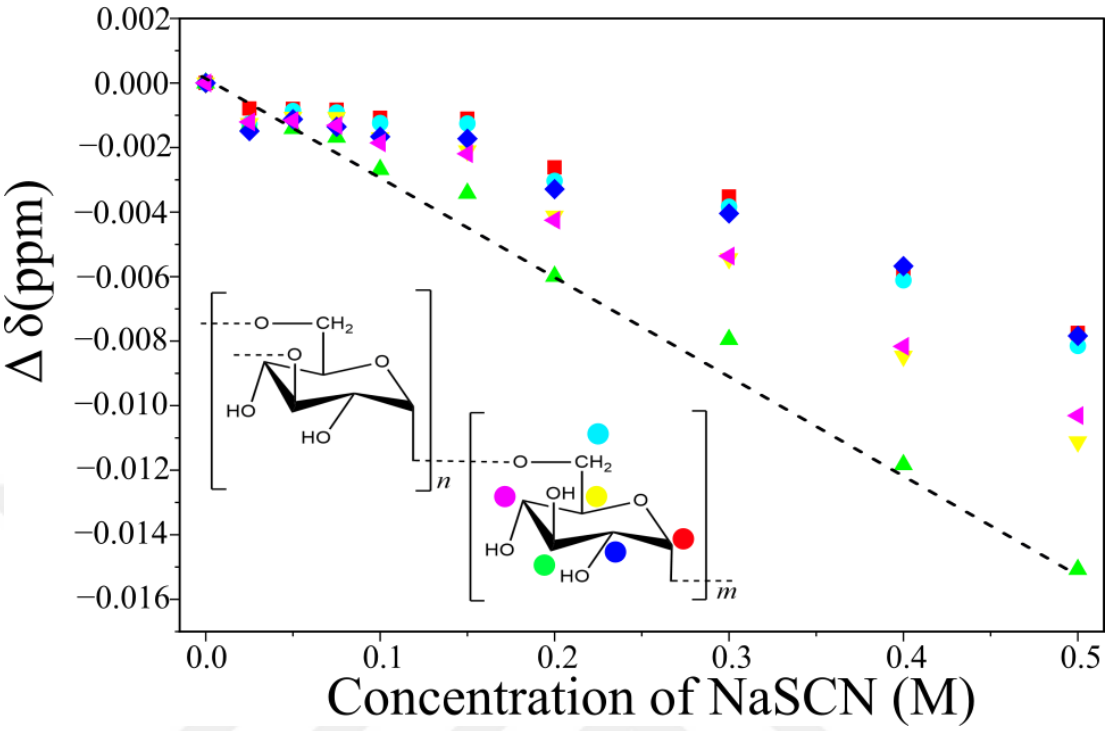

Figure 25: The changes in the peak positions of hydrogen are analyzed. The color-coding matches the different hydrogen peaks shown in the inset of the graph in different colors.

The changes in the peak positions of each hydrogen peak as a function of concentration are clearly nonlinear (The dashed black line is a guide to the eyes as a reference to a linear change in behavior). However, it does not resemble the classical binding-type behavior. Please note that all the corresponding peaks are acting similarly to each other as the concentration of NaSCN increases. This result suggests that there may be a different interaction mechanism between dextran and weakly hydrated Hofmeister anions, which has yet to be deciphered beyond the regular binding type of behavior.

After showing that the increasing NaSCN content causes a nonlinear change in the peak position of the dextran hydrogens, the same measurements and analysis are

performed in the presence of NaCl and Na_2SO_4, see Figure 26. Since it was shown in the previous data that all of the peaks act almost the same, the analysis is performed for only one peak. The peak corresponds to the hydrogen attached to the carbon, which is adjacent to the oxygen in the sugar ring is a relatively sharp singlet; this peak is analyzed for the sake of simplicity. The changes in the peak positions are linear, as expected in the presence of both strongly hydrated anions. The changes in the peak positions are linear, as expected in the presence of both strongly hydrated anions.

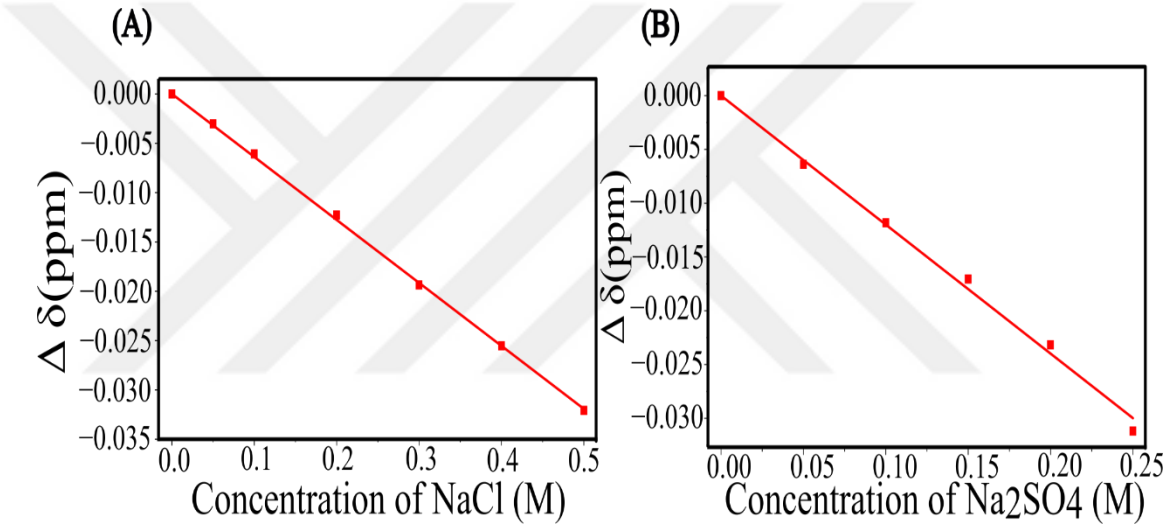

Figure 26: The change in the peak position of the hydrogen corresponds to the hydrogen attached to the carbon, which is adjacent to the oxygen in the sugar ring, as a function of concentrations of (A) NaCl and (B) Na_2SO_4

Up to this point, the findings presented in the previous figures were obtained by utilizing a large dextran polymer, which has a 70,000 Da molecular weight. For obtaining more information on the interaction between the dextran and weakly hydrated Hofmeister anions, additional NMR measurements with a lower molecular weight dextran, 6,000 Da, are also performed. The change in the peak position of the hydrogen corresponds to the hydrogen attached to the carbon, which is adjacent to the

oxygen in the sugar ring, as a function of the concentrations of NaSCN is plotted and fitted, see Figure 27. The data is fitted to a linear fit, and the lower molecular weight polymer showed no evidence of binding, as expected.[62]

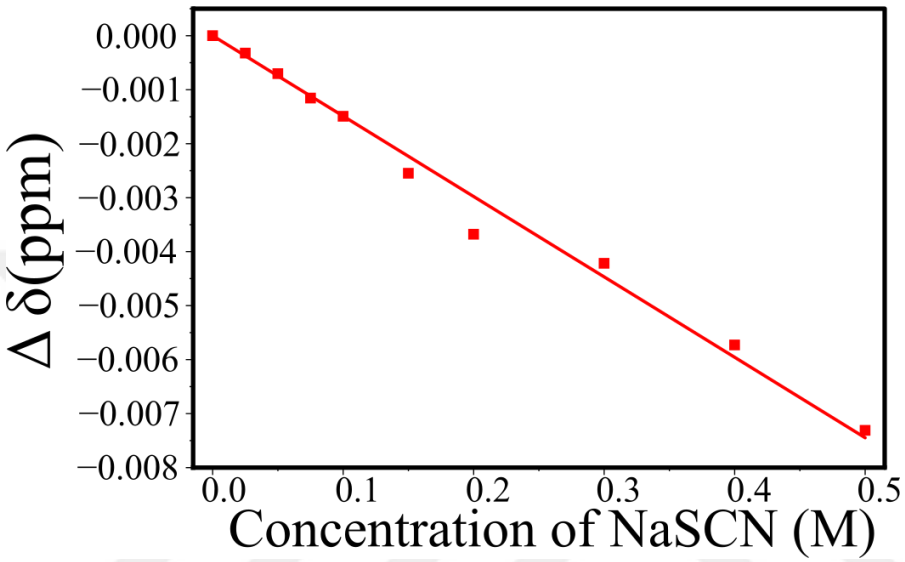

Figure 27: The change in the peak position of hydrogen corresponds to the hydrogen attached to the carbon, which is adjacent to the oxygen in the sugar ring, as a function of concentrations of NaSCN.

3.1.3 Is this effect universal for all sugar-based macromolecules with a side chain?

After showing that the side-chain of MC is responsible for the interactions between the macromolecule and the Hofmeister anions, the question arose whether any other sugar-based macromolecule with a side-chain shows the same type of interaction with the same anions. Another sugar-based macromolecule, which is also a thermoresponsive and water-soluble derivative of cellulose with a hydroxypropyl side-chain, hydroxypropyl cellulose, is used for this investigation. The same LCST measurements were performed with this model macromolecule in the presence of the

sodium salts of SCN^-, I^-, ClO_4^-, NO_3^-, Cl^-, HPO_4^{3-}, SO_4^{2-}, and CO_3^{2-} to see if the weakly hydrated anions can interact with HPC as well as MC.

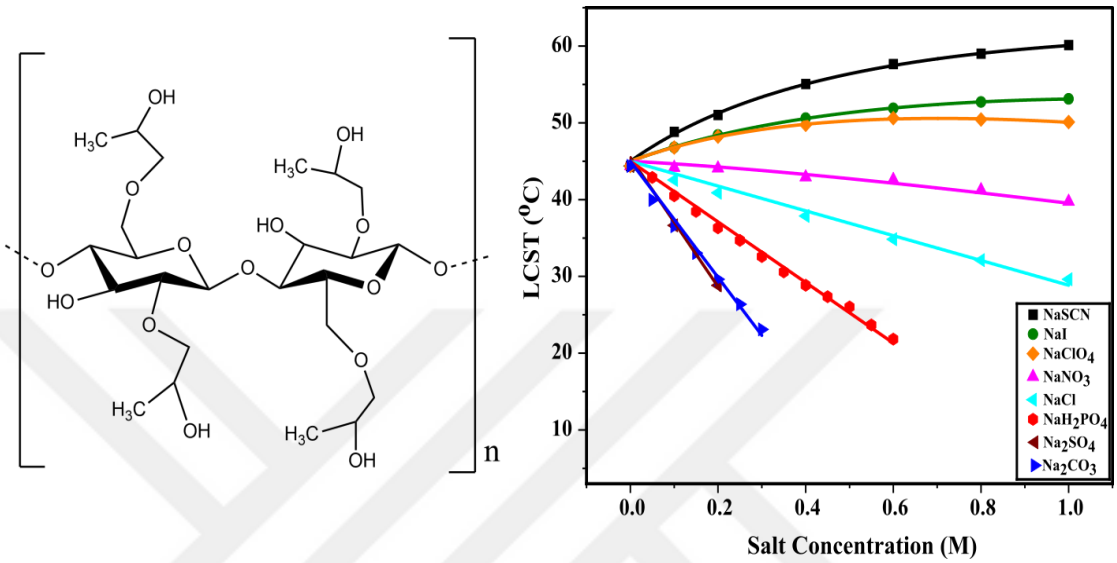

Figure 28: (Left) The molecular structure of Hydroxypropyl cellulose (HPC) and (Right) the fitted curves for the lower critical solution temperature of HPC as a function of sodium salts of eight different Hofmeister anions. Data courtesy of Sobia Farooq obtained from their master's thesis (unpublished), Bilkent University, 2024.

Figure 28 shows the LCST measurements of a 5mg/mL HPC sample, prepared as explained in Section 2.1.1, and dissolved in salt solutions of the salts indicated in the graph. The LCST of HPC in the absence of any salt is measured as 44 ± 0.5 °C. For all the samples in the presence of different salt concentration samples, the LCST value was measured and recorded to show the trend with the increasing concentration. The data were fitted according to the empirical formula explained in Chapters 1 and 3.1.1. The values for c, the linear coefficient with units °C/M, B_{max}, the maximum change in the phase transition temperature, and K_D the dissociation constant of the ion are listed in the following table.

Salt	Concentration Range	c (K.M^{-1})	K_D (M)	B_{max} (K)
NaSCN	0 - 1.0 M	-3.08	0.33	16.59
$NaClO_4$	0 - 1.0 M	-1.21	0.49	11.82
NaI	0 - 1.0 M	7.65	0.62	21.39
$NaNO_3$	0 - 1.0 M	7.74	0.97	6.21
NaCl	0 - 0.6 M	-16.2	-	-
NaH_2PO_4	0 - 0.6 M	-39.5	-	-
Na_2SO_4	0 - 0.3 M	-77.7	-	-
Na_2CO_3	0 - 0.3 M	-75.6	-	-

Table 2: Fit values for the parameters c, K_D, and B_{max} according to the empirical fit (Equation 1) for the LCST values of HPC solutions with salt content given in the second column. For the last four salts, the fit is linear, and there is no nonlinear term to report.

The LCST of HPC nonlinearly increases as the salt concentration of salting-in ions, namely NaSCN, NaI, $NaClO_4$, and $NaNO_3$, increases (see the curves indicated with black squares, green circles, orange squares, and magenta triangles). This nonlinear trend is correlated to a saturable type of binding behavior, which indicates that there is a direct interaction between the macromolecule and the ion. In contrast, the LCST is decreasing as the salting-out ions, namely, NaCl, NaH_2PO_4, Na_2SO_4, and Na_2CO_3. This linear decrease is evidence that there is no direct interaction between the macromolecule and the ion. As a result of this dataset, the given Hofmeister anions act on the HPC as they act on the MC. Meaning that, the same Hofmeister anions cause the same trends on these two different sugar-based macromolecules. It can be concluded from this data that this effect might be universal for all sugar-based macromolecules.

3.2. Developing a Methodology for Observing the Hydration Shell Structure for the Macromolecules by Utilizing the MCR Algorithm and ATR-FTIR Spectroscopy

Since the Hofmeister ions are classified based on their hydration capacity (strongly hydrated vs. weakly hydrated), and the hydration of small molecules affects their interaction with macromolecules, understanding the hydration structures of macromolecules is also crucial. In the literature, Raman Spectroscopy, along with the Multivariate Curve Resolution (MCR) algorithm, is widely used for observing the hydration shell of macromolecules with spectroscopic evidence.[158–160]

MCR is an algorithm that subtracts a spectrum from another with some optimization. The aim of using this algorithm is to subtract the bulk water spectrum from the water and solute spectrum to get the resulting spectrum containing only solute and hydration water structure, which is called the "solute correlated (SC) spectrum". The resulting spectra have no negative area and contain both the intramolecular modes from the solute and perturbations caused by the solute on the OH region of the water network.[161]

$$Whole\ Spectra = A * \ Solute\ Correlated\ Spectra + Bulk\ Spectra \qquad (3)$$

The equation above is the simplified version of the working principle of the MCR algorithm. The algorithm aims to subtract the "bulk spectra" from the "whole spectra" by optimizing the coefficient A in a way that no point in the resulting spectra has a negative value.

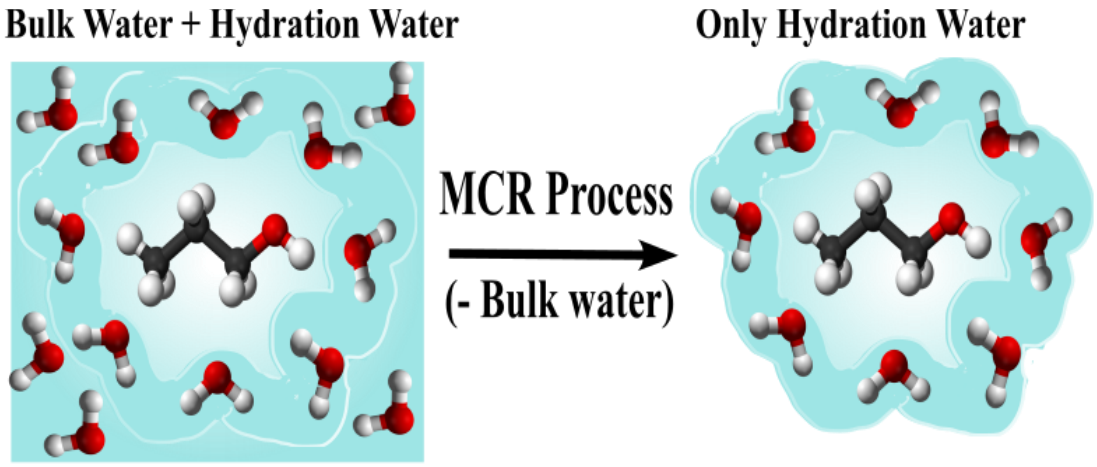

Figure 29: The illustration of the principle of the MCR algorithm. (Left) Shows the molecular-level picture of the spectrum that contains water and solute, propanol in this case, for the sake of simplicity. (Right) Shows the molecular-level picture of the solute correlated spectrum resulting from the MCR algorithm application, which contains the solute and the water molecules that participate in the hydration shell of this solute molecule.

This technique has been widely used in literature for spectroscopic evidence of how the hydration shell of the molecule changes with certain stimuli.[158–160] For macromolecules, Raman spectroscopy is used for the application of this algorithm due to its high signal-to-noise ratio. However, since Raman spectroscopy measurements are based on the light scattering principle, observing the collapsed state of the macromolecules with Raman measurements is not possible due to their elevated light scattering intensity. Even though in the literature, there are examples showing the hydration shells of macromolecules and proteins utilizing IR spectroscopy[162], there is no clear example of showing the collapsed state of macromolecules' hydration shells using IR SMCR. To overcome this difficulty, to develop a new methodology was necessary for observing the changes on the surface of the collapsed state of the macromolecules in this project. For this purpose, the Raman spectroscopy

measurements were replaced by ATR-FTIR measurements, and the MCR algorithm was performed on the resulting vibrational spectra. Expectedly, both analyses show similar results, and hydration of the macromolecules in the collapsed state can be observed. The experiment setup is explained in more detail in section 2.2.3.

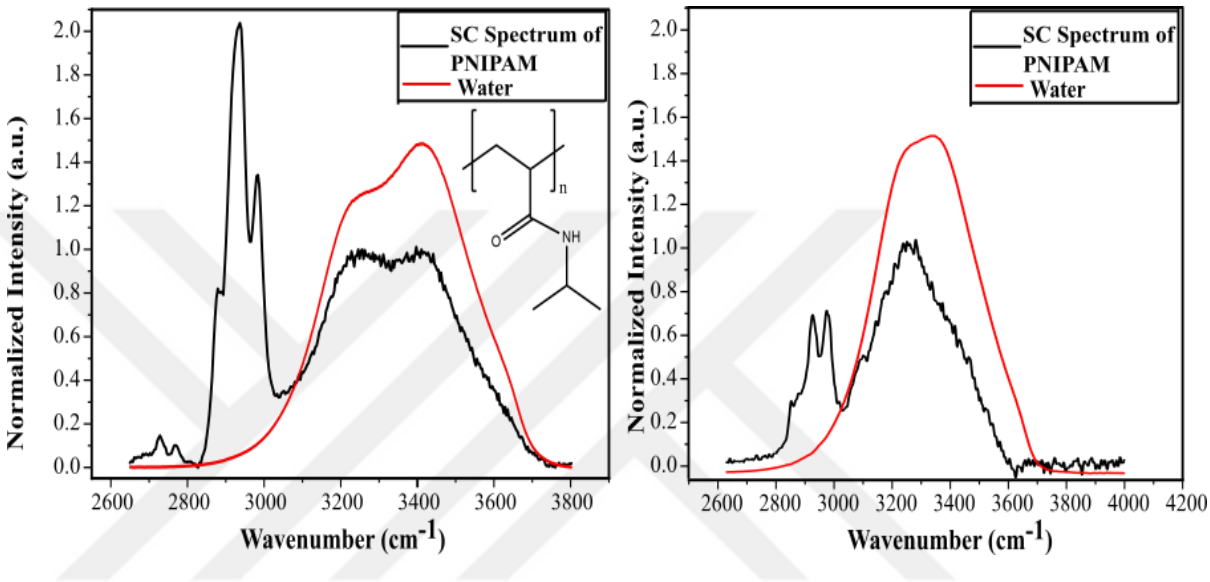

Figure 30: (Left) The Raman spectrum of pure water (red curve) and the resulting solute correlated spectrum of 20 mg/mL PNIPAM in water after MCR analysis in soluble state (black curve) with the molecular structure of PNIPAM inserted. (Right) The IR spectrum of pure water (red curve) and the resulting solute correlated spectrum of 20 mg/mL PNIPAM in water after MCR analysis in the soluble state (black curve).

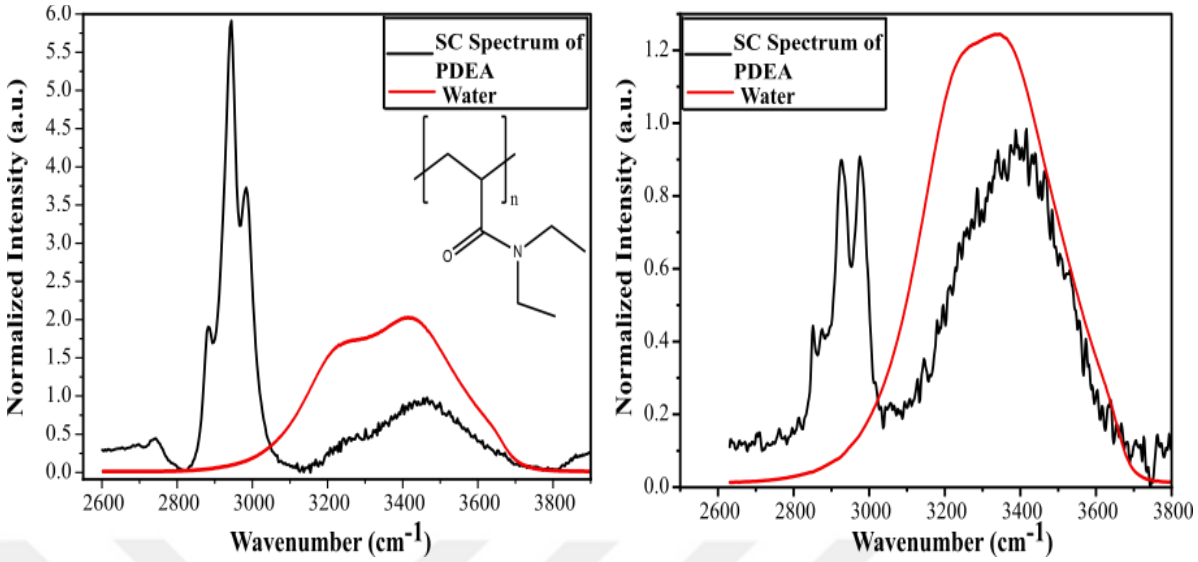

Figure 31: (Left) The Raman spectrum of pure water (red curve) and the resulting solute correlated spectrum of 20 mg/mL PDEA in water after MCR analysis in soluble state (black curve) with the molecular structure of PDEA inserted. (Right) The IR spectrum of pure water (red curve) and the resulting solute correlated spectrum of 20 mg/mL PDEA in water after MCR analysis in the soluble state (black curve).

In Figures 30 and 31, it is clear that both the Raman MCR and IR MCR analyses are useful for understanding the hydration behavior of macromolecules. Both techniques give similar SC spectra with minor differences in peak shapes and signal-to-noise ratios. The signal obtained from Raman spectroscopy measurements relies on the changes in the polarizability of the molecule during the vibration, and the O-H stretching vibrations of water molecules are not quite polarizable and yet still give a signal during the Raman spectroscopy measurements. Whereas the principle of IR spectroscopy is the dipole moment changes of the molecules during the vibrational transition. Since the CH stretching of the molecules doesn't cause significant changes in the dipole moment of the molecule, CH peaks are easier to observe in the Raman spectroscopy. These differences explain the different appearance of OH and CH peaks in Raman spectra versus ATR-FTIR spectra.[105,106,119,124,125,127,128,135,136,139,163–165]

Additionally, to obtain a better signal-to-noise ratio, IR measurements were performed with 512 scan numbers.

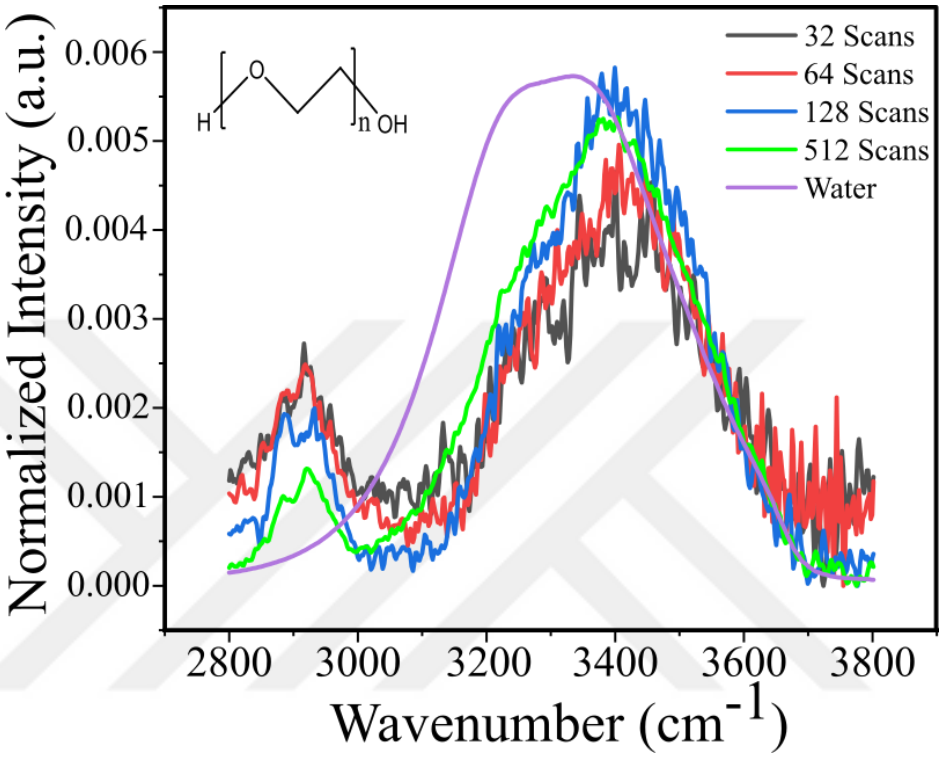

Figure 32: The multivariate curve resolution (MCR) analysis is performed with different scan numbers of IR spectra of polyethylene glycol (PEG), whose molecular structure is present in the inset of the graph. Among the four different tests, the analysis performed on the 512-scan measurement is found to have the best signal-to-noise ratio.

It can be concluded that from Figures 30, 31, and 32, ATR-FTIR spectroscopy measurements can be utilized instead of or together with the Raman spectroscopy measurements for observing the hydration shell structures of macromolecules, and performing these measurements with 512 scans has a good signal-to-noise ratio, which is enough for getting a reasonable signal-to-noise ratio after the MCR analysis. After providing evidence for the validity of this technique, it was utilized for observing how the hydration shell of the macromolecules in the collapsed state changes with additives

in the solutions with ATR-FTIR MCR analysis, with the measurements above the phase transition temperature (LCST).

3.3 Effects of Cosolvents on Macromolecules: Cononsolvency

In addition to the interactions of Hofmeister ions, the addition of other small molecules to the aqueous biological macromolecules can also alter the behavior of the macromolecules. For instance, the presence of small alcohols can lead to an increase or decrease in the solubility and hydration behavior of that macromolecule. A good example of this behavior is the cononsolvency behavior, which is a phenomenon that occurs when two good and miscible solvents become a bad solvent when they are mixed at certain ratios.[105,106,119,124,125,127,128,135,136,139] In this part of Chapter 3, the cononsolvency behavior of amide-based macromolecules is shown both by thermodynamic and spectroscopic techniques, and its universality and the underlying mechanism are discussed.

3.3.1 Addition of Alcohols to Aqueous Amide-Based Macromolecules

The effects of osmolytes, anions, and cations in the solutions on the solubility of macromolecules have been widely investigated in the literature for over a century.[32,33,42,59]Although most of the mechanisms regarding these interactions have been revealed, new findings continue to be added to the literature, as explained in the previous chapters in this study. However, there are some exceptional cases where the underlying mechanism is still under debate. Cononsolvency is one of these cases as explained in more detail in Chapter 1. This phenomenon occurs when two “good” and miscible solvents become a “bad” solvent when they are mixed at certain ratios. The

cosolvents for these types of systems are generally alcohol or other organic solvents.[136] In this study, the effect of methanol, ethanol, and isopropanol, which are the common cosolvents from the literature, on the solubility of PNIPAM and PDEA was observed at the molecular level to understand the origins of the "cononsolvency" phenomenon. In the first part of the experiment, the mole fraction of three different alcohols in PNIPAM/PDEA and water mixtures is increased, creating a solvent, cosolvent, and solute ternary system. The LCST values of PNIPAM and PDEA are recorded as the mole fractions of alcohols increase, see Figure 33. This data is in line with the literature. [117-122]

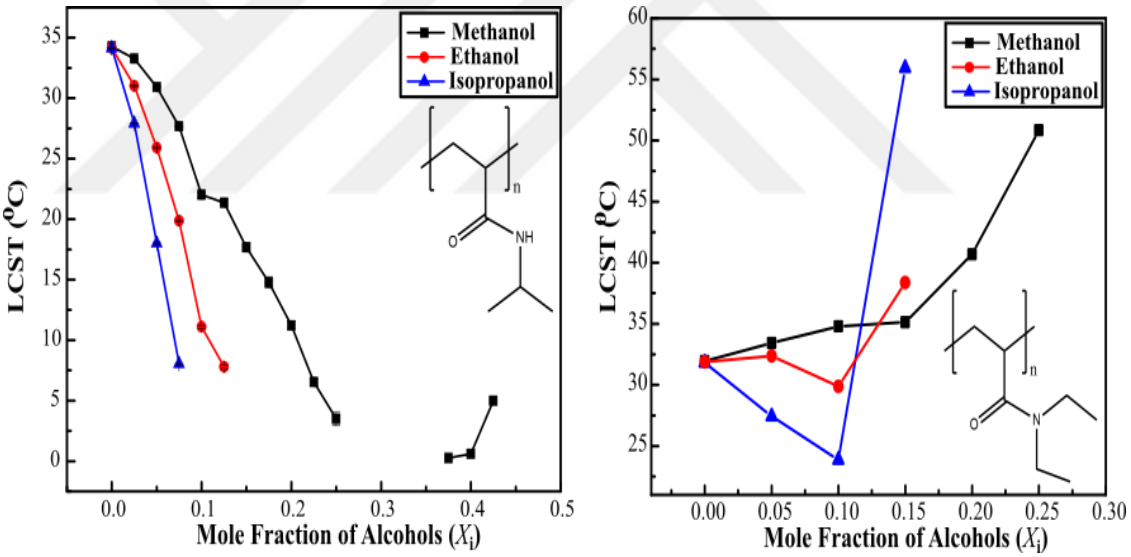

Figure 33: The molecular structures and the change of the LCST of (Left) PNIPAM and (Right) PDEA as the mole fraction of alcohols increases. Methanol (black squares and black curve), ethanol (the red circles and red curve), and isopropanol (the blue triangles and the blue curve) played the role as cosolvents.

In the absence of any cosolvents, the LCST of PNIPAM is measured as 34.30 ^{0}C. As the mole fraction of methanol, ethanol, and isopropanol increases, the LCST of PNIPAM decreases and shows a "cononsolvency" behavior. The gap between the 0.25

and 0.35 mole fraction of methanol indicated the points where the cononsolvency is observed the most, that is, the LCST goes below 0 ^{0}C and was not possible to measure with our current instrumentation. After 0.35 mole fraction of methanol, the LCST starts to increase again, showing the diminishing of cononsolvency behavior.

The LCST of PDEA in the absence of any cosolvents is measured as 32 ^{0}C. Even though PDEA has a very similar chemical structure to PNIPAM, it does not show a similar cononsolvency type of behavior with the increasing mole fraction of alcohols. Only for the small mole fractions of ethanol and isopropanol, there can be a slight decrease in the LCST of PDEA, which might be an indication of cononsolvency behavior. However, the significant increase in the LCST of PDEA in the elevated mole fractions of alcohols shows that this macromolecule does not behave the same as PNIPAM in the presence of cosolvents. There are other examples in the literature regarding the cononsolvency behavior of PDEA gels in the water/alcohol mixtures; however, a mechanistic study in the aqueous phase of this polymer was not well-established[166]. These findings brought to mind the possibility that the mechanism of this phenomenon might be highly dependent on the solvent-cosolvent interactions rather than the interactions between the macromolecule and solvent or cosolvent, since the two structurally similar macromolecules did not exhibit the same trends.

3.3.2 Solvent and Cosolvent Interactions: ATR-FTIR Spectra for Water-Alcohol Mixtures

For understanding the underlying mechanism of the cononsolvency effect on PNIPAM, it was crucial to understand what is happening between the solvent and cosolvent in the bulk. For this purpose, ATR-FTIR spectra of different mole fractions of alcohol-water contents

were obtained. Then the pure water spectrum was subtracted from the alcohol-water mixtures' spectra to get the "delta spectra", and the changes in the spectra as the alcohol content increases.

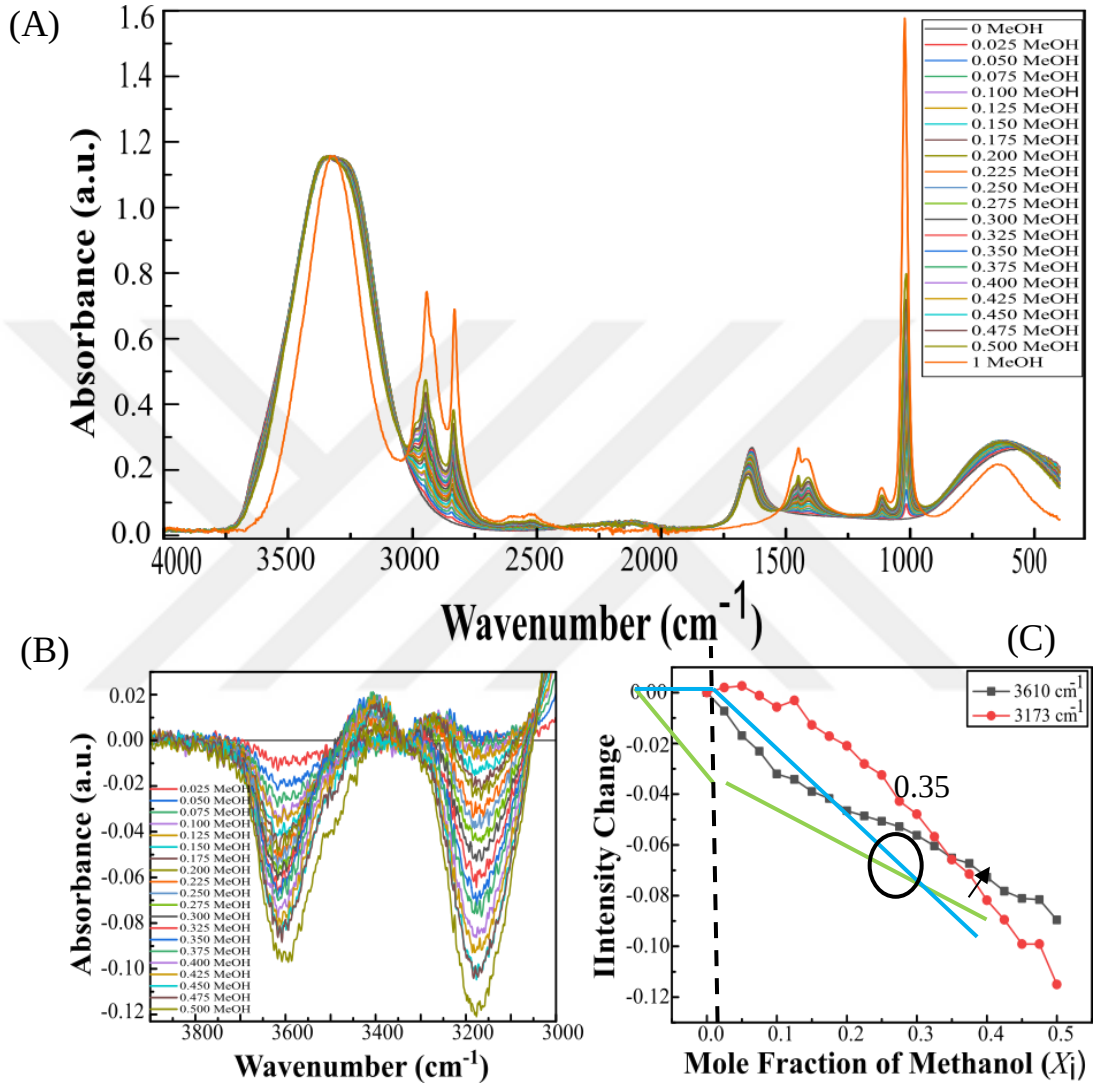

Figure 34: (A) The ATR-FTIR Spectra of methanol-water mixtures with differing methanol content. (B) The resulting spectra after subtracting the pure water spectrum from the methanol-water mixture spectra. Two different bands are resulting from the subtraction; the band around 3610 cm^{-1} corresponds to water molecules that form fewer hydrogen bonds with each other, and another band occurs around 3170 $cm^{-1,}$ which corresponds to water molecules that form more hydrogen bonds with each other, i.e., "ice-like water"[1]. (C) The change in the intensities of these two bands as the mole fraction of methanol increases.

Figure 34 shows how the H-bonding network of water changes as the methanol content increases. The intensity of the band found around 3610 cm^{-1} decreases substantially in the lower mole fractions of methanol, while the intensity of the band around 3170 cm^{-1} remains and decreases mildly. This result indicates that the less ordered water molecules are expelled from the network first with the addition of \. After a certain mole fraction of methanol, both types of water molecules could not hold onto the network, and the mediation of the alcohol significantly disrupts the water hydrogen bond network. Both types of water molecules are found to leave the water network in the same amount at the point where the methanol content reaches 0.35 mole fraction, which is the mole fraction where the addition of methanol causes the most cononsolvency behavior when added to aqueous PNIPAM solution. (See Figure 33)

The same ATR measurements and the delta analysis were performed for ethanol and isopropanol as well (see Figure 35). The behavior of two different OH bands belonging to water acted similarly to the methanol case; the water molecules that form fewer hydrogen bonds (band occurs at 3610 cm^{-1}), expelled from the water network first, and the strongly interacting water molecules (band occurs around 3170 cm^{-1}) get disrupted at higher mole fractions of alcohols. The point where both types of water molecules are found equal was determined around 0.125 mole fraction for ethanol and 0.1 mole fraction for isopropanol, which are the points the cononsolvency is observed the most with the addition of the alcohol of interest to the aqueous solution of PNIPAM.

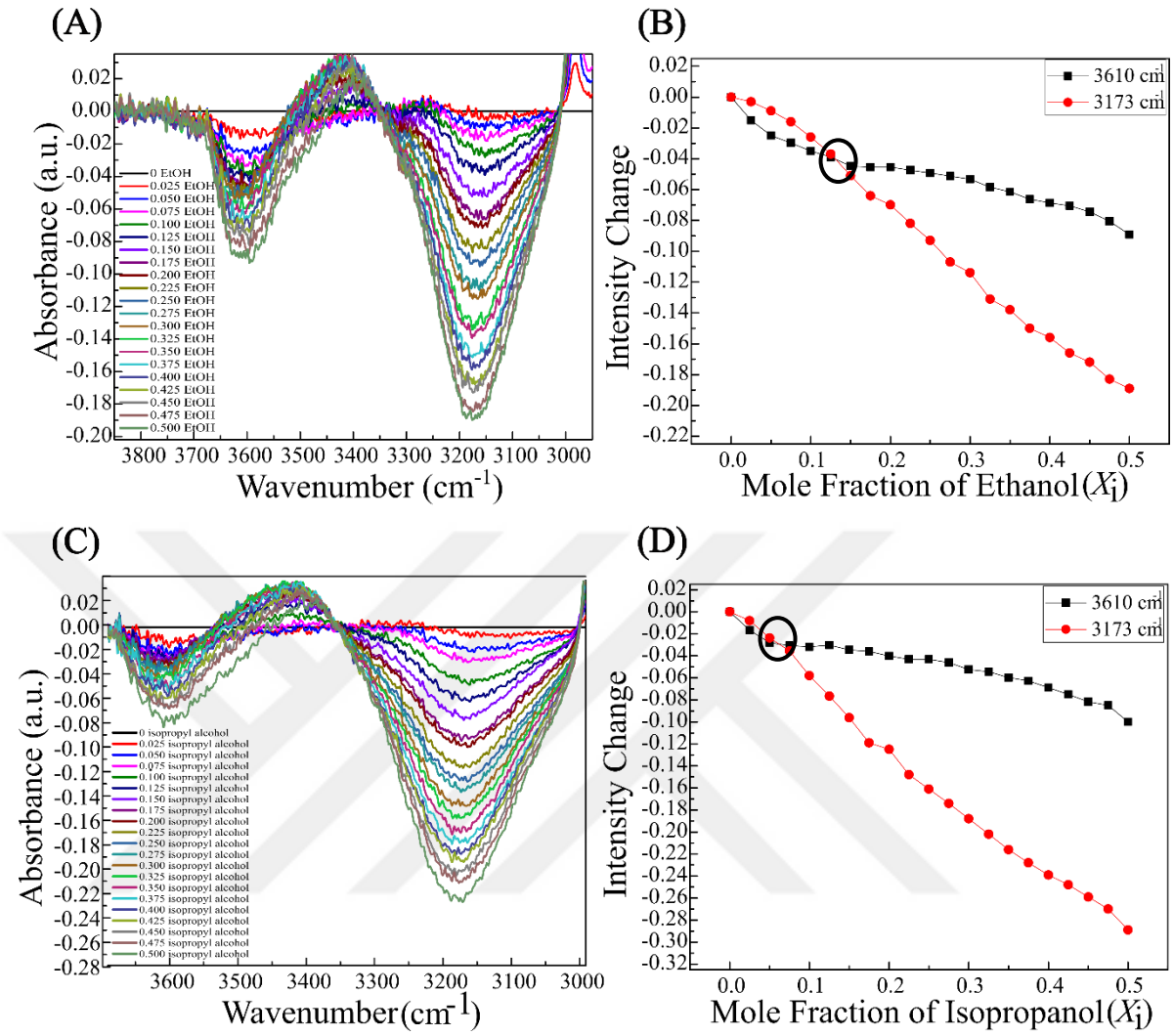

Figure 35: The resulting spectra after subtracting the pure water spectrum from the (A) ethanol-water mixture spectra, and (C) isopropanol-water mixture spectra. The changes in the intensities of two bands as the mole fraction of (B) ethanol and (D) isopropanol increase.

Figures 34 and 35 show that the interactions between alcohol and water should be related to the cononsolvency phenomenon. However, since both macromolecules (PNIPAM and PDEA) do not exhibit the same kind of behavior, this explanation is not sufficient on its own. Some factors specific to macromolecules must be playing an additional role in the mechanism of this phenomenon, such as the solvent accessible surface area (SASA) of the macromolecules.

3.3.3 The Driving Forces Behind the Cononsolvency Phenomenon is an Interplay Between Bulk and Surface

After observing the changes in the bulk properties via the addition of alcohols and the effect on the cononsolvency mechanism, further investigation on the changes in the surface properties of the macromolecule was carried out. The collapsed states of PNIPAM and PDEA were investigated via temperature-controlled ATR-FTIR measurements of ternary mixtures of macromolecule-solvent-cosolvent, as explained in Section 2.1.3 (See Figure 18). After these measurements, the multivariate curve resolution (MCR) analysis was performed on the spectra. For each mole fraction, the solvent-cosolvent mixture spectra were subtracted from the overall spectra as the "bulk spectra". This novel technique enables us to investigate how the surface of macromolecules and their hydration shell change in response to the addition of cosolvent to their aqueous solutions. The ATR-FTIR measurements were carried out with polymer-ethanol-water mixtures. Since the methanol is highly volatile, and the measurements were performed with 512 scans, which takes around half an hour for each measurement, the polymer-methanol-water mixtures were not suitable for this measurement setup, since long (> 30 min) measurement time enables changing the alcohol content of the sample solution due to low vapor pressure of methanol.

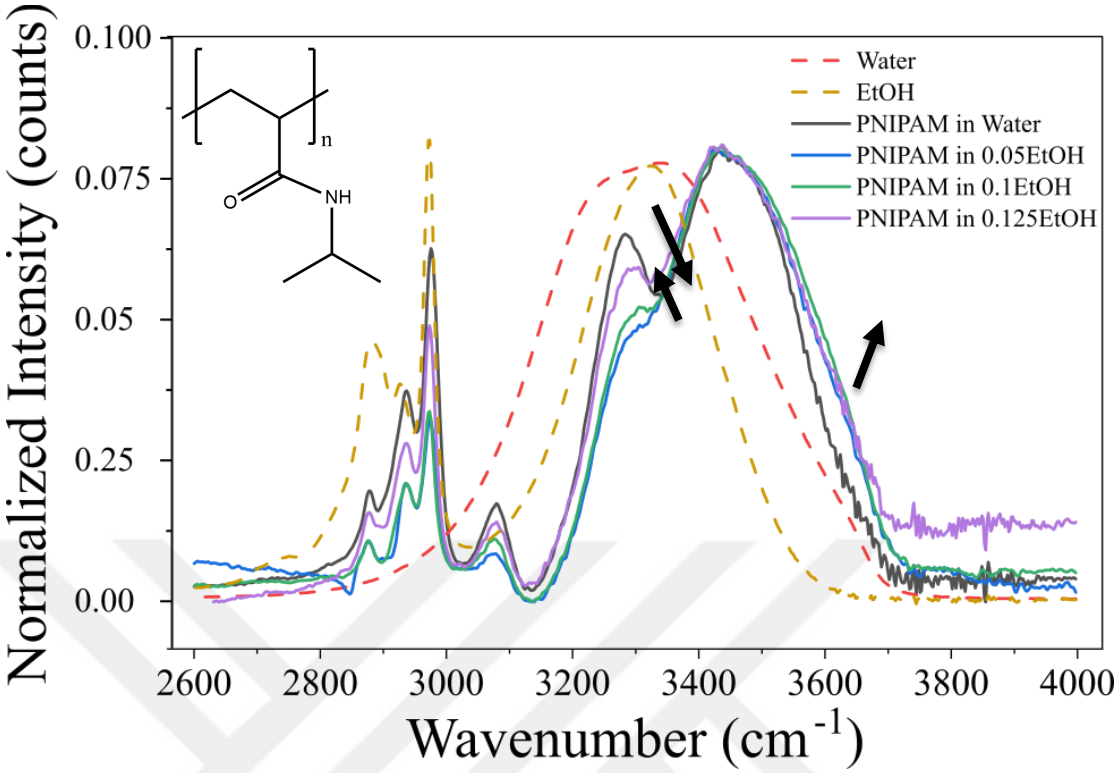

Figure 36: The resulting spectra of MCR analysis performed on the PNIPAM-Ethanol-Water Mixtures. The structure of PNIPAM is in the inset of the graph.

Figure 36 shows that the addition of ethanol changes the hydration structure of PNIPAM. The black curve indicates the hydration shell structure of PNIPAM in only water. After the addition of 0.05 mole fraction of ethanol to the system, the intensity of the peak located around 3300 cm^{-1} wavenumbers decreased, and via the further addition of ethanol, this peak started to increase again, but it is still lower in intensity compared to no ethanol containing sample. On the other hand, the peak intensity of 3600 cm^{-1} - 3650 cm^{-1} wavenumber range increases as the ethanol content increases. These spectral changes show that the addition of ethanol causes a change in the hydration shell of PNIPAM, and that can be evidence of alcohol accumulation on the surface of the polymer, which might lead to cononsolvency behavior. Since the mole fraction 0.125 is the ethanol content where we observe the cononsolvency the most,

and the LCST for PNIPAM could not be measured, the spectra for the more ethanol-containing samples could not be included.

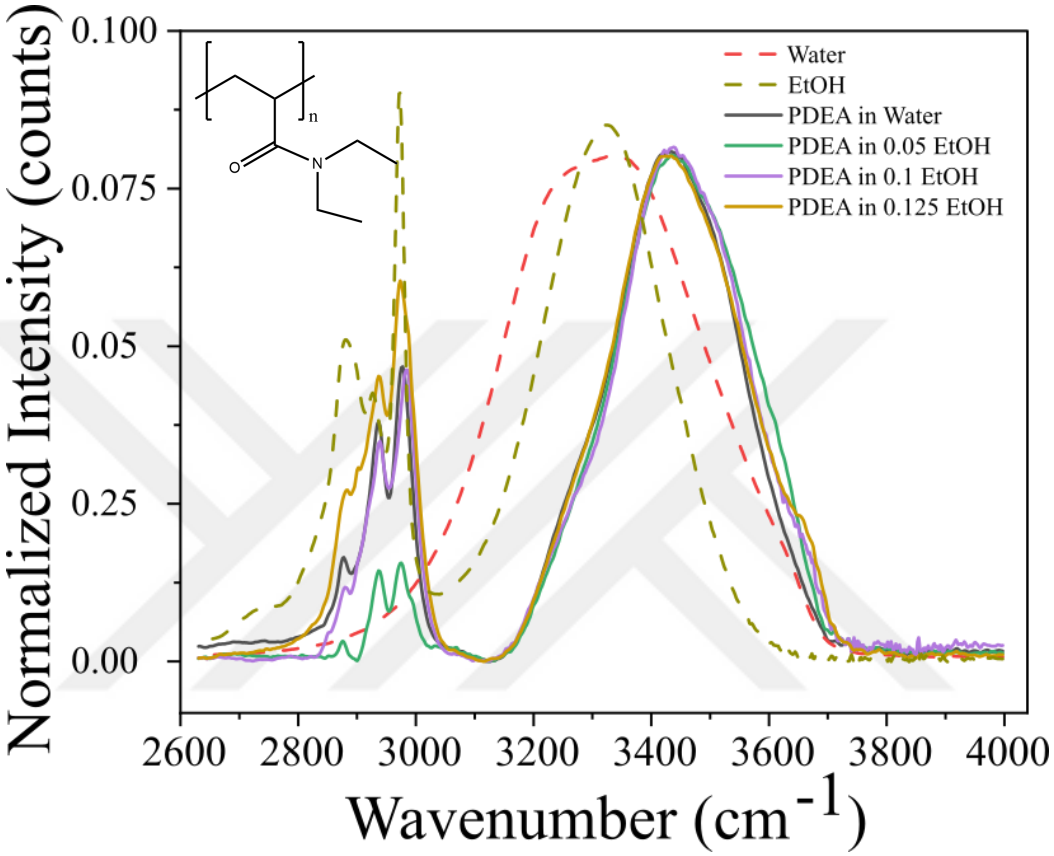

Figure 37: The resulting spectra of MCR analysis performed on the PDEA-Ethanol-Water Mixtures. The structure of PDEA is in the inset of the graph.

The same ATR-FTIR measurements and MCR analysis were also performed for PDEA-ethanol-water mixtures. The black curve is the hydration shell structure of PDEA. There is no significant spectral change observed for the hydration of the PDEA upon ethanol addition to the system. This result shows why PDEA does not show cononsolvency behavior as PNIPAM does, even though they have similar molecular structures.

3.3.4 Cononsolvency on Other Polymers

Poly(*N*-isopropylacrylamide) (PNIPAM) and Poly(*N*, *N*-diethylacrylamide) (PDEA) are the most widely used model polymers for the investigation of cononsolvency phenomenon. However, understanding how the other polymers act in similar systems is understanding the general mechanism for this phenomenon is crucial. For this reason, two different polymers, polypropylene oxide (PPO) and hydroxypropyl cellulose (HPC) used to observe whether these polymers exhibit the cononsolvency behavior or not.

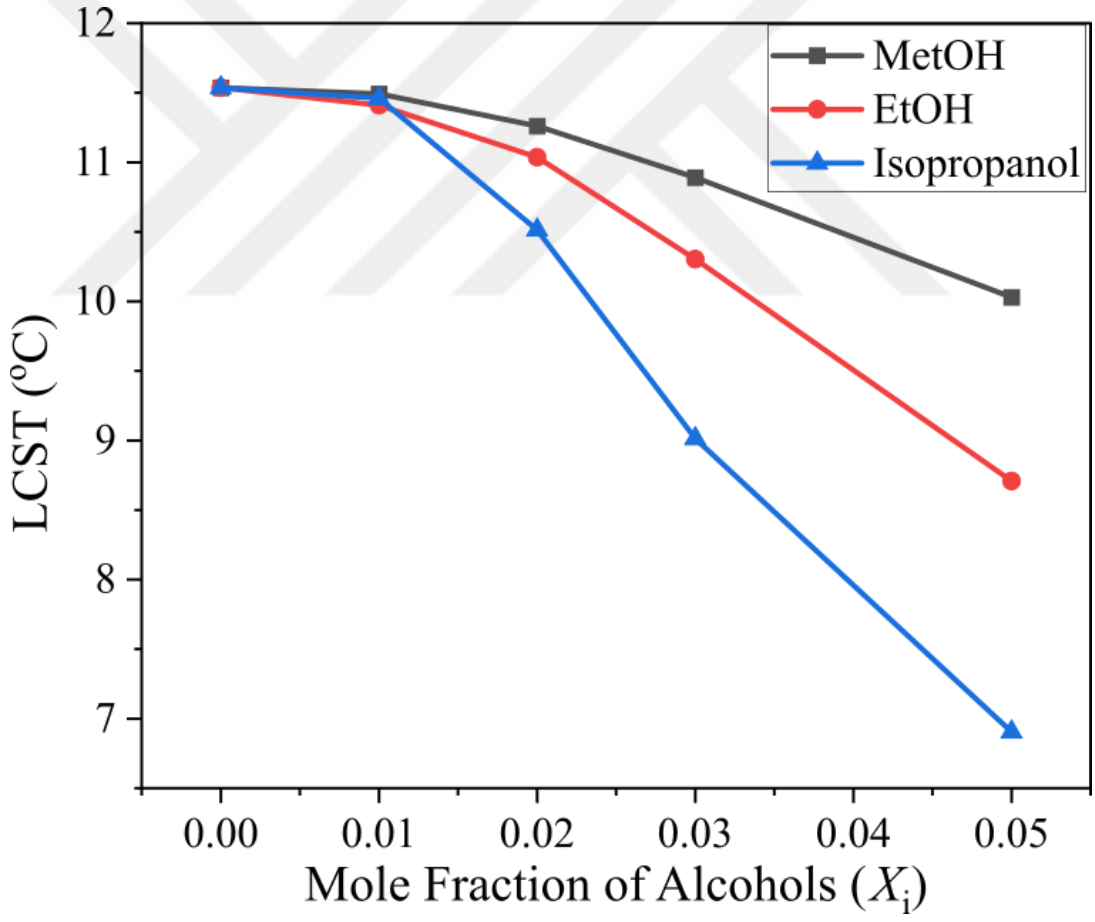

Figure 38: The molecular structures and the change of the lower critical solution temperature (LCST) of polypropylene oxide as the mole fraction of alcohols increases. Methanol (black squares and black curve), ethanol (the red circles and red curve), and isopropanol (the blue triangles and the blue curve) played the role of cosolvents.

The lower critical solution temperature (LCST) for PPO is around 15 ^{o}C. Figure 38 shows that methanol, ethanol, and isopropanol addition to the aqueous PPO solution causes a decrease in the LCST of PPO and indicates the cononsolvency behavior. Since the LCST of PPO goes below 0 ^{0}C, the LCST value for the higher mole fractions of alcohols could not be measured.

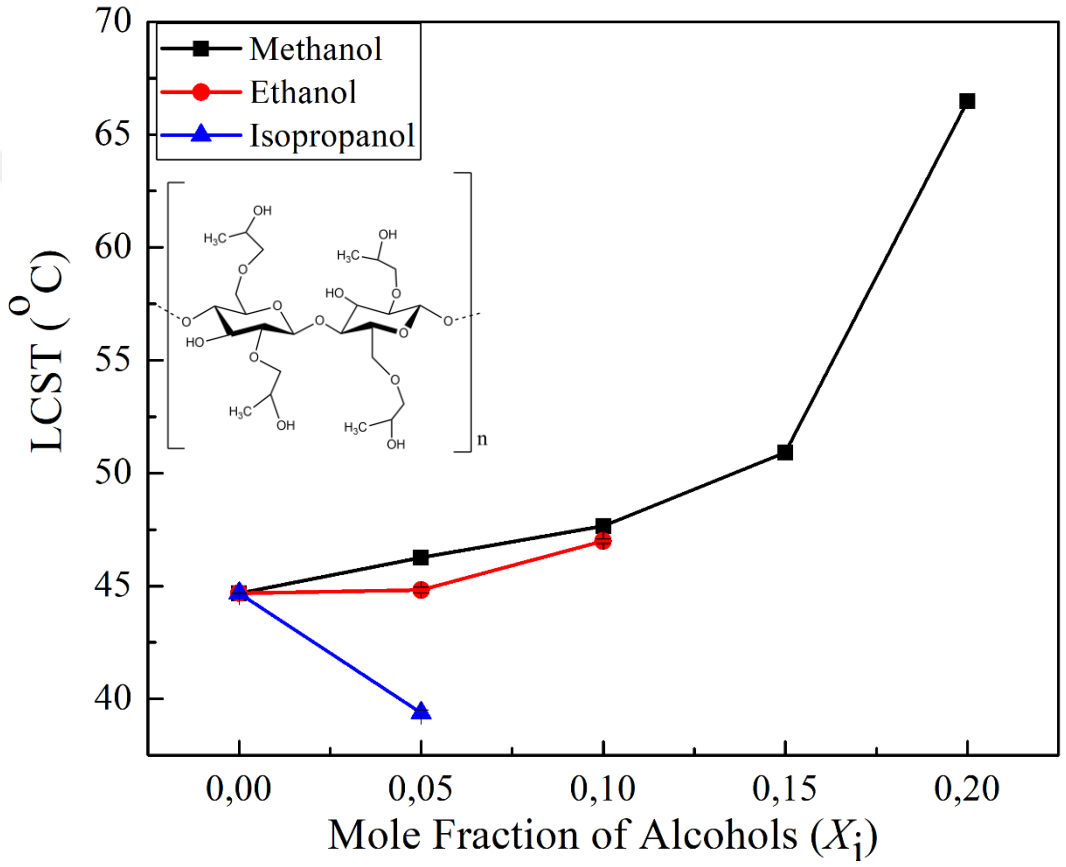

Figure 39: The molecular structures and the change of the lower critical solution temperature (LCST) of hydroxypropyl cellulose (HPC) as the mole fraction of alcohols increases. Methanol (black squares and black curve), ethanol (the red circles and red curve), and isopropanol (the blue triangles and the blue curve) played the role as cosolvents. Error bars represent the standard deviations for three different replicas of the measurements.

The LCST of HPC without any cosolvent is around 45 ^{o}C. The addition of methanol and ethanol increases the LCST, meaning that it does not cause cononsolvency behavior. However, the addition of isopropanol causes a decrease in the LCST of HPC. The LCST of HPC with further addition of isopropanol could not be recorded due to instrumental restrictions, since the LCST of these samples is not in the OptiMelt's heating range.

Figures 38 and 39 show that the cononsolvency behavior does not solely depend on solvent-cosolvent interactions since the same solvent-cosolvent systems do not result in the same behavior on different types of polymers. Instead, the interactions between the polymer and solvent/cosolvent play a crucial role in the mechanisms of the cononsolvency phenomenon.

Chapter 4 – Conclusion

The interactions of macromolecules have been investigated for decades. Understanding the effects of ions, osmolytes, and small molecules on macromolecules is crucial for lots of different aspects of physiologically relevant processes, such as biological functions, medical and therapeutic developments, and other industrial applications.[59,64,86] In this regard, concepts such as ion specificity hold great importance and have been drawing significant attention for over a century. The Hofmeister series was established by Franz Hofmeister in the late 19th century and has been investigated mostly on amide-based macromolecules such as poly(N-isopropylacrylamide) (PNIPAM) and poly (N, N-diethylacrylamide) (PDEA). The generalized mechanisms suitable for all types of macromolecules is still elusive. The thermodynamic and spectroscopic techniques are used and have proved the general idea that the "weakly-hydrated" Hofmeister anions can bind to macromolecules' specific sites, while the "strongly-hydrated" ones do not interact. Herein, for expanding our understanding of the interactions of Hofmeister anions with polymers, sugar-based macromolecules, namely methylcellulose (MC), hydroxypropyl cellulose (HPC), and dextran, are used as model macromolecules instead of amide-based macromolecules. Both thermodynamic and spectroscopic techniques were utilized to understand the effect of 11 most common Hofmeister anions. The lower critical solution temperatures (LCST) measurements demonstrated that weakly-hydrated anions, i.e. SCN^-, increase the LCST of MC and HPC nonlinearly as a function of their concentration, while the strongly hydrated ones, i.e., SO_4^{2-} or Cl^-, linearly decrease the LCST of both polymers. Note that, dextran is not a thermoresponsive polymer, as such it cannot be investigated with LCST measurements. Proton Nuclear Magnetic Resonance (1H-NMR) spectroscopy measurements showed

that the side chain of MC, the methyl groups, are responsible for the binding of weakly-hydrated Hofmeister anions. The ^{1}H-NMR measurements could not be applied to HPC since its spectra are too complicated to analyze. The ^{1}H-NMR measurements for side group absent dextran did not indicate any site-specific interactions. The results presented in this part showed that the sugar-based macromolecules can be good alternatives to amide-based macromolecules in variety of applications.

In the second part of the thesis, other small molecules that affect the properties of macromolecules in aqueous solutions were studied. The "Cononsolvency" phenomenon is one of the peculiar examples where two good and miscible solvents decrease the solubility of a polymer when they are mixed at certain ratios. The underlying mechanism of this counterintuitive phenomenon is still elusive. To understanding the underlying mechanism of cononsolvency effect, poly(N-isopropylacrylamide) (PNIPAM) and poly (N, N-diethylacrylamide) (PDEA) were used as model systems, and small alcohols, i.e., methanol, ethanol, and isopropanol used as cosolvents. The addition of all three alcohols to the aqueous solutions of PNIPAM causes a decrease in its solubility, and it was shown via LCST measurements. However, the PDEA did not exhibit the same type of behavior with the addition of the same cosolvents. For understanding the reason why these two systems act differently under the same conditions, spectroscopic investigations were performed. Attenuated Total Reflection – Fourier Transform Infrared spectroscopy (ATR-FTIR) measurements showed that the bulk property of water changes with the addition of alcohols, which might lead to less interaction with the polymer and cause its collapse. Since the phenomenon is not observed in both systems, even though PNIPAM and PDEA have similar molecular structures, the explanation that the bulk is responsible

for this phenomenon was not sufficient. For further explanations, the hydration properties and changes in the surfaces of the polymers were observed via a novel technique utilized ATR-FTIR spectroscopy combined with the Multivariate Curve Resolution (MCR) Algorithm. This algorithm aims to subtract the bulk spectra from the overall spectra to result in "solute correlated (SC)" spectra, which show the changes in the hydration shell of the polymer. The measurements were performed at a temperature above the LCST of the polymers, which enables the observation of the surface properties. The results showed that the addition of alcohol to the system causes significant changes in the hydration shell of PNIPAM, while it does not exhibit a significant change in the hydration shell of PDEA. These results confirmed that the driving forces behind the cononsolvency phenomenon are the interplay between the bulk and the surface. Additionally, the same LCST measurements were performed for HPC and polypropylene oxide (PPO), and both polymers showed opposite behaviors, akin to PNIPAM and PDEA, confirming the statement that the cononsolvency behavior depends on the interactions of the macromolecules with solvent/cosolvent systems. Yet solvation shell experiments are still in need for these polymers to clearly show the underlying mechanism behind cononsolvency.

References

1. Ben-Amotz, D. Water-Mediated Hydrophobic Interactions. *Annu Rev Phys Chem* **67**, 617–638 (2016).
2. Chen, K. *et al.* Experimental Observation of Screening and Amplification of Quantum Fluctuation in Aqueous Electrolyte Solution. *Journal of Physical Chemistry Letters* 6919–6925 (2025) doi:10.1021/acs.jpclett.5c01250.
3. Lakemond, C. M. M., De Jongh, H. H. J., Hessing, M., Gruppen, H. & Voragen, A. G. J. Soy glycinin: Influence of pH and ionic strength on solubility and molecular structure at ambient temperatures. *J Agric Food Chem* **48**, 1985–1990 (2000).
4. Zhang, Y., Furyk, S., Bergbreiter, D. E. & Cremer, P. S. Specific ion effects on the water solubility of macromolecules: PNIPAM and the Hofmeister series. *J Am Chem Soc* **127**, 14505–14510 (2005).
5. Baldwin, R. L. Temperature dependence of the hydrophobic interaction in protein folding. *Proc Natl Acad Sci U S A* **83**, 8069–8072 (1986).
6. Perez-gago, M. B. & Krochta, J. M. Denaturation time and temperature effects on solubility, tensile properties, and oxygen permeability of whey protein edible films. *J Food Sci* **66**, 705–710 (2001).
7. Hofmeister, F. Zur Lehre von der Wirkung der Salze - Sechste Mittheilung. Die Betheiligung gelöster Stoffe an Quellungsvorgängen. *Archiv für Experimentelle Pathologie und Pharmakologie* **28**, 210–238 (1891).
8. Hofmeister, F. 24. Zur Lehre von der Wirkung der Salze - Fünfte Mittheilung Untersuchungen über den Quellungsvorgang. *Archiv für Experimentelle Pathologie und Pharmakologie* **27**, 395–413 (1890).
9. v. Limbeck, R. Zur Lehre von der Wirkung der Salze - Vierte Mittheilung. Ueber die diuretische Wirkung der Salze. *Archiv für Experimentelle Pathologie und Pharmakologie* **25**, 69–86 (1889).
10. Hofmeister, F. Zur Lehre von der Wirkung der Salze - Zweite Mittheilung. *Archiv für Experimentelle Pathologie und Pharmakologie* **24**, 247–260 (1888).
11. Hofmeister, F. Zur Lehre von der Wirkung der Salze - Dritte Mittheilung. *Archiv für Experimentelle Pathologie und Pharmakologie* **25**, 1–30 (1888).
12. Bruce, E. E. *et al.* Molecular mechanism for the interactions of hofmeister cations with macromolecules in aqueous solution. *J Am Chem Soc* **142**, 19094–19100 (2020).
13. Shi, J., Lu, H. & Fu, Y.-Q. A Chemo-Mechanical Coupling Model for Multistaged Shape Recovery in a Multiarmed Amorphous Polymer. *Macromolecules* **58**, 6678–6687 (2025).
14. Han, L. & Ruotolo, B. T. Hofmeister salts recover a misfolded multiprotein complex for subsequent structural measurements in the gas phase. *Angewandte Chemie - International Edition* **52**, 8329–8332 (2013).

15. Keil, J. & van der Vegt, N. F. A. Buffer-Specific Interactions of Imidazolium with Elastin-Like Polypeptides. *Journal of Physical Chemistry B* (2025) doi:10.1021/acs.jpcb.5c03022.
16. Abernethy, J. L. Franz Hofmeister. The impact of his life and research on chemistry. *J Chem Educ* **44**, 177–180 (1967).
17. Péter, T. *et al.* Correlations Between Colloidal Stability and Peroxidase Activity of Prussian Blue Nanozymes in Salt Solutions. *Journal of Physical Chemistry B* (2025) doi:10.1021/acs.jpcb.5c01256.
18. Goodman, J., Attwood, D., Kiely, J., Coladas Mato, P. & Luxton, R. Modeling Peptide Nucleic Acid Binding Enthalpies Using MM-GBSA. *Journal of Physical Chemistry B* **126**, 9528–9538 (2022).
19. Pegram, L. M. *et al.* Why Hofmeister effects of many salts favor protein folding but not DNA helix formation. *Proc Natl Acad Sci U S A* **107**, 7716–7721 (2010).
20. Arteaga, S. J., Dolenz, B. J. & Znosko, B. M. Competitive Influence of Alkali Metals in the Ion Atmosphere on Nucleic Acid Duplex Stability. *ACS Omega* **9**, 1287–1297 (2024).
21. Lau, S. C. & Bilodeau, C. L. Effect of Monovalent Cations on the Structure and Dynamics of Multimodal Chromatographic Surfaces. *Langmuir* **40**, 6694–6702 (2024).
22. Guo, H. *et al.* Microfluidic Investigation of the Ion-Specific Effect on Bubble Coalescence in Salt Solutions. *Langmuir* **39**, 8234–8243 (2023).
23. Furuki, T. *et al.* Monovalent Ion Effect on Liquid-Liquid Phase Separation of Aqueous Polyphosphate-Salt Mixtures. *Journal of Physical Chemistry B* **128**, 11435–11440 (2024).
24. Bunkin, N. F. *et al.* Shaking-Induced Aggregation and Flotation in Immunoglobulin Dispersions: Differences between Water and Water-Ethanol Mixtures. *ACS Omega* **5**, 14689–14701 (2020).
25. Liu, B., Manica, R., Xu, Z. & Liu, Q. Ion specificity modulated inhomogeneous interfacial flow inhibits bubble coalescence in electrolyte solutions. (2020).
26. Li, D. *et al.* Bubble coalescence principle in saline water. *Proc Natl Acad Sci U S A* **122**, (2025).
27. Kerkan, A. *et al.* In Vitro Structural and Functional Studies of a Novel Cupredoxin, FtrB, from Brucella abortus 2308. *ACS Omega* **10**, 12653–12670 (2025).
28. Biswas, B. & Allen, H. C. Solution and Surface Solvation of Nitrate Anions with Iron(III) and Aluminum(III) in Aqueous Environments: A Raman and Vibrational Sum Frequency Generation Study. *Journal of Physical Chemistry A* **128**, 8938–8953 (2024).
29. Shmool, T. A., Martin, L. K., Matthews, R. P. & Hallett, J. P. Ionic Liquid-Based Strategy for Predicting Protein Aggregation Propensity and Thermodynamic Stability. *JACS Au* **2**, 2068–2080 (2022).

30. Lee, E., Choi, J. H. & Cho, M. The effect of Hofmeister anions on water structure at protein surfaces. *Physical Chemistry Chemical Physics* **19**, 20008–20015 (2017).
31. Charge asymmetry at aqueous hydrophobic interfaces and hydration shells.. *https://scholar.google.com/citations?view_op=view_citation&hl=en&user=wCE1otkAAAAJ&citation_for_view=wCE1otkAAAAJ:dfsIfKJdRG4C*.
32. Lo Nostro, P. & Ninham, B. W. Hofmeister phenomena: An update on ion specificity in biology. *Chem Rev* **112**, 2286–2322 (2012).
33. Jungwirth, P. & Cremer, P. S. Beyond hofmeister. *Nat Chem* **6**, 261–263 (2014).
34. Okur, H. I. *et al.* Beyond the Hofmeister Series: Ion-Specific Effects on Proteins and Their Biological Functions. *Journal of Physical Chemistry B* **121**, 1997–2014 (2017).
35. Cox, W. M., College, J. H. & Wolfenden, M. A. The viscosity of strong electrolytes measured by a differential method. *Proceedings of the Royal Society of London. Series A, Containing Papers of a Mathematical and Physical Character* **145**, 475–488 (1934).
36. Ionic Processes In Solution : Gurney, Ronald. W : Free Download, Borrow, and Streaming : Internet Archive. https://archive.org/details/ionicprocessesin031465mbp.
37. Omta, A. W., Kropman, M. F., Woutersen, S. & Bakker, H. J. Negligible effect of ions on the hydrogen-bond structure in liquid water. *Science (1979)* **301**, 347–349 (2003).
38. Kropman, M. F. & Bakker, H. J. Effect of ions on the vibrational relaxation of liquid water. *J Am Chem Soc* **126**, 9135–9141 (2004).
39. Kropman, M. F. & Bakker, H. J. Femtosecond mid-infrared spectroscopy of aqueous solvation shells. *J Chem Phys* **115**, 8942–8948 (2001).
40. Omta, A. W., Kropman, M. F., Woutersen, S. & Bakker, H. J. Influence of ions on the hydrogen-bond structure in liquid water. *J Chem Phys* **119**, 12457–12461 (2003).
41. Kropman, M. F. & Bakker, H. J. Vibrational relaxation of liquid water in ionic solvation shells. *Chem Phys Lett* **370**, 741–746 (2003).
42. Gurau, M. C. *et al.* On the mechanism of the Hofmeister effect. *J Am Chem Soc* **126**, 10522–10523 (2004).
43. Gurau, M. C. *et al.* Thermodynamics of phase transitions in Langmuir monolayers observed by vibrational sum frequency spectroscopy. *J Am Chem Soc* **125**, 11166–11167 (2003).
44. Robinson, D. R. & Jencks, W. P. The Effect of Concentrated Salt Solutions on the Activity Coefficient of Acetyltetraglycine Ethyl Ester. *J Am Chem Soc* **87**, 2470–2479 (1965).
45. Nandi, P. K. & Robinson, D. R. The Effects of Salts on the Free Energies of Nonpolar Groups in Model Peptides. *J Am Chem Soc* **94**, 1308–1315 (1972).

46. Nandi, P. K. & Robinson, D. R. The Effects of Salts on the Free Energy of the Peptide Group. *J Am Chem Soc* **94**, 1299–1308 (1972).
47. Hladílková, J. *et al.* Effects of end-group termination on salting-out constants for triglycine. *Journal of Physical Chemistry Letters* **4**, 4069–4073 (2013).
48. Paterová, J. *et al.* Reversal of the hofmeister series: Specific ion effects on peptides. *Journal of Physical Chemistry B* **117**, 8150–8158 (2013).
49. Rogers, B. A. *et al.* Weakly hydrated anions bind to polymers but not monomers in aqueous solutions. *Nat Chem* **14**, 40–45 (2022).
50. Bergbreiter, D. E., Hughes, R., Besinaiz, J., Li, C. & Osburn, P. L. Phase-selective solubility of poly(N-alkylacrylamide)s. *J Am Chem Soc* **125**, 8244–8249 (2003).
51. Yang, Y. *et al.* Reversible changes in solution pH resulting from changes in thermoresponsive polymer solubility. *J Am Chem Soc* **134**, 7378–7383 (2012).
52. Sun, J. *et al.* Effect of Molecular Structure on Thermoresponsive Behaviors of Pyrrolidone-Based Water-Soluble Polymers. *Macromolecules* **43**, 4041–4049 (2010).
53. Kadam, Y. *et al.* Induced micellization and micellar transitions in aqueous solutions of non-linear block copolymer Tetronic® T904. *J Colloid Interface Sci* **351**, 449–456 (2010).
54. Patel, K., Bharatiya, B., Kadam, Y. & Bahadur, P. Micellization and clouding behavior of EO-PO block copolymer in aqueous salt solutions. *J Surfactants Deterg* **13**, 89–95 (2010).
55. Yan, Y., Li, L. & Hoffmann, H. Clouding: Origin of phase separation in oppositely charged polyelectrolyte/surfactant mixed solutions. *Journal of Physical Chemistry B* **110**, 1949–1954 (2006).
56. Bloksma, M. M., Bakker, D. J., Weber, C., Hoogenboom, R. & Schubert, U. S. The effect of hofmeister salts on the LCST transition of poly(2-oxazoline)s with varying hydrophilicity. *Macromol Rapid Commun* **31**, 724–728 (2010).
57. Rembert, K. B., Okur, H. I., Hilty, C. & Cremer, P. S. An NH moiety is not required for anion binding to amides in aqueous solution. *Langmuir* **31**, 3459–3464 (2015).
58. Cho, Y. *et al.* Effects of Hofmeister Anions on the Phase Transition Temperature of Elastin-like Polypeptides. *J Phys Chem B* **112**, 13765 (2008).
59. Zhang, Y. & Cremer, P. S. Interactions between macromolecules and ions: the Hofmeister series. *Curr Opin Chem Biol* **10**, 658–663 (2006).
60. Cho, Y. *et al.* Effects of hofmeister anions on the phase transition temperature of elastin-like polypeptides. *Journal of Physical Chemistry B* **112**, 13765–13771 (2008).
61. Rembert, K. B. *et al.* Molecular Mechanisms of Ion-Specific Effects on Proteins. *J Am Chem Soc* **134**, 10039–10046 (2012).

62. Rogers, B. A. *et al.* Weakly hydrated anions bind to polymers but not monomers in aqueous solutions. *Nat Chem* **14**, 40–45 (2022).
63. Wang, A. & Bolen, D. W. A naturally occurring protective system in urea-rich cells: Mechanism of osmolyte protection of proteins against urea denaturation. *Biochemistry* **36**, 9101–9108 (1997).
64. Pasantes-Morales, H., De La Paz, L. D. O., Sepúlveda, J. & Quesada, O. Amino acids as osmolytes in the retina. *Neurochem Res* **24**, 1339–1346 (1999).
65. Sackett, D. L. Natural osmolyte trimethylamine N-oxide stimulates tubulin polymerization and reverses urea inhibition. *Am J Physiol Regul Integr Comp Physiol* **273**, (1997).
66. Fedotova, M. V., Kruchinin, S. E. & Chuev, G. N. Hydration structure of osmolyte TMAO: concentration/pressure-induced response. *New Journal of Chemistry* **41**, 1219–1228 (2017).
67. Li, J., Chen, J., An, L., Yuan, X. & Yao, L. Polyol and sugar osmolytes can shorten protein hydrogen bonds to modulate function. *Commun Biol* **3**, 1–8 (2020).
68. Sharma, G. S. & Singh, L. R. Polyols have unique ability to refold protein as compared to other osmolyte types. *Biochemistry (Moscow)* **82**, 465–473 (2017).
69. Bruździak, P., Panuszko, A. & Stangret, J. Influence of osmolytes on protein and water structure: A step to understanding the mechanism of protein stabilization. *Journal of Physical Chemistry B* **117**, 11502–11508 (2013).
70. Street, T. O., Bolen, D. W. & Rose, G. D. A molecular mechanism for osmolyte-induced protein stability. *Proc Natl Acad Sci U S A* **103**, 13997–14002 (2006).
71. Rani, A. & Venkatesu, P. Changing relations between proteins and osmolytes: a choice of nature. *Physical Chemistry Chemical Physics* **20**, 20315–20333 (2018).
72. Stasiulewicz, M., Panuszko, A., Bruździak, P. & Stangret, J. Mechanism of Osmolyte Stabilization-Destabilization of Proteins: Experimental Evidence. *Journal of Physical Chemistry B* **126**, 2990–2999 (2022).
73. Singh, L. R., Poddar, N. K., Dar, T. A., Kumar, R. & Ahmad, F. Protein and DNA destabilization by osmolytes: The other side of the coin. *Life Sci* **88**, 117–125 (2011).
74. Rabbani, G. & Choi, I. Roles of osmolytes in protein folding and aggregation in cells and their biotechnological applications. *Int J Biol Macromol* **109**, 483–491 (2018).
75. Almarza, J., Rincon, L., Bahsas, A. & Brito, F. Molecular mechanism for the denaturation of proteins by urea. *Biochemistry* **48**, 7608–7613 (2009).
76. Bennion, B. J. & Daggett, V. The molecular basis for the chemical denaturation of proteins by urea. *Proc Natl Acad Sci U S A* **100**, 5142–5147 (2003).
77. Heyda, J. *et al.* Urea and guanidinium induced denaturation of a Trp-cage miniprotein. *Journal of Physical Chemistry Part B* **115**, 8910–8924 (2011).

78. Heyda, J. *et al.* Guanidinium can both cause and prevent the hydrophobic collapse of biomacromolecules. *J Am Chem Soc* **139**, 863–870 (2017).
79. Withers', P. C., Morrison', G. & Guppy, M. Buoyancy Role of Urea and TMAO in an Elasmobranch Fish, the Port Jackson Shark, Heterodontus portusjacksoni. *https://doi.org/10.1086/physzool.67.3.30163765* **67**, 693–705 (1994).
80. Yoshiba, Y., Kiyosue, T., Nakashima, K., Yamaguchi-Shinozaki, K. & Shinozaki, K. Regulation of Levels of Proline as an Osmolyte in Plants under Water Stress. *Plant Cell Physiol* **38**, 1095–1102 (1997).
81. Khan, S., Hassan, M. I., Ahmad, F. & Islam, A. Osmolytes as a Promising Therapeutic Strategy for Protein Aggregation Diseases. *Cellular Osmolytes: From Chaperoning Protein Folding to Clinical Perspectives: Second Edition* 73–88 (2024) doi:10.1007/978-981-97-6001-5_5/TABLES/1.
82. Bruździak, P., Panuszko, A. & Stangret, J. Influence of osmolytes on protein and water structure: A step to understanding the mechanism of protein stabilization. *Journal of Physical Chemistry B* **117**, 11502–11508 (2013).
83. Verma, P. K. *et al.* Modulation of the hydrogen bonding structure of water by renal osmolytes. *Journal of Physical Chemistry Letters* **6**, 2273–2279 (2015).
84. Guo, F. & Friedman, J. M. Osmolyte-induced perturbations of hydrogen bonding between hydration layer waters: Correlation with protein conformational changes. *Journal of Physical Chemistry B* **113**, 16632–16642 (2009).
85. Jahan, I. & Nayeem, S. M. Effect of Osmolytes on Conformational Behavior of Intrinsically Disordered Protein α-Synuclein. *Biophys J* **117**, 1922–1934 (2019).
86. Parray, Z. A., Ahanger, I. A. & Islam, A. Potential of Osmolytes as Diagnostic Biomarkers in Various Diseases. *Cellular Osmolytes: From Chaperoning Protein Folding to Clinical Perspectives: Second Edition* 185–197 (2024) doi:10.1007/978-981-97-6001-5_10/FIGURES/2.
87. Ahanger, I. A., Hajam, I. B. & Wani, O. H. Modulation of conformational integrity and aggregation propensity of α-synuclein by osmolytes: Implications in therapeutic intervention of Parkinson's disease. *Prog Mol Biol Transl Sci* **211**, 63–87 (2025).
88. Kushwah, N., Jain, V. & Yadav, D. Osmolytes: A Possible Therapeutic Molecule for Ameliorating the Neurodegeneration Caused by Protein Misfolding and Aggregation. *Biomolecules 2020, Vol. 10, Page 132* **10**, 132 (2020).
89. Zhang, J., Yang, P. L. & Gray, N. S. Targeting cancer with small molecule kinase inhibitors. *Nat Rev Cancer* **9**, 28–39 (2009).
90. Ivy, S. P., Wick, J. Y. & Kaufman, B. M. An overview of small-molecule inhibitors of VEGFR signaling. *Nat Rev Clin Oncol* **6**, 569–579 (2009).

91. Wolan, D. W., Zorn, J. A., Gray, D. C. & Wells, J. A. Small-molecule activators of a proenzyme. *Science (1979)* **326**, 853–858 (2009).
92. Zorn, J. A. & Wells, J. A. Turning enzymes on with small molecules. *Nat Chem Biol* **6**, 179–188 (2010).
93. Wang, B., Barahona, M. & Buck, M. Amplification of small molecule-inducible gene expression via tuning of intracellular receptor densities. *Nucleic Acids Res* **43**, 1955–1964 (2015).
94. Malampati, S. *et al.* Targeting Aggrephagy for the Treatment of Alzheimer's Disease. *Cells* **9**, 311 (2020).
95. Hurtado, C. *et al.* Disruption of NOTCH signaling by a small molecule inhibitor of the transcription factor RBPJ. *Sci Rep* **9**, (2019).
96. Bedard, P. L., Hyman, D. M., Davids, M. S. & Siu, L. L. Small molecules, big impact: 20 years of targeted therapy in oncology. *The Lancet* **395**, 1078–1088 (2020).
97. Comission, E., Safer, G., Zabriskie, D. W. & Brady, J. EudraLex The Rules Governing Medicinal Products in the European Union Volume 4 EU guidelines for Good Manufacturing Practice for Medicinal Products for Human and Veterinary Use Annex 2 Manufacture of Biological active substances and Medicinal Products for. *Handbook of Pharmaceutical Biotechnology* **4**, 319 (2012).
98. Hautke, A. *et al.* CAG-Repeat RNA Hairpin Folding and Recruitment to Nuclear Speckles with a Pivotal Role of ATP as a Cosolute. *J Am Chem Soc* **145**, 9571–9583 (2023).
99. Hautke, A., Voronin, A., Idiris, F., Schug, A. H. & Ebbinghaus, S. Cellular ATP levels are paramount for governing stability and LLPS of CAG repeat-containing RNAs inside cell. *Biophys J* **121**, 311a (2022).
100. Klotz, I. M. , R. G. P. , S. A. R. Macromolecule-small molecule interactions. Strong binding and cooperativity in a model synthetic polymer. *Biochemistry* **8**, 4752–4756 (1969).
101. Klotz, I. M. Protein Interactions with Small Molecules. *Acc Chem Res* **7**, 162–168 (1974).
102. Sukenik, S., Sapir, L., Gilman-Politi, R. & Harries, D. Diversity in the mechanisms of cosolute action on biomolecular processes. *Faraday Discuss* **160**, 225–237 (2013).
103. Karlstrom, G., Carlsson, A. & Lindman, B. Phase Diagrams of Nonionic Polymer-Water Systems. Experimental and Theoretical Studies of the Effects of Surfactants and Other Cosolutes. *Journal of Physical Chemistry* **94**, 5005–5015 (1990).
104. Wolf, B. A. & Blaum, G. Measured and calculated solubility of polymers in mixed solvents: Monotony and cosolvency. *Journal of Polymer Science: Polymer Physics Edition* **13**, 1115–1132 (1975).

105. Scherzinger, C., Schwarz, A., Bardow, A., Leonhard, K. & Richtering, W. Cononsolvency of poly-N-isopropyl acrylamide (PNIPAM): Microgels versus linear chains and macrogels. *Curr Opin Colloid Interface Sci* **19**, 84–94 (2014).
106. Mills, C. E., Ding, E. & Olsen, B. D. Cononsolvency of Elastin-like Polypeptides in Water/Alcohol Solutions. *Biomacromolecules* **20**, 2167–2173 (2019).
107. Strickley, R. G. Solubilizing Excipients in Oral and Injectable Formulations. *Pharm Res* **21**, 201–230 (2004).
108. Seedher, N. & Kanojia, M. Co-solvent solubilization of some poorly-soluble antidiabetic drugs Solubilization antidiabetic drugs. *Pharm Dev Technol* **14**, 185–192 (2009).
109. Mardles, E. Study of the Solvents of Some Cellulose Esters. *J Soc Chem Ind Trans* **42**, T127–T142 (1923).
110. Winnik, F. M., Ringsdorf, H. & Venzmer, J. Methanol-Water as a Co-nonsolvent System for Poly(JV-isopropylacrylamide). *Macromolecules* **23**, 2415–2416 (1990).
111. Zhang, Y., Carvalho, W. S. P., Fang, C. & Serpe, M. J. Volatile organic compound vapor detection with responsive microgel-based etalons. *Sens Actuators B Chem* **290**, 520–526 (2019).
112. Kleinschmidt, D. *et al.* Microgel organocatalysts: modulation of reaction rates at liquid–liquid interfaces. *Mater Adv* **1**, 2983–2993 (2020).
113. Krieg, E. & Shih, W. M. Selective Nascent Polymer Catch-and-Release Enables Scalable Isolation of Multi-Kilobase Single-Stranded DNA. *Angewandte Chemie International Edition* **57**, 714–718 (2018).
114. Morris, M. A. *et al.* Democratizing the rapid screening of protein expression for materials development. *Mol Syst Des Eng* **8**, 227–239 (2023).
115. O'Connell, R. A., Sharratt, W. N., Aelmans, N. J. J., Higgins, J. S. & Cabral, J. T. SANS Study of PPPO in Mixed Solvents and Impact on Polymer Nanoprecipitation. *Macromolecules* **55**, 1050–1059 (2022).
116. Van Duinen, D., Butt, H. J. & Berger, R. Two-Stage Collapse of PNIPAM Brushes: Viscoelastic Changes Revealed by an Interferometric Laser Technique. *Langmuir* **18**, 24 (2019).
117. Yu, Y. *et al.* Tunable Friction by Employment of Co-Non-Solvency of PNIPAM Brushes. *Polymer (Guildf)* **102**, 372–378 (2016).
118. Niebuur, B. J. *et al.* Pressure Dependence of Water Dynamics in Concentrated Aqueous Poly(N-isopropylacrylamide) Solutions with a Methanol Cosolvent. *Macromolecules* **54**, 4387–4400 (2021).
119. Yang, M. & Zhao, K. Cononsolvency of poly(N-isopropylacrylamide) in methanol aqueous solution—insight by dielectric spectroscopy. *J Polym Sci B Polym Phys* **55**, 1227–1234 (2017).

120. Mukherji, D. *et al.* Relating side chain organization of PNIPAm with its conformation in aqueous methanol. *Soft Matter* **12**, 7995–8003 (2016).
121. Grinberg, V. Y. *et al.* Energetics and Mechanisms of poly(N-isopropylacrylamide) Phase Transitions in Water-Methanol Solutions. *Macromolecules* **53**, 10765–10772 (2020).
122. Lang, X., Xu, E. X., Wei, Y., Walters, L. N. & Hore, M. J. A. Isomeric and structural effects in polymer cononsolvent systems. *Polymer (Guildf)* **170**, 190–197 (2019).
123. Su, Y., Dan, M., Xiao, X., Wang, X. & Zhang, W. A new thermo-responsive block copolymer with tunable upper critical solution temperature and lower critical solution temperature in the alcohol/water mixture. *J Polym Sci A Polym Chem* **51**, 4399–4412 (2013).
124. Scherzinger, C., Schwarz, A., Bardow, A., Leonhard, K. & Richtering, W. Cononsolvency of poly-N-isopropyl acrylamide (PNIPAM): Microgels versus linear chains and macrogels. *Curr Opin Colloid Interface Sci* **19**, 84–94 (2014).
125. Mills, C. E., Ding, E. & Olsen, B. D. Cononsolvency of Elastin-like Polypeptides in Water/Alcohol Solutions. *Biomacromolecules* **20**, 2167–2173 (2019).
126. Hofmann, C. H. *et al.* Methanol-induced change of the mechanism of the temperature- and pressure-induced collapse of N-substituted acrylamide copolymers. *J Polym Sci B Polym Phys* **53**, 532–544 (2015).
127. Kyriakos, K. *et al.* Quantifying the Interactions in the Aggregation of Thermoresponsive Polymers: The Effect of Cononsolvency. *Macromol Rapid Commun* **37**, 420–425 (2016).
128. Geiger, C. *et al.* PMMA- b-PNIPAM Thin Films Display Cononsolvency-Driven Response in Mixed Water/Methanol Vapors. *Macromolecules* **54**, 3517–3530 (2021).
129. Wang, F., Shi, Y., Luo, S., Chen, Y. & Zhao, J. Conformational transition of poly(N-isopropylacrylamide) single chains in its cononsolvency process: A study by fluorescence correlation spectroscopy and scaling analysis. *Macromolecules* **45**, 9196–9204 (2012).
130. Hore, M. J. A., Hammouda, B., Li, Y. & Cheng, H. Co-nonsolvency of poly(n-isopropylacrylamide) in deuterated water/ethanol mixtures. *Macromolecules* **46**, 7894–7901 (2013).
131. Transformations of Poly-N-Vinylcaprolactam in Aqueous-Organic Mixtures. https://www.elibrary.ru/item.asp?id=13242518.
132. Cortez-Lemus, N. A. & Licea-Claverie, A. Poly(N-vinylcaprolactam), a comprehensive review on a thermoresponsive polymer becoming popular. *Prog Polym Sci* **53**, 1–51 (2016).

133. Pooch, F., Teltevskij, V., Karjalainen, E., Tenhu, H. & Winnik, F. M. Poly(2-propyl-2-oxazoline)s in Aqueous Methanol: To Dissolve or not to Dissolve. *Macromolecules* **52**, 6361–6368 (2019).
134. Amiya, T., Hirokawa, Y., Hirose, Y., Li, Y. & Tanaka, T. Reentrant phase transition of N-isopropylacrylamide gels in mixed solvents. *J Chem Phys* **86**, 2375–2379 (1987).
135. Zuo, T. *et al.* Water/Cosolvent Attraction Induced Phase Separation: A Molecular Picture of Cononsolvency. *Macromolecules* **52**, 457–464 (2019).
136. Bharadwaj, S. *et al.* Cononsolvency of thermoresponsive polymers: where we are now and where we are going. *Soft Matter* **18**, 2884–2909 (2022).
137. Bischofberger, I., Calzolari, D. C. E., De Los Rios, P., Jelezarov, I. & Trappe, V. Hydrophobic hydration of poly-N-isopropyl acrylamide: A matter of the mean energetic state of water. *Sci Rep* **4**, 1–7 (2014).
138. Heyda, J., Muzdalo, A. & Dzubiella, J. Rationalizing polymer swelling and collapse under attractive cosolvent conditions. *Macromolecules* **46**, 1231–1238 (2013).
139. Dalgicdir, C., Rodríguez-Ropero, F. & Van Der Vegt, N. F. A. Computational Calorimetry of PNIPAM Cononsolvency in Water/Methanol Mixtures. *Journal of Physical Chemistry B* **121**, 7741–7748 (2017).
140. Nayar, D., Folberth, A. & Van Der Vegt, N. F. A. Molecular origin of urea driven hydrophobic polymer collapse and unfolding depending on side chain chemistry. *Physical Chemistry Chemical Physics* **19**, 18156–18161 (2017).
141. Dwek, R. A. Glycobiology: Toward understanding the function of sugars. *Chem Rev* **96**, 683–720 (1996).
142. Somerville, C. Cellulose synthesis in higher plants. *Annu Rev Cell Dev Biol* **22**, 53–78 (2006).
143. VAN DER VIES, J. Two methods for the determination of glycogen in liver. *Biochemical Journal* **57**, 410 (1954).
144. Handley, C. J., Samiric, T. & Ilic, M. Z. Structure, Metabolism, and Tissue Roles of Chondroitin Sulfate Proteoglycans. *Adv Pharmacol* **53**, 219–232 (2006).
145. Muzzarelli, R. A. A., Greco, F., Busilacchi, A., Sollazzo, V. & Gigante, A. Chitosan, hyaluronan and chondroitin sulfate in tissue engineering for cartilage regeneration: A review. *Carbohydr Polym* **89**, 723–739 (2012).
146. Cook, G. M. Glycoproteins in membranes. *Biol Rev Camb Philos Soc* **43**, 363–391 (1968).
147. ASPINALL, G. O. Chemistry of Cell Wall Polysaccharides. *Carbohydrates: Structure and Function* 473–500 (1980) doi:10.1016/B978-0-12-675403-2.50018-1.
148. Sutherland, I. W. Bacterial Surface Polysaccharides: Structure and Function. *Int Rev Cytol* **113**, 187–231 (1988).

149. Garcia-Vallejo, J. J. & Van Kooyk, Y. DC-sign. C-type lectin with prominent role in immune system. *Glycoscience: Biology and Medicine* 649–659 (2015) doi:10.1007/978-4-431-54841-6_133/FIGURES/2.
150. Kiessling, L. L., Young, T., Gruber, T. D. & Mortell, K. H. Multivalency in Protein–Carbohydrate Recognition. *Glycoscience* 2483–2523 (2008) doi:10.1007/978-3-540-30429-6_64.
151. Putnam, D., Gentry, C. A., Pack, D. W. & Langer, R. Polymer-based gene delivery with low cytotoxicity by a unique balance of side-chain termini. *Proceedings of the National Academy of Sciences* **98**, 1200–1205 (2001).
152. Wei, Z., Zhao, J., Chen, Y. M., Zhang, P. & Zhang, Q. Self-healing polysaccharide-based hydrogels as injectable carriers for neural stem cells. *Sci Rep* **6**, 1–12 (2016).
153. Hubbell, J. A. Materials as morphogenetic guides in tissue engineering. *Curr Opin Biotechnol* **14**, 551–558 (2003).
154. Duncan, R. Polymer therapeutics as nanomedicines: new perspectives. *Curr Opin Biotechnol* **22**, 492–501 (2011).
155. Wang, J., Wang, D., Zhang, Y. & Dong, J. Synthesis and Biopharmaceutical Applications of Sugar-Based Polymers: New Advances and Future Prospects. *ACS Biomater Sci Eng* **7**, 963–982 (2021).
156. Azzam, T. *et al.* Cationic polysaccharides for gene delivery. *Macromolecules* **35**, 9947–9953 (2002).
157. Torres, F. G., Troncoso, O. P., Urtecho, A., Soto, P. & Pachas, B. Recent Progress in Polysaccharide-Based Materials for Energy Applications: A Review. *ACS Appl Mater Interfaces* **17**, 13179–13196 (2025).
158. Perera, P. N., Browder, B. & Ben-Amotz, D. Perturbations of water by alkali halide ions measured using multivariate raman curve resolution. *Journal of Physical Chemistry B* **113**, 1805–1809 (2009).
159. Perera, P., Wyche, M., Loethen, Y. & Ben-Amotz, D. Solute-induced perturbations of solvent-shell molecules observed using multivariate raman curve resolution. *J Am Chem Soc* **130**, 4576–4577 (2008).
160. Perera, P. N. *et al.* Observation of water dangling OH bonds around dissolved nonpolar groups. *Proceedings of the National Academy of Sciences* **106**, 12230–12234 (2009).
161. Ben-Amotz, D. Hydration-Shell Vibrational Spectroscopy. *J Am Chem Soc* **141**, 10569–10580 (2019).
162. Sun, Y. & Petersen, P. B. Solvation Shell Structure of Small Molecules and Proteins by IR-MCR Spectroscopy. *Journal of Physical Chemistry Letters* **8**, 611–614 (2017).
163. Bates, J. B. Fourier Transform Infrared Spectroscopy. *Science (1979)* **191**, 31–37 (1976).
164. Mulvaney, S. P. & Keating, C. D. Raman Spectroscopy. *Anal Chem* **72**, (2000).

165. Wartewig, S. . IR and Raman spectroscopy : fundamental processing. 175 (2003).
166. Liu, B., Wang, J., Ru, G., Liu, C. & Feng, J. Phase Transition and Preferential Alcohol Adsorption of Poly(N,N-diethylacrylamide) Gel in Water/Alcohol Mixtures. *Macromolecules* **48**, 1126–1133 (2015).

Appendix A: The Size Exclusion Chromatography (SEC) Measurement for the Methylcellulose

The methylcellulose used for the investigation of the ion specificity was purchased commercially. However, its molecular weight and polydispersity index (PDI) were not reported. To ensure that the chain length of the polymer is suitable for this research, Size Exclusion Chromatography (SEC) measurement was performed. The Agilent 1260 Infinity II GPC/SEC System was used for the measurements. The detector of the device was the refractive index (RI), and it is suitable for measuring macromolecules that have 200-10^7 Da average molecular weight. Agilent GPC Offline Analysis Software was used for the analysis. The average molecular weight of MC was determined to be around 145,000 Da, and its PDI is determined as 1.2.

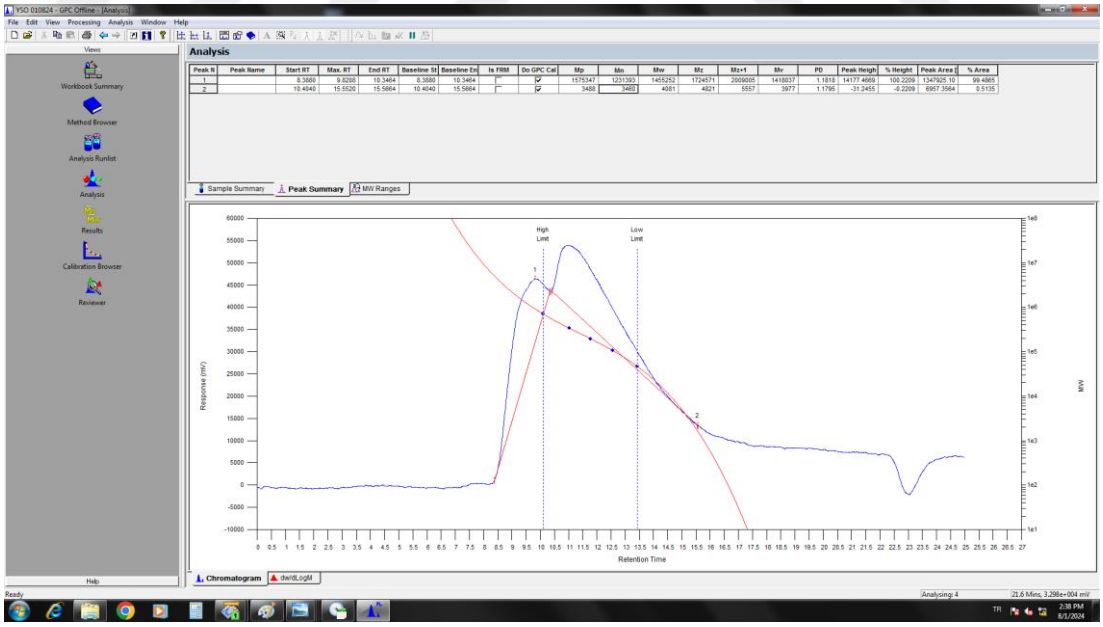

Figure 40: The Screenshot from the Software Agilent GPC Offline Analysis, showing the average molecular weight chromatogram of MC.